STRUCTURAL STUDIES ON SILVER(I) COMPLEXES CONTAINING PHENYLCYANAMIDO LIGANDS AND URANYL(VI) COMPLEXES WITH β-KETOPHENOLATES

A Dissertation presented in partial fulfilment for the Degree of Master of Science in Chemistry at Massey University

Roger Joseph Cresswell

1992

Acknowledgements

Much of this work would not have been possible without the gratefully acknowledged contributions from the following people:

Drs E.W. Ainscough and A.M. Brodie for their supervision, enthusiasm and encouragement throughout this project.

Dr J.M. Waters for her guidance and expertise with the X-ray crystallography.

Drs M.S. Shongwe, A. Mair, Mr Y. Wu and all the members of the inorganic chemistry research group for helpful discussions and for making life in the lab enjoyable.

Mr J.M. Allen, DSIR, for running mass spectra.

Drs K.W. Jolley and G.M. Williams and Mr A.N. Parbhu for help in running NMR spectra.

Ms A. Wallace for preparing of 1,4-dicyanamidobenzene and 4-methoxyphenylcyanamide.

Abstract

This thesis is divided into two parts. In Section One studies on the interaction of phenylcyanamides with silver(I) are reported. Section Two describes the results of studies on the complexes formed from β-ketophenol ligands and the uranyl ion.

Section One

Chapter 1 is a brief overview of the use of phenylcyanamides in forming coordination complexes with transition metals.

In Chapter 2 the preparation of a series of silver complexes of the general formula $[Ag(Ph_3P)_3(pcyd)]$, where pcyd is a phenylcyanamido anion, is described. The crystal structures of $[Ag(Ph_3P)_3(4\text{-}Brpcyd)]$ and $[Ag(Ph_3P)_3(4\text{-}MeOpcyd)]$ have been determined, in which the silver atom occupies a distorted tetrahedral environment, and the latter complex has a very short terminal C-N bond within the 4-methoxyphenylcyanamido ligand.

Chapter 3 provides a comparison of all those transition metal complexes of phenylcyanamides that have been structurally characterised.

Section Two

Chapter 4 is a brief overview of the use of β-diketonate ligands in forming dinuclear complexes, especially those in which the uranyl ion (UO_2^{2+}) is present.

In Chapter 5 the preparation of the mononuclear complexes $[UO_2(HL^1)_2(MeOH)]$, $[UO_2(HL^2)_2(EtOH)]$, the heterobinuclear complexes $[UO_2Mn(L^1)_2(EtOH)]\cdot 1.5H_2O$, and $[UO_2Mn(L^2)_2(EtOH)]\cdot 2H_2O$ and the oxo-ligand adducts $[UO_2(HL^1)_2(Ph_3AsO)]\cdot 2H_2O$, $[UO_2(HL^2)_2(Ph_3PO)]$ and $[UO_2(HL^2)_2(Ph_3AsO)]$ (H_2L^1 = 1-(2-hydroxyphenyl)-3-butanedione and H_2L^2 = 1-(2-hydroxyphenyl)-3-phenyl-1,3-propanedione) is described. The complexes have been characterized by a variety of physicochemical techniques and the crystal structures of $[UO_2(HL^1)_2(EtOH)]$ and $[UO_2(HL^2)_2(EtOH)]\cdot EtOH$ determined. Both complexes contain seven coordinate uranium(VI) in a pentagonal bipyramidal geometry in which the two bidentate β-diketonato ligands and the ethanol ligand make up the equatorial pentagonal plane. For the complex $[UO_2(HL^1)_2(EtOH)]$ the HL^1 ligands are in a *trans* arrangement with respect to one another, whereas for the $[UO_2(HL^2)_2(EtOH)]\cdot EtOH$ complex the HL^2 ligands adopt a *cis* arrangement. However, in solution variable temperature ^1H NMR spectra indicate that the *cis* and *trans* isomers are in equilibrium for both complexes.

Abbreviations

TMTSF	tetramethyltetraselenafulvalene
DCNQI	N,N'-dicyanoquinonediimine
LMCT	ligand to metal charge transfer
pcydH	phenylcyanamide
2,3-Cl_2pcydH	2,3-dichlorophenylcyanamide
3-ClpcydH	3-chlorophenylcyanamide
4-ClpcydH	4-chlorophenylcyanamide
4-MepcydH	4-methylphenylcyanamide
4-BrpcydH	4-bromophenylcyanamide
4-NO_2pcydH	4-nitrophenylcyanamide
bipy	2,2'-dipyridyl
phen	1,10-phenanthroline
Me_2phen	2,9-dimethyl-1,10-phenanthroline
dppm	bis(diphenylphosphino)methane
dppe	1,2-bis(diphenylphosphino)ethane
H_2L^1	1-(2-hydroxyphenyl)-1,3-butanedione
H_2L^2	1-(2-hydroxyphenyl)-3-phenyl-1,3-propanedione
acac	acetylacetone
hfa	1,1,1,5,5,5-hexafluoroacetylacetone
Hpicmet	benzoylpicolinoylmethane
Hnicmet	nicotinoylmethane
bhppH_3	bis(2-hydroxyphenyl)-1,3-propanedione
LSIMS	liquid secondary ion mass spectroscopy

Table of Contents

SECTION ONE
PHENYLCYANAMIDO COMPLEXES OF SILVER(I)

CHAPTER ONE

INTRODUCTION

1.1 Molecular Metals and the Cyanamide Group

The first organic superconductor at atmospheric pressure, the perchlorate salt of the radical cation of tetramethyltetraselenafulvalene (**1**) $(TMTSF)_2ClO_4$ (T_c = 1K), was discovered in 1981[1]. More recently organic superconductors based on the sulphur compound bis(ethylene dithio)-tetrathiafulvalene (**2**) have been prepared[2,3].

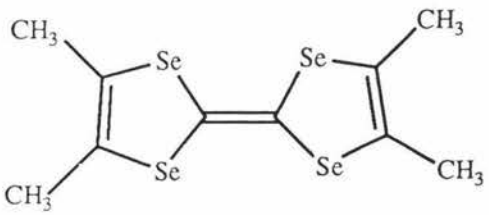

TMTSF (**1**)

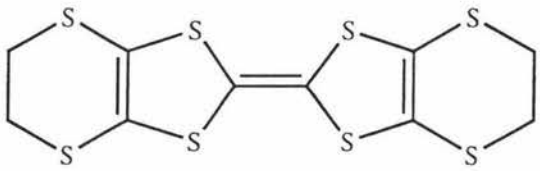

(**2**)

These organic charge transfer crystals involve stacking of the radical-cations to form quasi- one-dimensional "organic metals".

The N,N'- dicyanoquinonediimines (DCNQIs) were recently synthesised to act as electron acceptors in organic charge transfer complexes[4].

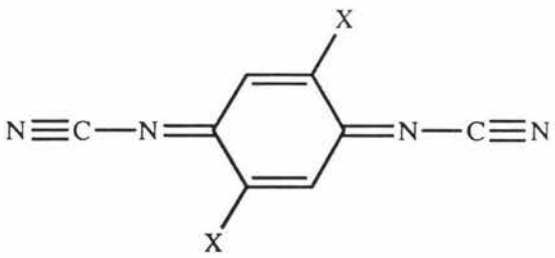

The copper salts of radical anions of 2,5- di- substituted derivatives, having stoichiometry $(2\text{-Me,5-X-DCNQI})_2M$, where X = Me, I, Cl, M = Cu, exhibit metallic conductivity at low

temperatures. For example, (2,5-Me_2-DCNQI)$_2$Cu has a conductivity of σ = 500,000 S cm^{-1} at 3.5K[5]. In the X-ray structure of this example the 2,5-Me_2-DCNQI ligands bridge copper ions that are in a distorted tetrahedral environment and are co-ordinated to four cyanamide groups (RNCN) from four individual ligands. The copper ions are arranged in chains, each surrounded by four stacks of 2,5-Me_2-DCNQI molecules (Fig 1.1).

The high electrical conductivity is attributed to the π-stacks; transverse conductivity occurs via NCN - Cu - NCN bridges within individual stacks. This multidimensionality is based on the empirical evidence of (i) no esr signal in either the X-band or Q-band, (ii) high conductivity with no phase transition point, and (iii) low temperature X-ray diffraction and XPS studies which indicate the copper exists in a mixed valence state (the average oxidation state being 1.3 per copper)[5].

The coordination chemistry and physicochemical properties of the related cyanamides are therefore of interest since they have an important role in the understanding of the high conductivity of radical anion salts of N,N'-dicyanoquinonediimines.

1.2 The Coordination Chemistry of Phenylcyanamides

Cyanamides (**3**) are highly reactive molecules. They are used as starting materials in a wide variety of organic syntheses. Calcium cyanamide (CaNCN) is used as a direct application fertiliser and is also the basic starting material for the industrial preparation of a great range of substances including polymers, medicinals, thiourea, dicyandiamide and melamine plastics.

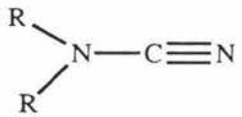

(3)

The predominant reaction of cyanamides is that of polymerisation, involving the addition of a cyanamide ion to the nitrile group of an undissociated cyanamide molecule, e.g. cyanamide (H_2NCN) slowly dimerises on standing to form dicyandiamide.

Figure 1.1 The crystal structure of $(2,5\text{-}Me_2\text{-}DCNQI)_2Cu$

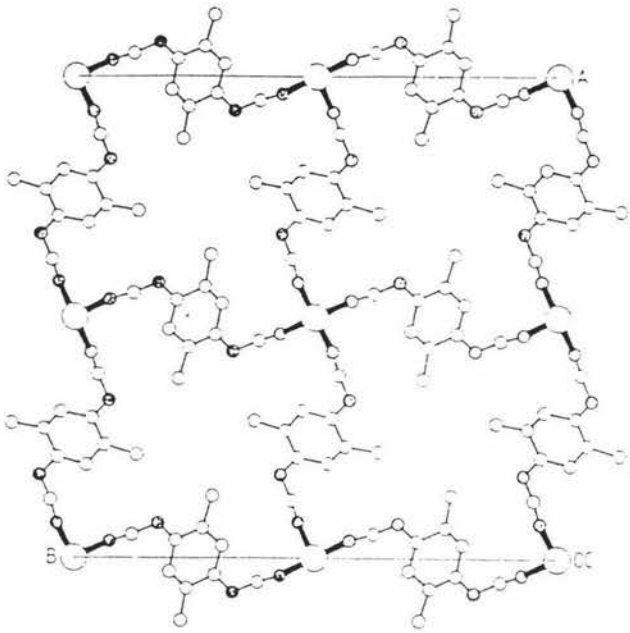

a, *b*-Projection of the crystal structure of $(2,5\text{-}DM\text{-}DCNQI)_2Cu$ (H atoms omitted for clarity). ○ = Cu, ○ = C, ○ = N.

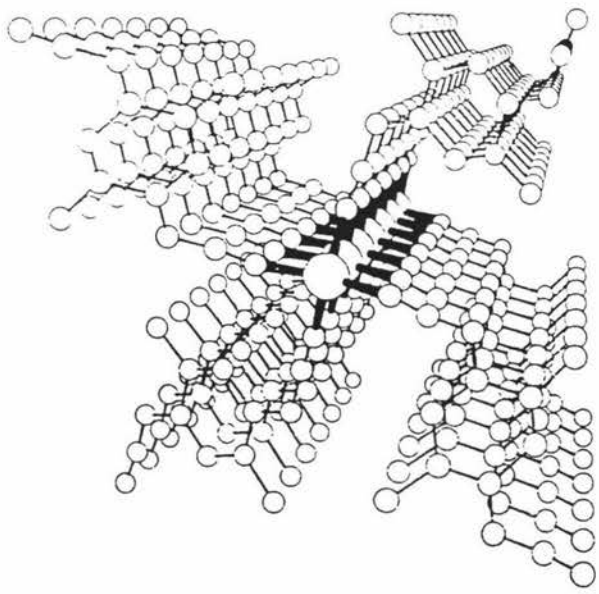

Perspective view of the crystal structure along the *c* axis; the chain of copper atoms is surrounded by four stacks of 2,5-DM-DCNQI molecules (H atoms not shown). ○ = Cu, ○ = C, ○ = N.

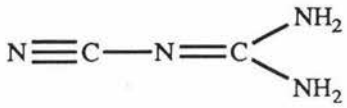

(Dicyandiamide)

Cyanamides present a potentially versatile ligand type in that they possess two functional groups linked directly together. As monodentate ligands, they may coordinate to a metal through either the cyano group (**5**) or the lone pair of electrons on the amido group (**4**).Coordination through the cyano group may involve the σ(**5a**) or π(**5b**) electrons resulting in a μ- type bond. As bidentate ligands they may coordinate to two different metal atoms.

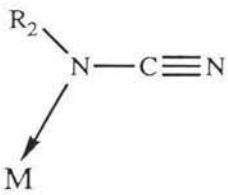

(**4**)

(**5a**)

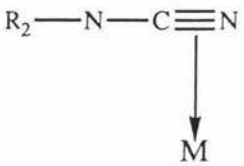

(**5b**)

Phenylcyanamides (**6**) are less prone to autopolymerisation than cyanamide and mono-alkyl substituted cyanamides, and can be synthesised readily in high yields[6].

The amine proton of the neutral phenylcyanamides is highly acidic, due to the conjugate anion being resonance stabilised.

The anionic phenylcyanamide ligand is a strong π-donor because the nitrogen lone pairs can be delocalised into the nitrile π system.

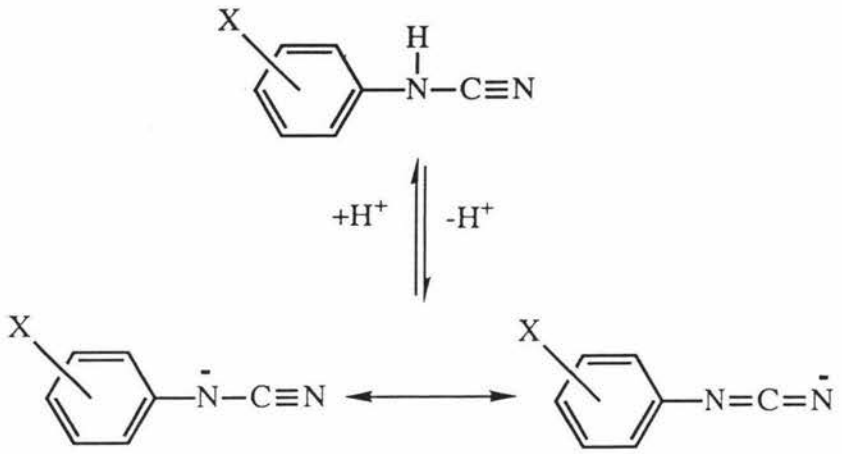

(6a) (6b)

Anionic phenylcyanamides behave like pseudohalides in their ligating properties[7]. Pseudohalides are polyatomic mesomerically stabilised monoanions which exhibit numerous parallels with the halides. Their ambidentate nature and ability to act as bridging ligands are characteristics in common with pseudohalides.

Despite their added stability and ambidentate character, the phenylcyanamides (both neutral and anionic) have received little attention - of the handful of reports published the majority have appeared since 1989 [7-14].

Hollebone and Nyholm, when studying the physical and spectroscopic properties of a series of transition metal pseudohalide complexes, reported a number of halogen-substituted phenylcarbodiimide complexes of copper(II), formulated as $[Ph_4As]_2[Cu(L)_4]$[15]. No spectroscopic data were published to support the assertion that the ligand exists in the carbodiimide form (**6b**) rather than the cyanamide(**6a**) form.

A series of pentaammine ruthenium(III) complexes of neutral and anionic phenylcyanamides have been prepared[10-12]. The electronic spectra of either neutral or anionic ruthenium(III) complexes show ligand to metal charge transfer (LMCT) bands arising from either one non-bonding, or two non-degenerate non-bonding electron pairs, respectively. In these complexes the neutral or anionic ligand coordinates end-on *via* the nitrile nitrogen, the carbodiimide form predominating. The short Ru - N bond distance and nearly linear Ru - N - C bond angle in the X-ray structure of

$[(NH_3)_5Ru(2,3\text{-}Cl_2pcyd)][SO_4]\cdot EtOH$, where 2,3-$Cl_2$pcydH is 2,3-dichlorophenylcyanamide, show a significant degree of π-bonding between the cyanamide group and the ruthenium(III) [10,12] (Fig. 1.2).

The coordination chemistry of neutral phenylcyanamide ligands to the pentaammine ruthenium(II) moiety shows they are capable of acting as π-acceptor ligands, stabilising the Ru(II) oxidation state (even though they possess π-donor properties), whereas anionic phenylcyanamides preferentially coordinate to Ru(III)[11].

A pentaammine mixed-valence complex $[(NH_3)_5Ru(II)(L)Ru(III)(NH_3)_5]$, where L^{2-} = 1,4-dicyanamido-2,3,5,6-tetrachlorobenzene dianion was prepared in an attempt to observe electronic coupling between π-donor Ru(II) and π-acceptor Ru(III), bridged by L^{2-} , via a superexchange mechanism, but only weak coupling was measured[13].

Two copper complexes of anionic phenylcyanamides have been prepared[14] in an attempt to model the copper site in the molecular metal $Cu(DCNQI)_2$. The X-ray crystal structures of $[(bipy)_2Cu(2,3\text{-}Cl_2pcyd)][PF_6]$ and $[(bipy)Cu(2,3\text{-}Cl_2pcyd)_2]$ show the anionic phenylcyanamide ligands are bound end-on to Cu(II) and although some π interaction occurs as evidenced from a LMCT band, assigned to a cyanamido anion pπ ---> $d_{x^2-y^2}$ Cu(II) transition, this is predominantly a σ bonding interaction (Fig. 1.3) [14].

This group's interest in the coordinating properties of phenylcyanamides arose from the observation that the reaction of N-phenylthiourea with an ethanolic solution of copper(II) acetate / 2,2'-bipyridine resulted in the desulphurisation of the phenylthiourea to afford a complex of stoichiometry $[\{Cu(bipy)(pycd)_2\}_2]$[8], where bipy is 2,2'-dipyridyl and pcydH is phenylcyanamide. The X-ray crystal structures of two copper(II) complexes with anionic phenylcyanamides, namely $[\{Cu(bipy)(pycd)_2\}_2]$ and $[\{Cu(phen)(3\text{-}Clpycd)(CH_3CO_2)\}_2]\cdot 2H_2O$ (phen is 1,10-phenanthroline and 3-ClpcydH is 3-chlorophenylcyanamide), were determined and revealed three different coordination modes were available to phenylcyanamido ligands when bound to copper(II)[7] (Fig. 1.4 a,b) . These modes involve (i) terminal coordination

via the nitrile nitrogen (**7a**), (ii) μ-1,3-bridging through the amido and nitrile nitrogens (**7b**), and (iii) μ-1,1-bridging via the nitrile nitrogen(**7c**).

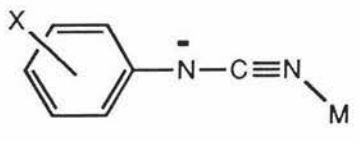

(**7a**)

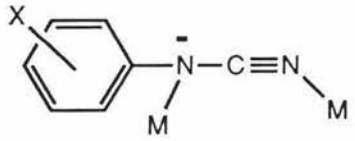

(**7b**)

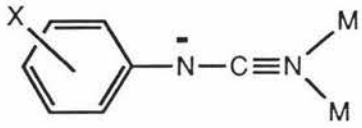

(**7c**)

Several copper(I) complexes of the types $[Cu_2(dppe)_3(pcyd)_2]\cdot 2Me_2CO$ and $[\{Cu(PPh_3)_2(pcyd)\}_2]$, where dppe is 1,2-bis(diphenylphosphino)ethane and pcyd is a phenylcyanamide anion, were synthesised and compared with previously reported halide and pseudohalide complexes. A strong parallel with the analogous azido complexes of copper (I) and copper (II)[9].was observed. The X-ray crystal structures of $[Cu(dppe)_3(4\text{-}Clpcyd)_2]\cdot 2Me_2CO$ and $[\{Cu(PPh_3)_2(4\text{-}Mepcyd)\}_2]$ were determined, the former consisting of centrosymmetric dimer involving terminally bound 4-chlorophenylcyanamido ligands; the latter contains μ-1,3-anionic (mode **7b**) ligands (Fig. 1.4 c,d).

1.3 This Present Study

Univalent silver readily forms complexes with N-donor ligands and also tertiary phosphines and has coordination numbers of two, three and four. One of the aims of this study was to extend the coordination chemistry of anionic phenylcyanamides to include that of mixed ligand complexes of silver(I) with triphenylphosphine and phenylcyanamido ligands.

Chapter Two presents the synthesis and characterisation of some silver (I) complexes , including a series of compounds with the general formula of $[Ag(Ph_3P)_3(pcyd)]$. The physicochemical and spectroscopic properties of these complexes are described, including the single crystal x-ray

structures of [$Ag(Ph_3P)_3$(4-Brpcyd)] and[$Ag(Ph_3P)_3$(4-MeOpcyd)] respectively. This study allowed the monitoring of the influence that the phenyl substituents have on the electronic structure of the complexes.

Chapter Three involves a comparison of all the transition metal complexes of anionic phenylcyanamides that have been structurally characterised in order to investigate the nature of the bonding of phenylcyanamido ligands.

Figure 1.2 The crystal structure of the $[Ru(NH_3)_5(2,3\text{-}Cl_2pcyd)]^{2+}$ ion

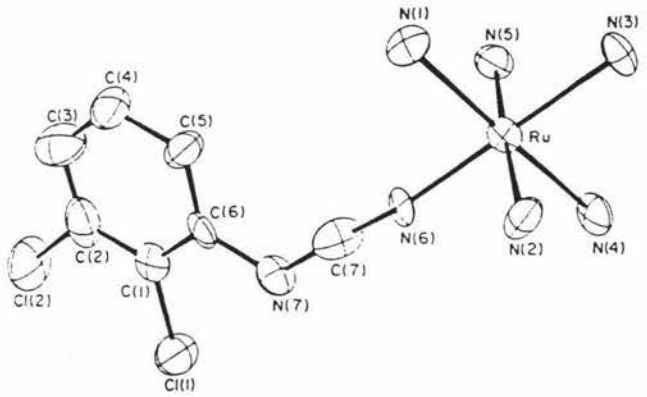

ORTEP drawing of the complex $[(NH_3)_5Ru(2,3\text{-}Cl_2pcyd)]\text{-}[SO_4]\cdot C_2H_5OH$. The sulfate ion and ethanol have not been included for the sake of clarity.

ref [12]

Figure 1.3 Copper(II) complexes of bipyridine and phenylcyanamido ligands

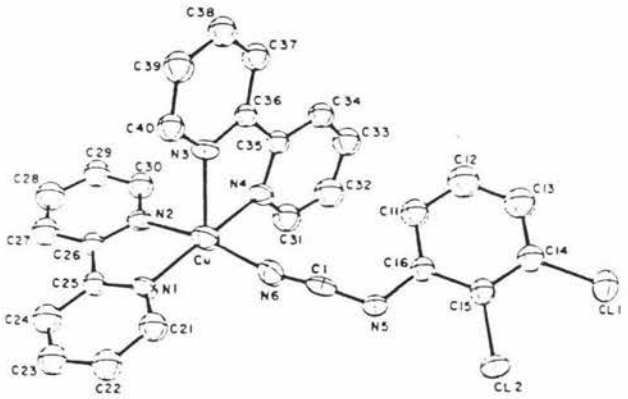

(a) ref [14]

Plot of $[(bpy)_2Cu(2,3\text{-}Cl_2pcyd)][PF_6]$ (1) with atom number scheme. The PF_6 anion has been omitted for clarity.

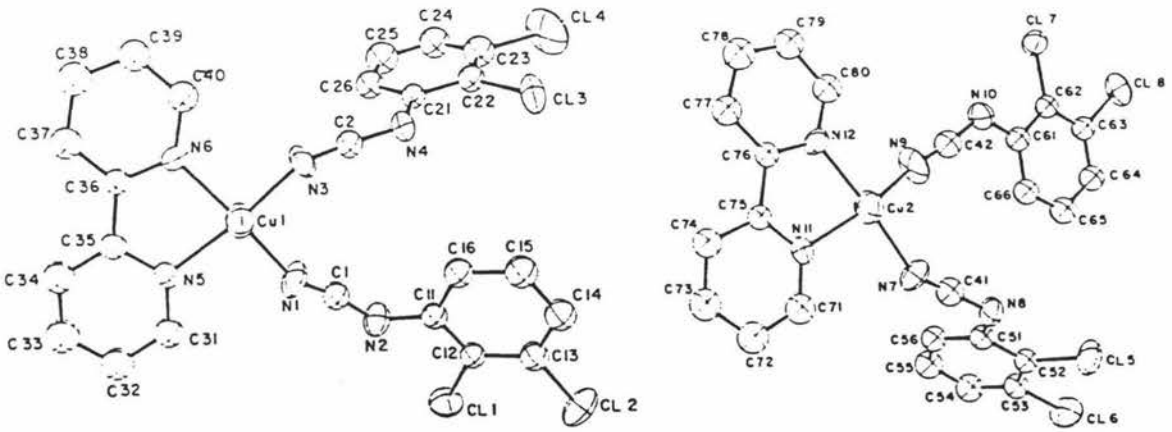

Plot of the two inequivalent configurations of $[(bpy)Cu(2,3\text{-}Cl_2pcyd)_2]$ (2) with atom number scheme.

(b) ref [14]

Figure 1.4 Phenylcyanamido complexes of copper(I) and copper(II)

(a)

ref [7]

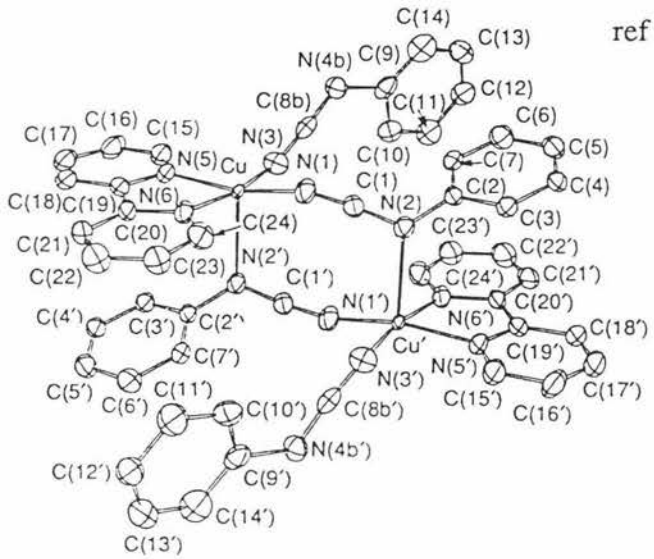

Structure of the complex $[\{Cu(bipy)(PhNCN)_2\}_2]$ showing the numbering system used

(b)

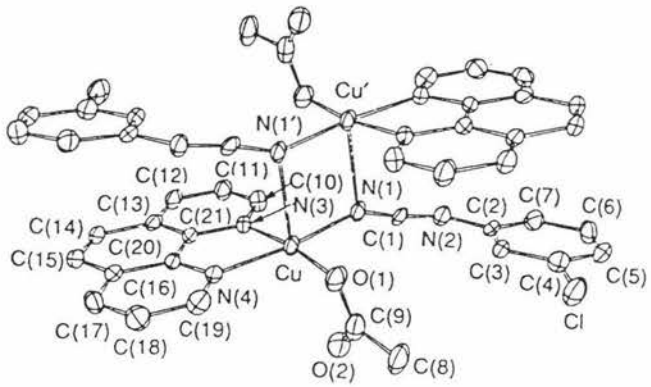

Structure of the complex $[\{Cu(phen)(3\text{-}ClC_6H_4NCN)(CH_3CO_2)\}_2]\cdot 2H_2O$. The numbering system is shown for one monomer unit

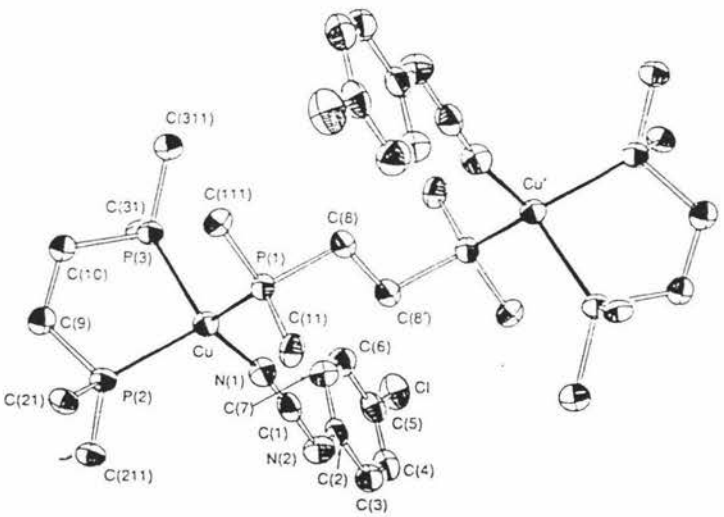

(c)

The structure of the complex $[Cu_2(dppe)_2(4\text{-}ClC_6H_4NCN)_2]$, showing the numbering system used. Ellipsoids are drawn at the 50% probability level. Only the first atoms of the phenyl rings of the dppe ligands are shown, the remainder having been omitted for clarity

ref [9]

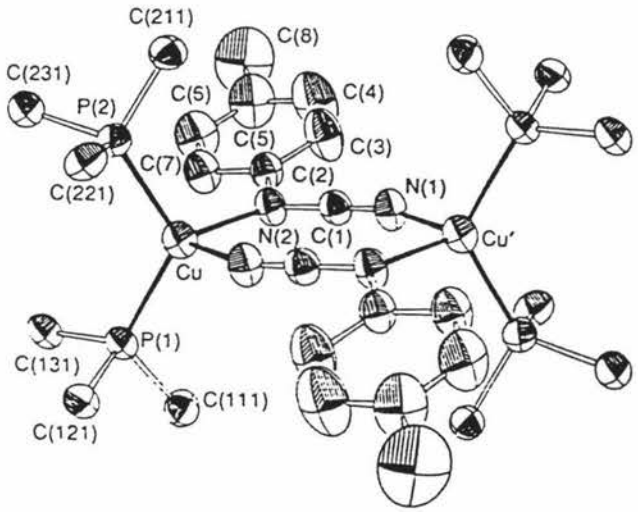

(d)

The structure of the complex $[\{Cu(PPh_3)_2(4\text{-}MeC_6H_4\text{-}NCN)\}_2]$, showing the numbering system used. Ellipsoids are drawn at the 50% probability level. Only the first atoms of the phenyl rings of the

CHAPTER TWO

SILVER(I) PHENYLCYANAMIDO TRIPHENYLPHOSPHINE COMPLEXES

2.1 Synthesis of the Complexes

A series of complexes of the general formula $[Ag(Ph_3P)_3(pcyd)]$, where pcydH = a substituted phenylcyanamide, have been prepared by the addition of triphenylphosphine to the appopriate silver(I) phenylcyanamido salt in a 3:1 ratio.

Two further complexes characterised as [Ag(dppm)(4-Brpcyd)] and $[Ag(Me_2phen)(2\text{-}Clpcyd)]$, where dppm = bis(diphenylphosphino)methane and Me_2phen = 2,9-dimethyl-1,10-phenanthroline, have been synthesised by addition of the appropriate ligand to the corresponding silver(I) phenylcyanamido salt in a 1:1 ratio.

The complexes prepared in this chapter are listed in Table 2.1 along with their melting points, elemental analyses and infrared data.

2.2 Results and Discussion

2.2.1 Infrared Spectra

The infrared ν(CN) frequencies are listed for each compound in Table 2.1 and generally fall in the range 2070 - 2140 cm^{-1}. Comparison of these values with the ν(CN) frequencies of the phenylcyanamido silver salts, [Ag(pcyd)], show a shift of up to 30 cm^{-1} to higher wavenumbers. This trend of an increase in the infrared frequency of the CN triple bond upon the formation of the nitrogen - metal bond has also been observed in ruthenium(III) complexes of neutral phenylcyanamides and in copper(I) and copper (II) phenylcyanamido complexes [7,9,10]. The interpretation of the direction of these frequency shifts is not straightforward[16] and cannot be described solely in terms of changes in the electron distribution within the bonds.Thus the infrared results obtained indicate that the phenylcyanamido ligands are coordinated via the terminal nitrogen, in the complexes prepared, but a detailed analysis of the precise coordination mode is limited.

2.2.2 Molar Conductivities

The molar conductance of 10^{-3} mol l^{-1} solutions of the tris(triphenylphosphine) phenylcyanamido silver(I) complexes in acetone reveal that the appropriate phenylcyanamido ligand remains coordinated in solution.

Complex	Conductivity [a] ($S\ cm^2\ mol^{-1}$)
$[Ag(Ph_3P)_3(2\text{-}Clpcyd)]$	13
$[Ag(Ph_3P)_3(2\text{-}Mepcyd)]$	2
$[[Ag(Ph_3P)_3(4\text{-}Brpcyd)]$	11
$[Ag(Ph_3P)_3(4\text{-}Clpcyd)]$	13
$[Ag(Ph_3P)_3(4\text{-}MeOpcyd)]$	4
$[Ag(Ph_3P)_3(4\text{-}NO_2pcyd)]$	24

[a] In acetone (typical values for 1:1 electrolytes range from 100-130)

2.2.3 ^{31}P NMR Spectroscopy

It has been observed that silver-phosphorus complexes show an averaged ^{31}P chemical shift that is temperature dependent, and that only on cooling to -80 °C did the Ag-P spin-spin coupling become observable[17,18]. The ^{31}P NMR spectrum of $[Ag(Ph_3P)_3(4\text{-}Brpcyd)]$ at room temperature shows a singlet at 3.3 ppm, due to three equivalent phosphorus atoms, with the Ag-P spin-spin coupling not being observed.

Table 2.1
Analytical, melting point and IR data for Silver(I) phenylcyanamido complexes

Complex	Analysis[a]				M.P.	ν(CN)
	%C	%H	%N	%P	(°C)	(cm^{-1})
[$Ag(Ph_3P)_3$(2-Clpcyd)]	69.2 (70.0)	4.6 (4.7)	2.6 (2.7)	8.7 (8.9)	188-190	2100
[$Ag(Ph_3P)_3$(4-Clpcyd)]	69.2 (70.0)	4.8 (4.7)	2.3 (2.7)	9.2 (8.9)	180-182	2093
[$Ag(Ph_3P)_3$(4-Brpcyd)]	67.3 (67.2)	4.5 (4.5)	2.3 (2.5)	8.5 (8.5)	153-155	2110
[$Ag(Ph_3P)_3$(4-MeOpcyd)]	70.8 (71.5)	4.9 (5.0)	2.3 (2.7)	9.4 (8.9)	168-171	2100
[$Ag(Ph_3P)_3$(4-NO_2pcyd)]	69.0 (69.3)	4.9 (4.7)	4.0 (4.0)	8.7 (8.8)	187-189	2121
[$Ag(Ph_3P)_3$(2-Mepcyd)]	70.5 (72.6)	5.1 (5.1)	1.9 (2.7)	8.9 (9.1)	154-155	2073
[$Ag(Me_2$phen)(2-Clpcyd)]	53.6 (53.9)	3.4 (3.5)	12.0 (12.0)		221-225	2134
[Ag(dppm)(4-Brpcyd)]	55.9 (55.8)	3.7 (3.8)	4.2 (4.1)	9.0 (9.1)	231-235	2107

[a] calculated values given in parentheses

2.3 The Single Crystal X-ray Structure of [(4-bromophenylcyanamido-κN) tris(triphenylphosphine-κP) silver(I)], [$Ag(Ph_3P)_3$(4-Brpcyd)]

Thermal ellipsoid diagrams for the title compound showing the atomic numbering scheme used are depicted in Figures 2.3.1 and 2.3.2 respectively. Figure 2.3.3 shows the packing of the molecules within the unit cell. Bond length and angle data are given in Tables 2.2 and 2.3 respectively.

The complex crystallises as a discrete monomer in which the silver atom adopts a distorted tetrahedral geometry, the silver atom being coordinated to three triphenylphosphine phosphorus atoms and a terminal cyano nitrogen atom from the 4-bromophenylcyanamido ligand. The Ag-P bond distances are 2.543(1), 2.569(1) and 2.564(1) Å respectively. Very few monomeric tetrahedral silver - tertiary phosphine complexes have been structurally characterised, hence direct comparisons are difficult. Some typical values of Ag-P distances in tetrahedral complexes are given in Table 2.4. The calculated Ag-P single bond length, based upon the sum of the tetrahedral covalent radii, is calculated to be 2.44 Å[19]. The Ag-P bond distances in this complex are larger than this, but are in good agreement with those in the close structural analogues, [$Ag(Ph_3P)_3(NO_3)$] and [$Ag(Ph_3P)_3Cl$]. The Ag-N bond distance is 2.288(4) Å, being 0.321 and 0.193 Å longer than in the copper(I) phenylcyanamido complexes [$Cu_2(dppe)_3$(4-Clpcyd)$_2$]·$2Me_2CO$ and[{$Cu(Ph_3P)_2$(4-Mepcyd)}$_2$] respectively[9]. Some observed Ag-N bond lengths are given in Table 2.5 and are comparable with that observed in this complex. The angles about the silver atom deviate from the ideal tetrahedral angle of 109.5°, with the P-Ag-P angles being generally larger and the N-Ag-P angles more acute, allowing the accommodation of three bulky phosphine molecules and the relatively less bulky phenylcyanamido ligand around the silver.

The three triphenylphosphine ligands have regular bond distances and angles, comparable with those observed in other silver(I) and copper(I) triphenylphosphine complexes[9,20,22]; the average P-C bond length is 1.830(2) Å. The Ag-P-C angles range from 110.3(1) to 121.0(1)°, all greater than the ideal tetrahedral angle, while the C-P-C angles are all smaller than ideal, ranging from 101.8(1)

to 104.6(1)°. The P-C-C angles, oriented towards the pseudo-threefold axis of the triphenylphosphine ligands, have angles larger than the ideal trigonal angle. In contrast, those in the opposite orientation have angles smaller than than the ideal. This is due to weak intramolecular phenyl ··· phenyl repulsions within the triphenylphosphine ligands[20] (Table 2.7).

In this compound the phenylcyanamido ligand coordinates via the terminal nitrogen only. The cyanamido moiety deviates from linearity as demonstrated by the N(1) - C(1) - N(2) angle of 172.5(6)°, possibly due to steric repulsions. The atoms of the phenyl ring belonging to the 4-bromophenylcyanamido ligand are coplanar, but steric pressures force a rotation (35.4°) of the phenyl ring with respect to the plane defined by the silver atom and the cyanamido group (Table 2.6). This can be seen from the close non-bonding intramolecular approaches made by the hydrogen atoms of the phosphine and phenylcyanamide phenyl rings (Table 2.7).

The two resonance structures for the phenylcyanamido anion are shown below.

(I) (II)

From the bond distances within the Ph -N(2) - C(1) - N(1) moiety, the contribution of each canonical form may be inferred. The observed C(2) - N(2), N(2) - C(1) and N(1) - C(1) lengths are 1.407(5), 1.290(6) and 1.149(6) Å respectively. These bond distances indicate that both resonance structures are important but that the actual structure is closer to (I) than (II). The N(2) -C(2) bond length of 1.407(5) Å is shorter than expected for a C-N single bond (1.472(5) Å)[36]. This reduction in bond length possibly arises because of delocalisation of the negative charge on N(2) into the phenyl ring (in spite of the ring being tilted) via the following resonance forms, which are stabilised by the inductive effect of the bromine atom.

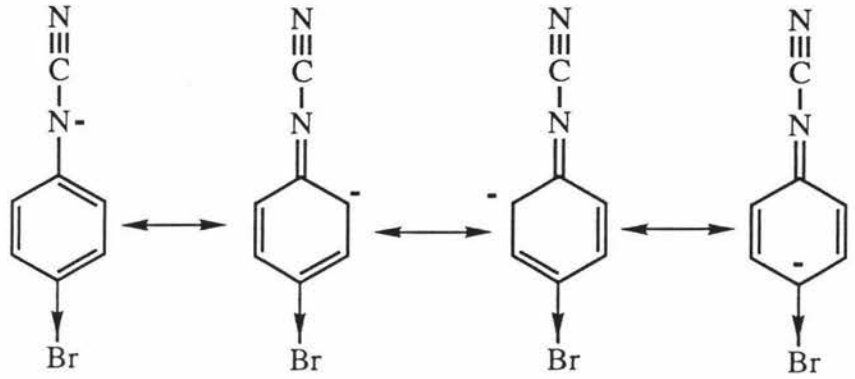

The N(2)-C(1) bond distance of 1.290(6) approaches the value expected for a C-N double bond (1.287 Å [19]), indicating that there is a finite contribution made to the overall electronic structure by the carbodiimide form (II). However, this effect cannot be ascribed solely to the effect of the hybridisation of carbon and nitrogen atoms. If the effects of resonance forms (I) and (II) are taken into account, then the N(2)-C(1) distance will have a value which is intermediate between those of a single and double bond, whereas the nitrilo distance N(1)-C(1) will have a value which corresponds to partially double and partially triple bond character. Despite the shorter N(2)-C(1) distance, the N(1)-C(1) bond length is no longer than the expected C-N triple bond distance (1.158(2)[36]). This phenomenon of markedly shortened bonds linked directly to triple bonds occurs in many other compounds, for example, isothiocyanates[31], $S(CN)_2$[32,33], H_2NCN[34] and $Se(SCN)_2$[35]. It is still unclear what other factors are important in causing such short C-N distances. These findings are in accord with the results of other structures involving phenylcyanamido ligands with ruthenium(III), copper(I) and copper(II)[7-9,12,14]. A detailed comparison of these structures is given in the next chapter.

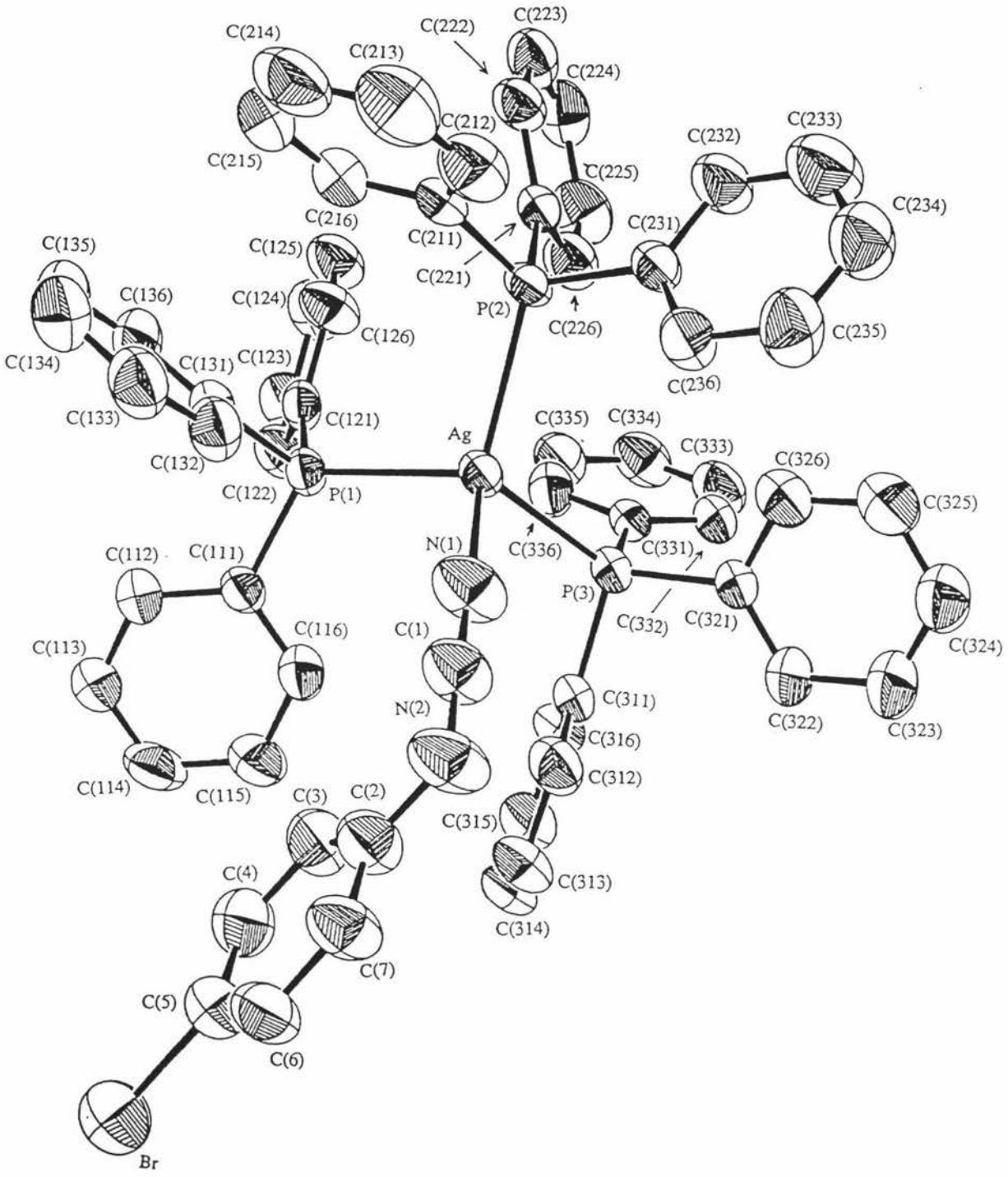

Figure 2.3.1 ORTEP Diagram of $[Ag(Ph_3P)_3(4\text{-Brpcyd})]$ showing the numbering scheme used. Ellipsoids are drawn at the 50% probability level. Hydrogen atoms are omitted for clarity.

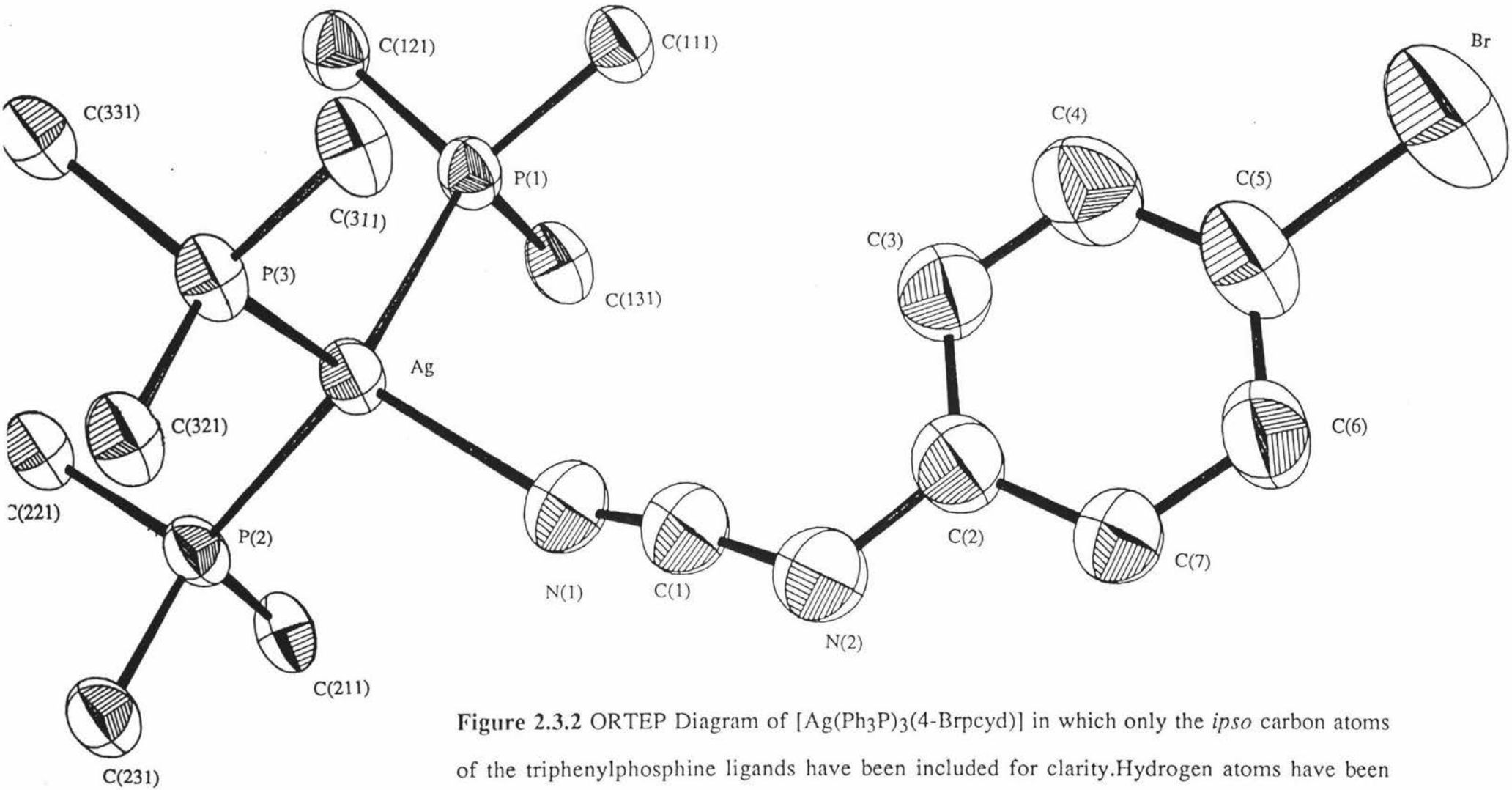

Figure 2.3.2 ORTEP Diagram of $[Ag(Ph_3P)_3(4\text{-Brpcyd})]$ in which only the *ipso* carbon atoms of the triphenylphosphine ligands have been included for clarity.Hydrogen atoms have been ommitted.

Figure 2.3.3 Unit cell packing diagram of $[Ag(Ph_3P)_3(4\text{-}Brpcyd)]$

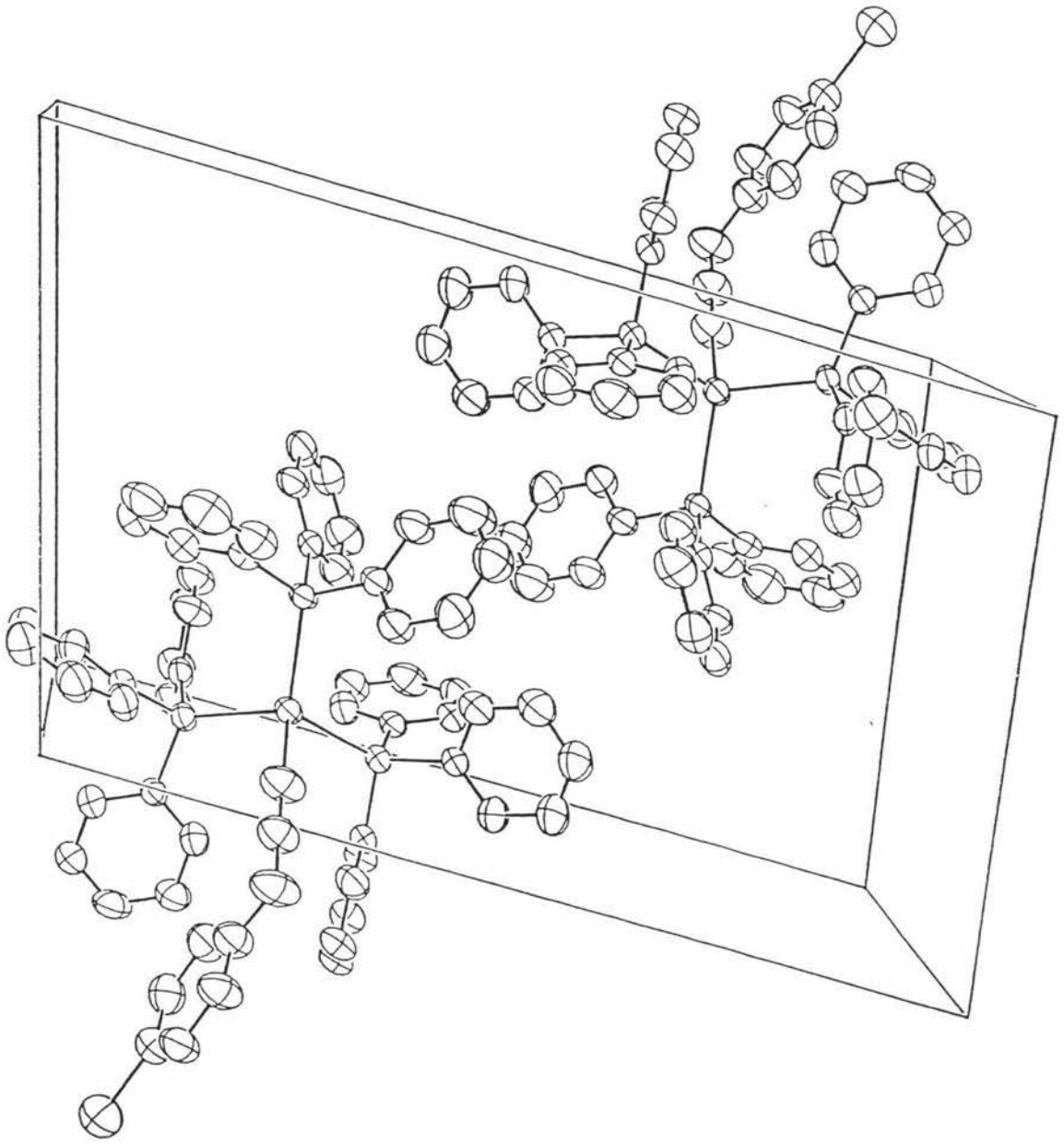

Table 2.2 Selected Bond Lengths (Å) for [Ag(Ph$_3$P)$_3$(4-Brpcyd)] (estimated standard deviations in parentheses)

coordination sphere

Ag - P(1)	2.543(1)	Ag - P(2)	2.569(1)
Ag - P(3)	2.564(1)	Ag - N(1)	2.288(4)

phenylcyanamido ligand

N(1) - C(1)	1.149(6)	N(2) - C(2)	1.407(5)
C(1) - N(2)	1.290(6)	Br - C(5)	1.886(2)

phosphine ligands

P(1) - C(111)	1.831(2)	P(2) - C(211)	1.845(2)
P(1) - C(121)	1.823(2)	P(2) - C(221)	1.832(2)
P(1) - C(131)	1.826(2)	P(2) - C(231)	1.824(2)
P(3) - C(311)	1.834(2)	P(3) - C(321)	1.828(2)
P(3) - C(331)	1.825(2)		

Phenyl rings C-C = 1.395, C-H = 0.960 Å

Table 2.3 Selected Bond Angles for [Ag(Ph$_3$P)$_3$(4-Brpcyd)] (estimated standard deviations in parentheses)

Coordination Sphere

P-Ag-P		*P-Ag-N*	
P(1)-Ag-P(2)	107.9	P(1)-Ag-N(1)	105.0(1)
P(1)-Ag-P(3)	116.3	P(2)-Ag-N(1)	112.7(1)
P(2)-Ag-P(3)	116.7	P(3)-Ag-N(1)	97.4(1)

Phenylcyanamido ligand

Ag-N(1)-C(1)	159.1(4)	N(1)-C(1)-N(2)	172.5(6)
C(1)-N(2)-C(2)	120.2(4)	Br-C(5)-C(4)	118.9(1)
Br-C(5)-C(6)	121.1(1)		

Ag-P-C

Ag-P(1)-C(111)	119.7(1)	Ag-P(2)-C(211)	121.0(1)
Ag-P(1)-C(121)	114.7(1)	Ag-P(2)-C(221)	111.0(1)
Ag-P(1)-C(131)	110.3(1)	Ag-P(2)-C(231)	114.5(1)
Ag-P(3)-C(311)	112.0(1)		
Ag-P(3)-C(321)	117.7(1)		
Ag-P(3)-C(331)	115.3(1)		

C-P-C

C(111)-P(1)-C(121)	103.3(1)	C(111)-P(1)-C(131)	104.6(1)
C(121)-P(1)-C(131)	102.7(1)	C(211)-P(2)-C(221)	104.0(1)
C(211)-P(2)-C(231)	101.8(1)	C(221)-P(2)-C(231)	102.5(1)
C(311)-P(3)-C(321)	103.5(1)	C(311)-P(3)-C(331)	102.4(1)
C(321)-P(3)-C(331)	104.3(1)		

P-C-C

P(1)-C(111)-C(112)	121.5(1)	P(1)-C(111)-C(116)	118.4(1)
P(1)-C(121)-C(122)	122.6(1)	P(1)-C(121)-C(126)	117.2(1)
P(1)-C(131)-C(132)	115.0(1)	P(1)-C(131)-C(136)	124.9(1)
P(2)-C(211)-C(212)	121.1(1)	P(2)-C(211)-C(216)	118.4(1)
P(2)-C(221)-C(222)	124.0(1)	P(2)-C(221)-C(226)	116.0(1)

(table continued over page)

Table 2.3 continued

P(2)-C(231)-C(232)	122.3(1)	P(2)-C(231)-C(236)	117.6(1)
P(3)-C(311)-C(312)	117.4(1)	P(3)-C(311)-C(316)	122.5(1)
P(3)-C(321)-C(322)	122.4(1)	P(3)-C(321)-C(326)	117.6(1)
P(3)-C(331)-C(332)	123.3(1)	P(3)-C(331)-C(336)	116.6(1)

Table 2.4 Ag - P Bond Lengths (Å) in Complexes Containing Tetrahedral Silver(I) (estimated standard deviations in parentheses)

Compound	Bond Distance (Å)	Reference
$[Ag(Ph_3P)Cl]_4$	2.382(3)	[20]
$[Ag(Et_3P)Br]_4$	2.402(5)	[21]
$[Ag(Ph_3P)Br]_4$	2.422(4)	[20]
$[Ag(Ph_3P)I]_4$	2.459(4)	[20]
$[Ag(Ph_3P)_2Cl]_2$	2.470(2)	[22]
$[Ag(Ph_3P)_2(SCN)]_2$	2.479(5)	[23]
$[Ag(Ph_3P)_2]_2[Ni\{S_2C=C(CN)_2\}_2]$	2.485(4)	[24]
$[Ag(Ph_3P)_3Cl]$	2.543(1)	[25]
$[Ag(Ph_3P)_3$(4-MeOpcyd)]	2.549(2)	
$[Ag(Ph_3P)_3$(4-Brpcyd)]	2.559(1)	
$[Ag(Ph_3P)_3(NO_3)]$	2.567(2)	[26]
$[Ag(Ph_3P)_4]PF_6$	2.657(2)	[27]

Table 2.5 Ag-N Bond Lengths (Å) for Selected Silver(I) Complexes (estimated standard deviations in parentheses)

Compound	Bond Distance (Å)	Reference
$[Ag\{p$ Me-Ph$)_3P\}\{BH_2(pz)_2\}]$ [28]	2.194(4)	[28]
$[Ag(Me_5tet)(NO_3)]_2$ [29]	2.216(10), 2.233(10)	[29]
$[Ag(1\text{-Ph-}3,5\text{-}Me_2pz)_3]^+$ [30]	2.243(3)	[30]
$[Ag(Ph_3P)_3$(4-Brpcyd)]	2.288(4)	
$[Ag(Ph_3P)_3$(4-MeOpcyd)]	2.295(8)	

pz = pyrazole, tet = tetrazole

Table 2.6 Planes of "Best-Fit" for [Ag(Ph_3P)$_3$(4-Brpcyd)] (estimated standard deviations in parentheses)

Plane	Atom	Deviation(Å)
1. [Ag-N(1)-C(1)-N(2)]	Ag	-0.0002(19)
	N(1)	-0.0055(59)
	C(1)	0.0191(59)
	N(2)	-0.0099(59)
2. [C(2)-C(3)-C(4)-C(5)-C(6)-C(7)]	C(2)	-0.0003(36)
	C(3)	0.0009(36)
	C(4)	-0.0007(36)
	C(5)	0.0000(36)
	C(6)	0.0006(36)
	C(7)	-0.0004(36)
	Br	-0.0317(8)
	Ag	0.7888(18)
	N(1)	0.6004(57)
	N(2)	-0.0021(57)
	C(1)	0.2993(57)

Equation of Plane $Ax + By + Cz + D = 0$

Plane	A	B	C	D
1	0.070	0.036	-0.997	-5.070
2	-0.155	0.569	-0.808	-4.978

Table 2.7 Intramolecular Non-Bonding Contacts (<3.0 Å) for [Ag(Ph_3P)$_3$(4-Brpcyd)]

H(3) ··· H(116)	2.85
H(3) ··· H(313)	2.97
Intra-triphenylphosphine contacts	
H(112) ··· H(136)	2.84
H(116) ··· C(311)	2.66
H(126) ··· H(216)	2.18
H(126) ··· H(136)	2.89
H(212) ··· C(231)	2.51
H(222) ··· C(211)	2.68
H(222) ··· H(232)	2.87
H(226) ··· C(336)	2.75
H(232) ··· C(221)	2.55
H(312) ··· H(322)	2.97
H(316) ··· C(331)	2.51

2.4 The Single Crystal X-Ray Structure of [(4-methoxyphenylcyanamido-κN) tris(triphenylphosphine-κP) silver(I)], [Ag(Ph$_3$P)$_3$(4-MeOpcyd)].

The structure of [Ag(Ph$_3$P)$_3$(4-MeOpcyd)] is similar to that described for [Ag(Ph$_3$P)$_3$(4-Brpcyd)]. The complex is monomeric, with the silver atom coordinated to three triphenylphosphine phosphorus atoms and a terminal nitrogen atom from the 4-methoxyphenylcyanamido ligand in a distorted tetrahedral environment. A thermal ellipsoid diagram, showing the atomic numbering scheme is given in Figure 2.4.1, with a unit cell packing diagram given in Figure 2.4.2. Bond distances and angles are given in Tables 2.8 and 2.9 respectively.

Ag-P and Ag-N bond distances are comparable with those in the previous structure (Tables 2.4 and 2.5). All the P-Ag-P angles are greater than the ideal tetrahedral angle, whereas the P-Ag-N angles are all less than the ideal, thus relieving the steric strain of the triphenylphosphine ligands.

The most striking feature of this structure is that although a measure of electron delocalisation is observed throughout the cyanamido moiety, with C(1) - N(2) and N(2) - C(2) bond distances of 1.404(18) and 1.428(11) Å respectively, the N(1) - C(1) bond distance is very short at 1.001(16) Å. The cyanamido moiety is close to linear with a N(1) - C(1) - N(2) bond angle of 174(1)°. This evidence suggests that the resonance equilibrium is shifted closer towards the cyanamido resonance form (I) in this structure. The Ag - N(1) - C(1) bond angle of 140.7(8)° (cf 159.1(4)° in [Ag(Ph$_3$P)$_3$(4-Brpcyd)]) deviates significantly from the ideal angle of 180° that is expected for the cyanamido resonance form coordinating through a σ bonding interaction *via* the terminal nitrogen lone pair to the silver. The actual bonding description will have contributions from both the cyanamido (I) and carbodiimide (II) resonance forms such that the bond angle may lie between 120 and 180°. Another factor in the differences between the cyanamido groups in these two silver structures is the electron-withdrawing and -donating abilities of the substituents on the phenyl rings of the phenylcyanamido ligands. For [Ag(Ph$_3$P)$_3$(4-MeOpcyd)] the electron-donating methoxy group provides further electron density to the terminal nitrogen, thus the N(1) - C(1) bond length is shorter than that in [Ag(Ph$_3$P)$_3$(4-Brpcyd)] for which the inductive effect of the

bromine atom removes electron density from the nitrile nitrogen. Thus the σ and π basicity of the phenylcyanamido ligands can be "tuned" as electron-donating or -withdrawing substituents effect the electron density coefficient of the π non-bonding molecular orbitals [12].

As in the previous structure the phenyl ring of the 4-methoxyphenylcyanamido is tilted (angle = 78.6°) with respect to the cyanamido moiety due to steric repulsions and reduced electron delocalisation from the cyanamido group (Tables 2.10 and 2.11).

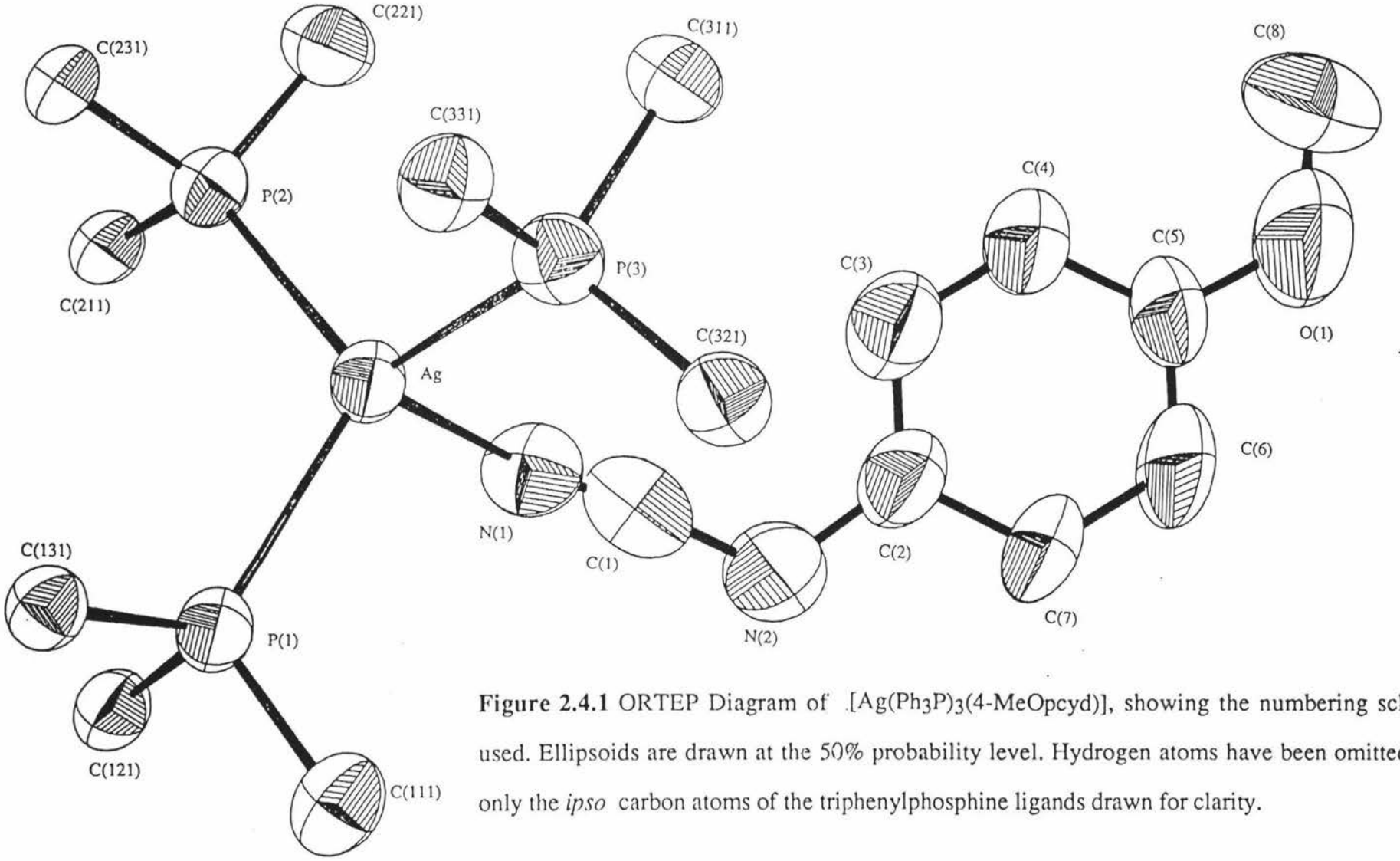

Figure 2.4.1 ORTEP Diagram of [$Ag(Ph_3P)_3$(4-MeOpcyd)], showing the numbering scheme used. Ellipsoids are drawn at the 50% probability level. Hydrogen atoms have been omitted and only the *ipso* carbon atoms of the triphenylphosphine ligands drawn for clarity.

Figure 2.4.2 Unit cell packing diagram of $[Ag(Ph_3P)_3(4\text{-MeOpcyd})]$

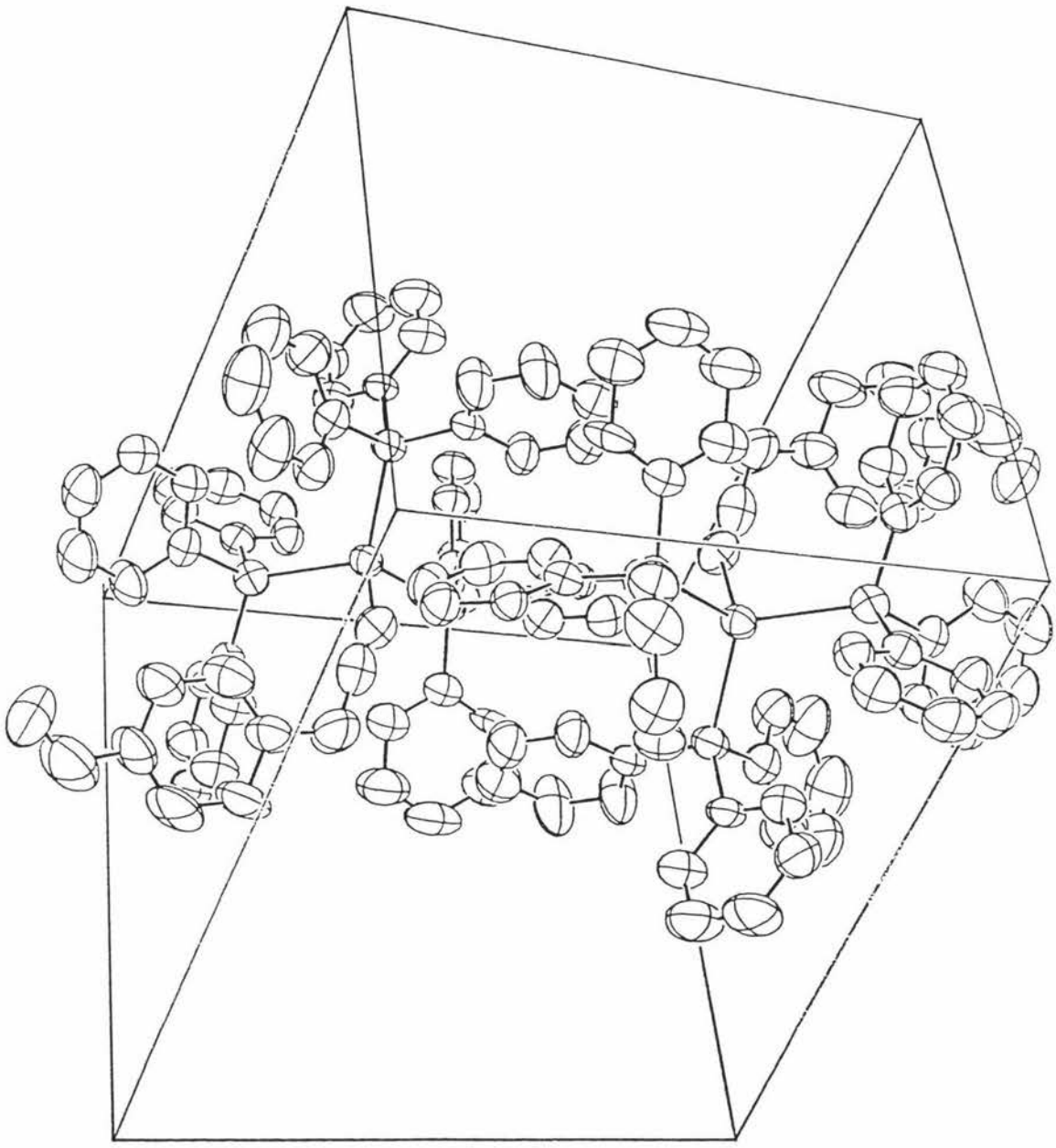

Table 2.8 Selected Bond Lengths (Å) for [Ag(Ph$_3$P)$_3$(4-MeOpcyd)] (estimated standard deviations in parentheses)

coordination sphere			
Ag - P(1)	2.526(2)	Ag - P(2)	2.543(2)
Ag - P(3)	2.577(2)	Ag - N(1)	2.295(8)
phenylcyanamido ligand			
N(1) - C(1)	1.001(16)	N(2) - C(2)	1.428(11)
C(1) - N(2)	1.404(18)	O(1) - C(5)	1.369(13)
O(1) - C(8)	1.284(18)		
phosphine ligands			
P(1) - C(111)	1.824(6)	P(2) - C(211)	1.820(5)
P(1) - C(121)	1.823(4)	P(2) - C(221)	1.817(6)
P(1) - C(131)	1.832(5)	P(2) - C(231)	1.831(6)
P(3) - C(311)	1.832(5)	P(3) - C(321)	1.829(6)
P(3) - C(331)	1.826(5)		

Phenyl rings C-C = 1.395, C-H = 0.960 Å

Table 2.9 Selected Bond Angles (°) for [Ag(Ph3P)3(4-MeOpcyd)] (estimated standard deviations in parentheses)

Coordination Sphere

P-Ag-P		*P-Ag-N*	
P(1)-Ag-P(2)	114.6(1)	P(1)-Ag-N(1)	102.5(2)
P(1)-Ag-P(3)	115.7(1)	P(2)-Ag-N(1)	104.3(2)
P(2)-Ag-P(3)	113.4(1)	P(3)-Ag-N(1)	104.3(2)

Phenylcyanamido ligand

Ag-N(1)-C(1)	140.7(8)	N(1)-C(1)-N(2)	174(1)
C(1)-N(2)-C(2)	116.5(8)	C(8) - O(1) - C(5)	122(1)
O(1) - C(5) - C(4)	123.7(7)	O(1) - C(5) - C(6)	116.3(8)

Ag-P-C

Ag-P(1)-C(111)	115.8(2)	Ag-P(2)-C(211)	119.7(2)
Ag-P(1)-C(121)	115.1(2)	Ag-P(2)-C(221)	111.6(3)
Ag-P(1)-C(131)	114.1(2)	Ag-P(2)-C(231)	112.4(2)
Ag-P(3)-C(311)	117.6(2)		
Ag-P(3)-C(321)	115.6(2)		
Ag-P(3)-C(331)	112.4(2)		

C-P-C

C(111)-P(1)-C(121)	100.6(2)	C(111)-P(1)-C(131)	106.6(3)
C(121)-P(1)-C(131)	103.0(3)	C(211)-P(2)-C(221)	102.4(3)
C(211)-P(2)-C(231)	103.7(3)	C(221)-P(2)-C(231)	105.6(3)
C(311)-P(3)-C(321)	103.6(3)	C(311)-P(3)-C(331)	102.4(3)
C(321)-P(3)-C(331)	103.4(2)		

P-C-C

P(1)-C(111)-C(112)	122.1(5)	P(1)-C(111)-C(116)	117.8(4)
P(1)-C(121)-C(122)	122.5(3)	P(1)-C(121)-C(126)	117.5(4)
P(1)-C(131)-C(132)	124.2(4)	P(1)-C(131)-C(136)	115.8(4)
P(2)-C(211)-C(212)	122.4(4)	P(2)-C(211)-C(216)	117.6(3)

(table continued over page)

Table 2.9 continued

P(2)-C(221)-C(222)	116.7(5)	P(2)-C(221)-C(226)	123.1(5)
P(2)-C(231)-C(232)	116.7(5)	P(2)-C(231)-C(236)	123.2(4)
P(3)-C(311)-C(312)	117.5(4)	P(3)-C(311)-C(316)	122.2(4)
P(3)-C(321)-C(322)	116.9(3)	P(3)-C(321)-C(326)	123.0(4)
P(3)-C(331)-C(332)	117.5(3)	P(3)-C(331)-C(336)	122.4(4)

Table 2.10 Planes of "Best-Fit" for [Ag(Ph_3P)$_3$(4-MeOpcyd)] (estimated standard deviations in parentheses)

Plane	Atom	Deviation(Å)
1. [Ag-N(1)-C(1)-N(2)]	Ag	0.0000(14)
	N(1)	0.0149(98)
	C(1)	-0.0414(98)
	N(2)	0.0128(83)
2. [C(2)-C(3)-C(4)-C(5)-C(6)-C(7)]	C(2)	0.0003(75)
	C(3)	-0.0001(75)
	C(4)	-0.0001(75)
	C(5)	0.0000(75)
	C(6)	0.0002(75)
	C(7)	-0.0004(75)
	O(1)	-0.0068(117)
	C(8)	-0.4291(168)
	Ag	0.0048(14)
	N(1)	0.1112(107)
	N(2)	0.5574(84)
	C(1)	0.3844(117)

Equation of Plane $Ax + By + Cz + D = 0$

Plane	A	B	C	D
1	0.114	0.950	-0.290	-2.999
2	-0.603	0.036	-0.797	-6.120

Table 2.11 Intramolecular Non-Bonding Contacts (<3.0 Å) for [Ag(Ph$_3$P)$_3$(4-MeOpcyd)]

H(3) ··· H(222)	2.72
H(3) ··· H(322)	2.79
Intra-triphenylphosphine contacts	
H(112) ··· H(132)	2.59
H(112) ··· H(122)	2.89
H(116) ··· C(322)	2.86
H(122) ··· C(131)	2.54
H(132) ··· C(112)	2.66
H(136) ... H(216)	2.69
H(212) ··· C(221)	2.54
H(216) ··· C(121)	2.67
H(226) ··· C(231)	2.70
H(232) ··· H(312)	2.35
H(232) ··· H(331)	2.72
H(236) ··· C(211)	2.59
H(315) ··· H(326)	2.84
H(316) ··· H(335)	2.40
H(316) ··· C(321)	2.55
H(326) ··· C(331)	2.55

2.5 Silver Phenylcyanamido Complexes with Bidentate Ligands

The complexes [Ag(dppm) (4-Brpcyd)] and [Ag(Me$_2$phen)(2-Clpcyd)], where Me$_2$phen is 2,9-dimethyl-1,10-phenanthroline and dppm is bis(diphenylphosphino)methane, have been prepared by the addition of the appropriate bidentate ligand to the corresponding silver phenylcyanamido salt in a 1:1 ratio. The elemental analyses and IR data are given in Table 2.1.The ν(CN) frequencies are similar to those of the previously described complexes and therefore the phenylcyanamido ligands are most likely coordinating through the terminal nitrogen.

Further characterisation was limited by their insolubility in suitable solvents.

Examples of three-coordinate silver(I) are few[29,30], and it is possible to write a four coordinate dimeric structure (IV) in place of the trigonal coplanar one (III). Thus the coordination geometry about the silver in these two complexes cannot be assigned unambiguously.

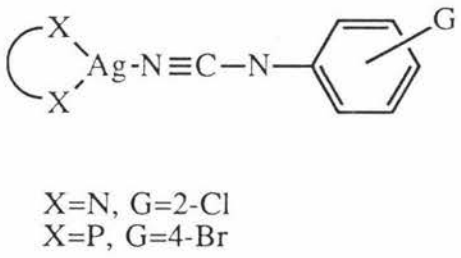

X=N, G=2-Cl
X=P, G=4-Br

(III)

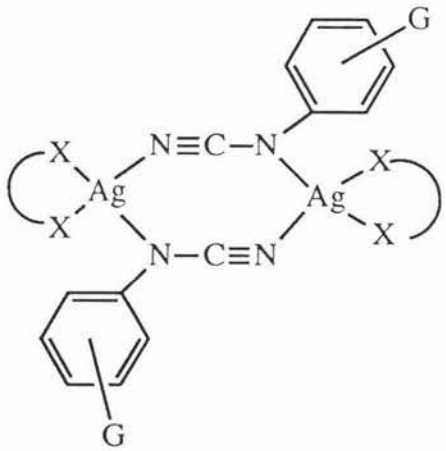

(IV)

2.6 The Interaction of $Ag(ClO_4)$ with 1,4-Dicyanamidobenzene

The addition of a methanolic solution of 1,4-dicyanamidobenzene to silver perchlorate in methanol immediately produced a bright purple precipitate. Substituted 1,4-dicyanamidobenzenes are susceptible to air oxidation to form blue radical anions[13]. Elemental analysis yielded a Ag: ligand ratio of 2:1. The observation of an ESR signal ($g_{\perp}$=1.98) would suggest that the compound is either the disilver salt of the radical anion of 1,4-dicyanobenzene, or contains an impurity of the radical anion. Analysis: %C = 25.5 (25.8), %H = 1.1 (1.1), %N = 15.2 (15.2), with calculated figures in parentheses for $Ag_2C_8H_4N_4$.

The addition of triphenylphosphine to this radical anion salt in a 6:1 ratio produced a light blue precipitate, with the filtrate subsequently yielding a green solid. These two compounds have proved difficult to characterise.

2.7 Summary

A series of silver(I) complexes containing a phenylcyanamido ligand and three triphenylphosphine ligands have been prepared. IR data and the X-ray crystal structures of [$Ag(Ph_3P)_3$(4-Brpcyd)] and [$Ag(Ph_3P)_3$(4-MeOpcyd)] show that for this series the complexes are monomeric, with the silver atom in a tetrahedral environment and the phenylcyanamido ligand is coordinated *via* the terminal cyano nitrogen. The structural details for the cyanamide ligands are dependent on the nature of the substitution on the phenyl ring.

With bidentate ligands the silver(I) complexes [Ag(dppm)(4-Brpcyd)] and [$Ag(Me_2$phen)(2-Clpcyd)] have also been prepared, but their structures have not been resolved.

When silver perchlorate is reacted with 1,4-dicyanamidobenzene the purple disilver salt of the 1,4-dicyanamidobenzene radical anion is probably formed.

2.8 Experimental

2.8.1 Sources of Chemicals

Silver perchlorate and bis(diphenylphosphino)methane were from Aldrich, triphenylphosphine from Merk, 2,9-dimethyl-1,10-phenanthroline from Ega-Chemie, and were used as supplied.

All solvents were laboratory grade and used as supplied with the exception of methanol and dichloromethane, which were dried according to the methods described in "Purification of Organic Chemicals"[37].

2.8.2 Preparation of the Phenylcyanamides

Two different synthetic routes were used in the preparation of the phenylcyanamide ligands, the first involved two steps: (i) the conversion of an aniline to it's analogous phenylthiourea[38], and (ii) desulphurisation to form the appropriate phenylcyanamide[39]. The second method was the direct conversion of an aniline to the corresponding phenylcyanamide using cyanogen bromide[40].

2.8.2.(a) The Synthesis of Phenylcyanamides from the Phenylthioureas

(i) the synthesis of the phenylthioureas via the anilines:

Ammonium thiocyanate (17g, 0.33 mol) was dissolved in dry acetone in a 500 cm^3 three necked flask fitted with a dropping funnel. Through the dropping funnel, benzoyl chloride (28.2g, 0.2 mol) was added dropwise with constant stirring. After the addition was complete the flask was placed in an oil bath at 70 - 80°, and the mixture refluxed with stirring for five minutes. To this, a solution of aniline (18.6g, 0.2 mol) in dry acetone (50 cm^3) was added at such a rate that the mixture refluxed gently. A yellow precipitate (α-benzoyl-β-phenylthiourea) was obtained when the mixture was added to 1.5 l of water. This precipitate was isolated by filtration and heated for five minutes in a boiling solution of sodium hydroxide (30g) in water (270 cm^3). The resulting solution was filtered to remove any insoluble material, acidified with concentrated hydrochloric acid, then made slightly basic with ammonium hydroxide. Upon standing overnight, a white precipitate of phenylthiourea (22.5g, 73%) separated, m.p. 150-153° (lit. 151-153°)[16].

(ii) the desulphurisation of phenylthioureas to yield the corresponding phenylcyanamides:

To a boiling suspension of phenylthiourea (11.8g, 0.1 mol) in water (150 cm^3), a boiling aqueous solution (150 cm^3) of potassium hydroxide (56.0g, 1.0 mol) was added, and immediately followed by a hot saturated solution of lead acetate (38.0g, 0.1 mol). The reaction mixture was boiled for six minutes and then cooled to 0°C, the lead sulphide being removed by filtration. On acidification of the colourless filtrate with glacial acetic acid (60 cm3) at 0-5°C (addition of ice), a white crystalline precipitate of phenylcyanamide (7.6g, 65%, m.p= 107-109°) separated, forming large lustrous needles which were recrystallised from benzene-light petroleum. The substituted phenylcyanamides; 4-bromophenylcyanamide, 2-methylphenylcyanamide, and 4-nitrophenylcyanamide, were prepared by an analogous method using the corresponding substituted phenylthioureas derived from the appropriate aniline. The overall equations for the synthesis of phenylcyanamide (pcydH) are given below:

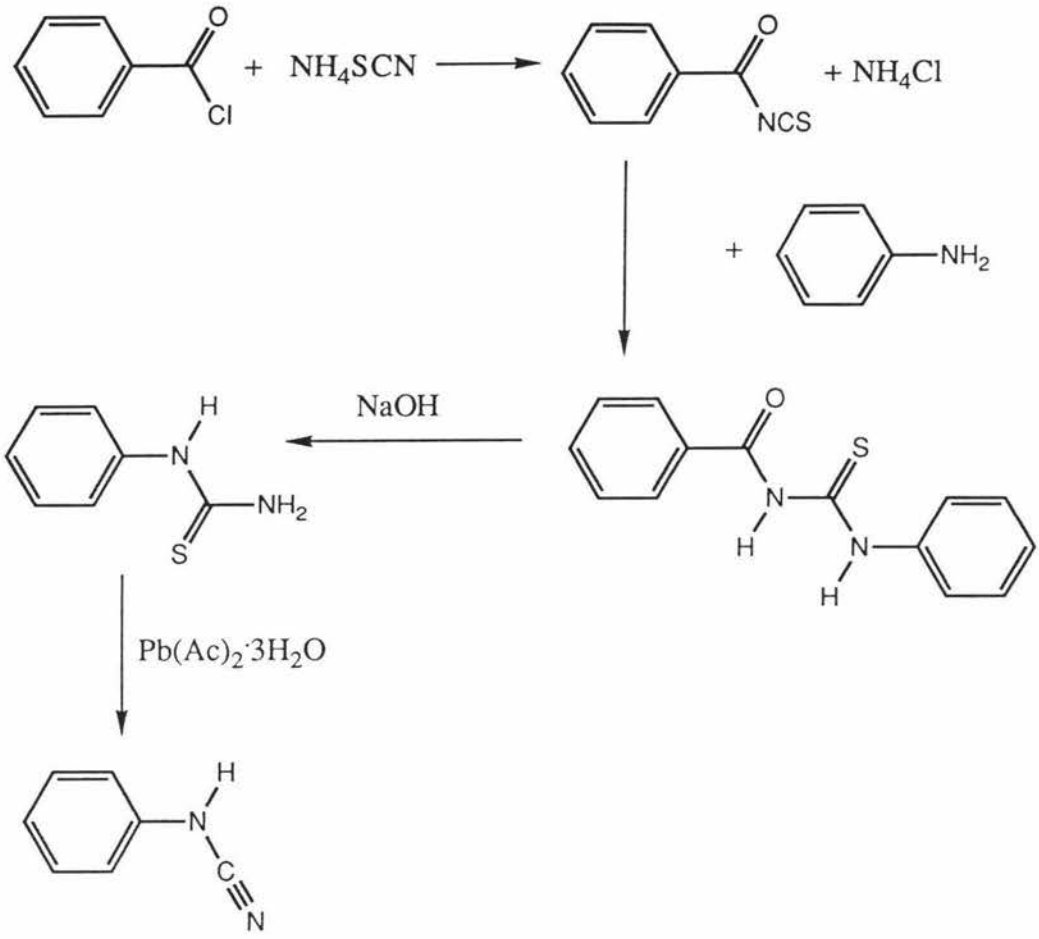

2.8.2.(b) The Synthesis of Phenylcyanamides Directly from the Corresponding Anilines

4-methoxyphenylcyanamide:

4-Anisidine (23.0g, 187 mmol) was dissolved in ethanol (50 cm^3) and water (50 cm^3) and placed in a 500 cm^3 three necked flask fitted with a thermometer, condenser and 100 cm^3 dropping funnel. Cyanogen bromide (10.6g, 100 mmol) in ethanol (50 cm^3) was added dropwise with constant stirring, under ice-water cooling. After the addition was complete, the mixture was stirred for half an hour and then added to 500 cm^3 of water. The precipitate obtained was dissolved in chloroform, filtered to remove any insoluble material, and the resulting solution dried over magnesium sulphate.

Pentane was added to the dry chloroform solution until crystallisation just occured. The light purple crystals were isolated by vacuum filtration (5.3g, 36%, m.p =74-77°).

This method was also used to prepare 2- chloro- and 4-chlorophenylcyanamide, which were recrystallised from benzene-light petroleum. The overall equation for the synthesis of 4-methoxyphenylcyanamide is given below:

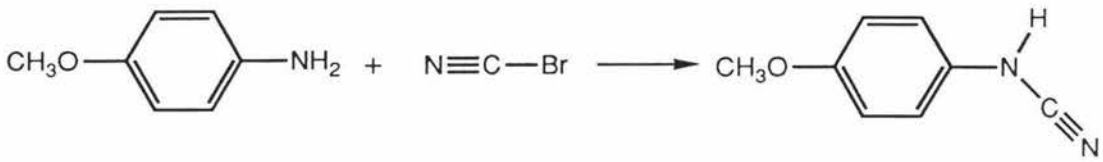

2.8.3 The Preparation of 1,4-Dicyanamidobenzene

The method employed was CNBr treatment of the appropriate amine as used above and in the preparation of 1,3-phenylenedicyanamide[41]:

1,4-phenylenediamine (4.0g, 37 mmol) was dissolved in aqueous ethanol (40 cm^3, 1:1) and placed in a 250 cm^3 three necked flask fitted with a condensor, thermometer and a 100 cm^3 dropping funnel. To this solution was slowly added, in a dropwise manner, cyanogen bromide (8.5g, 80 mmol) in ethanol (40 cm^3), keeping the mixture at a temperature of less than ten degrees. After stirring for 1.5 hours a light purple precipitate was filtered under reduced pressure and washed with small amounts of aqueous ethanol and dried *in- vacuo*.

2.8.4 The Preparation of Ag(I) Phenylcyanamido Salts

Salts of the formulation Ag[pcyd] were prepared according to the method of Hollebone[15] by mixing methanolic solutions of silver perchlorate and the neutral ligand in a 1:1 ratio to produce flocculent white precipitates.

2.8.5 The Preparation of the Complexes [Ag(Ph_3P)$_3$(pcyd)]

Triphenylphosphine (3 mmol) in dichloromethane (30 cm^3) was added to a suspension of the silver phenylcyanamido salt (1 mmol) in dichloromethane (20 cm^3) and left to stir until the suspension had dissolved. The volume of the solution was halved by rotary evaporation and hexane added until precipitation occured. The solid was collected by filtration under reduced pressure, washed with ethanol and dried *in-vacuo*.

(Yields: {Ag(Ph_3P)$_3$(4-Brpcyd)], 25% (white); [Ag(Ph_3P)$_3$(4-Clpcyd)], 38% (white); [Ag(Ph_3P)$_3$(4-NO_2pcyd)], 65% (yellow); [Ag(Ph_3P)$_3$(4-MeOpcyd)],73% (light purple); [Ag(Ph_3P)$_3$(2-Clpcyd)], 69% (white); and [Ag(Ph_3P)$_3$(2-Mepcyd)], 26% (white))

2.8.6 The Preparation of [Ag(dppm)(4-Brpcyd)]

To a suspension of Ag[4-Brpcyd] (0.388g, 1.3 mmol) in hot acetonitrile (20 cm^3)was added a solution of dppm (0.494g, 1.3 mmol) in hot acetonitrile (20 cm^3) and the mixture was refluxed. After ten minutes refluxing the Ag[4-Brpcyd] had dissolved and within twenty minutes a cream-coloured solid had precipitated. The solid was isolated by vacuum filtration, washed with ethanol and dried *in-vacuo*. (Yield = 89%)

2.8.7 The Preparation of [Ag(Me_2phen)(2-Clpcyd)]

2,9-dimethyl-1,10-phenanthroline (0.108g, 0.52 mmol) in dichloromethane (10 cm^3) was added to a suspension of Ag[2-Clpcyd] (0.134g, 0.52 mmol) in dichloromethane (10 cm^3) to form a colourless solution. The solution was stirred for several minutes in which a cream precipitate appeared, which was filtered under reduced pressure, washed with ethanol and dried *in-vacuo*. (Yield = 48%)

2.8.8 The Reaction of Ag(4-Brpcyd) with Ph_3P in a 1:1.5 Ratio

To a solution of Ph_3P (0.787g, 3 mmol) in toluene (20 cm^3) was added Ag[4-Brpcyd] (0.608g, 2 mmol) and the mixture stirred at room temperature for 30 minutes and then at 50°C for 1 hour. The solution was filtered and warm n-butanol (25 cm^3) added to the filtrate. Upon standing for three days colourless crystal were observed and isolated by filtration. Two types of crystals were detected of which one type was characterised as the tris-triphenylphosphine complex [$Ag(Ph_3P)_3$(4-Brpcyd)]. The second crystal form was thin elongated needles which melted at 99-101 °C and were not characterised.

2.9 X-Ray Crystallography

Four single crystal X-ray crystallographic structures were determined in this work. As the general procedure for the data collection was similar in all four cases a more detailed account is given only for the first structure. Tables summarising the crystal and data collection parameters for all the structures are given in their corresponding experimental sections.

2.10 The Crystal Structure Determination of [(4-bromophenylcyanamido-κN) tris(triphenylphosphine-κP) silver(I)], [$Ag(Ph_3P)_3$(4-Brpcyd)].

2.10.1 Crystal Preparation

Transparent parallelepiped crystals of the complex were obtained by slow evaporation of a toluene solution to which warm n-butanol had been added. The crystal selected for X-ray diffraction had the approximate dimensions of 0.24 x 0.28 x 0.48mm, extinguished plane polarised light, and appeared to be single. The crystal was attached to a glass fibre using "Araldite" adhesive and mounted on a goniometer head.

2.10.2 Unit Cell Parameters

Seventeen low angle reflections ($6.2 < \theta < 6.9°$) were located using the automatic "search" routine. Three areas of reciprocal space ($\chi = 20°, 0°, -20°$) were searched to obtain these reflections, so as to avoid coplanarity. An orientation matrix was calculated and preliminary unit cell parameters were obtained by least-squares refinement of the setting angles for the seventeen reflections. A thin shell of data was collected ($17° < \theta < 18°$) from which twenty four moderately strong reflections were chosen, to replace the seventeen low angle reflections, and which fulfilled the following criteria:

(i) wide range of ϕ values covering 360°

(ii) χ values distributed within the range ±40°

(iii) selection of high values for *h*, *k*, and *l*

(iv) relatively intense diffracted beams

Accurate setting angles were obtained for these reflections, from which refined unit cell parameters were calculated by least-squares refinement of the setting angles. The diffraction symmetry was characteristic of the triclinic class. The refined cell dimensions were:

$a = 9.927(2)$Å $\quad b = 13.755(2)$Å $\quad c = 20.256(2)$Å

$\alpha = 102.67(1)°$ $\quad \beta = 94.61(1)°$ $\quad \gamma = 106.32(1)°$

Cell volume = 2559.48Å^3

2.10.3 Data Collection

Data were collected at room temperature on a Enraf-Nonius CAD-4 diffractometer using non-monochromated molybdenum radiation. For very intense reflections, a Zr attenuator was automatically inserted during the data collection. The attenuation factor was previously determined as 12.34. Data were collected using the $\omega/2\theta$ scan technique where the ω scan angle is given by:

$$\omega = DOMA + DOMB*\tan\theta°$$

DOMA is dependent on the crystal mosaic spread and divergence of the primary beam. The term DOMB*tanθ compensates for reflection widening at high theta angles due to $\alpha1/\alpha2$ splitting. For Mo radiation, DOMB = 0.344. Background measurements were made by automatically extending each scan by 25% at each side of the peak. The height of the detector aperture was fixed at 4mm. The width of the horizontal aperture (APT) was varied automatically according to the relationship:

$$APT = APTA + APTB*\tan\theta \text{ mm}$$

DOMA and APTA were determined experimentally by inspection of some typical reflection profiles.

Each scan consisted of a ninety-six step intensity profile which is divided into background and intensity measurements as follows:

Left background	BGL	Steps 1-16
Intensity	INT	Steps 17-80
Right background	BGR	Steps 81-96

A "prescan" of each reflection using a fixed scan speed of $16.48/NPI_{pre}°min^{-1}$, gave an initial net intensity I§. If the $\sigma(I)§/I$ of this prescan measurement ($SIGMA_{pre}$) was greater than a specified acceptance parameter (SIG_{pre}), then the reflection was considered to be unobserved and no further measurement was made.

---

§ $I = INT - 2*(BGL+BGR)$

$\sigma(I) = (INT+4*(BGL+BGR))^{1/2}$

For observed data, if the relative $\sigma(I)/(I)$ value of the prescan was less than or equal to a specified value of $\sigma(I)/(I)$ (SIGMA), then the data were of acceptable quality and no further measurements were made. A second scan was undertaken for those observed data with a relative $\sigma(I)/(I)$ for the prescan greater than the specified value of $\sigma(I)/(I)$. The final scan speed parameter (NPI) was then calculated to produce data of acceptable quality, based on the prescan measurement, the required $\sigma(I)/(I)$ value, and the maximum allowable time to be spent on each reflection (IT_{max}). First the maximum allowable scan speed parameter (NPI_{max}) was calculated from the maximum allowable time and the ω scan angle as:

$$NPI_{max} = \frac{IT_{max}}{3*\omega}$$

Then NPI, the scan speed parameter for the final scan was calculated as :

$$NPI = NPI_{pre}*\left[\frac{SIGMA_{pre}}{SIGMA}\right]^2$$

If the value for NPI was greater than NPI_{max}, then NPI was reset to NPI_{max} with the final scan being measured at a scan speed of $16.48/NPI°min^{-1}$.

During the course of the data collection, the intensities of three standard reflections were measured every 7200 seconds of X-ray exposure time. These reflections were measured to a required $\sigma(I)/I$ of 0.012. This allowed corrections to be applied for any crystal decomposition which may have occured during data processing.

The orientation of the crystal was checked by monitoring the same three standard reflections after every one hundred measurements had been made. Deviations of greater than 0.1° between the observed and calculated positions of the 3 diffracted beams were considered unacceptable. When this occured, the setting angles of the twenty four reflections used to calculate accurate cell dimensions were remeasured, and the orientation matrix adjusted accordingly.

2.10.4 Data Processing

A total of 9496 reflections was measured for the *h*, *k*, *l* range 0 -->12, -16 --> 16, -25 --> 25, to a maximum of $\theta = 22°$.

The unit cell volume indicated two molecules per unit cell which suggests space group $P\bar{1}$ rather than P1. Subsequent successful refinement confirmed this space group.

The raw intensities of the diffracted beams, I_{raw}, were calculated from the expression:

$$I_{raw} = \frac{20.1166*ATN}{NPI} *[INT-2*(BGL+BGR)]$$

Observed structure factor amplitudes, F_{obs}, were calculated from the raw intensities after correction for Lorentz and polarisation effects as given by:

$$F_{obs} = \frac{I_{raw}}{Lp}$$

where Lp is the Lorentz-polarisation factor

The standard deviations of the square of the observed structure factor amplitudes, $\sigma(F_{obs})$, being calculated from $\sigma(F_{obs}^2)$ and F_{obs} by:

$$\sigma(F_{obs}) = \sqrt{F_{obs}^2+\sigma(F_{obs}^2)} - Fobs$$

The crystal was exposed to the X-ray beam for a total of 57.9 hours, with an average loss of intensity for the three standard reflections measured of 0.1%, in that time.

Empirical absorption corrections were applied, by the selection of four suitably strong reflections, with χ values > 85.2°. The intensities of these reflections were measured accurately in steps of 10° over the ϕ range 0 to 360°. The maximum intensity for each curve was considered to be 100% transmission, with transmission factors for the other points calculated relative to this maximum, then averaged for all curves. Corrections were applied to the observed structure factors using these averaged transmission values and the orientation matrix for the crystal. Minimum and maximum transmission values were 85.7 and 100%, with the minimum and maximum absorption corrections applied being 0.926 and 1.000 respectively.

8931 unique data were measured with 761 equivalent reflections being averaged, 369 reflections considered unobserved, to give an agreement factor for observed data based on intensity of 0.022.

2.10.5 Structure Solution and Refinement

Inspection of a Patterson map suggested a possible Ag site at (x,y,z) = (0.2871,0.1436,0.2686) [from the Patterson vector (0.5742,0.2871,0.5371) correponding to 2x,2y,2z]. A structure factor calculation based on this position gave a residual, R, of 0.42, where:

$$R = \frac{\Sigma \, | \, |F_{obs}| - |F_{calc}| \, |}{\Sigma \, |F_{obs}|}$$

Calculation of an electron density map, based on the phasing contribution of the Ag atom, revealed the positions of the three phosphorus atoms. A series of electron density maps and least-squares calculations revealed all non-hydrogen atom positions and gave a residual of 0.22. In susequent refinement, all phenyl rings were refined as rigid groups (C-C = 1.395Å). Hydrogen atoms were placed in calculated positions (C-H = 0.96Å) and were constrained to ride on their associated carbon atoms. The isotropic thermal parameters of the hydrogen atoms in individual phenyl rings were constrained to be equal and refined as such. Anisotropic thermal motion was assumed for all non-hydrogen atoms in the final stages of refinement.

For the 493 parameters and 5614 observed reflections, for which $F_{obs}^2 > 3\sigma(F_{obs}^2)$, the final full-matrix least- squares refinement cycle converged to values of R = 0.035 and $R_w = 0.040$ respectively, where:

$$Rw = \frac{\Sigma\sqrt{w} \, | \, |F_{obs}| - |F_{calc}| \, |}{\Sigma\sqrt{w} \, |F_{obs}|}$$

The function minimised was $\Sigma \, w(|F_{obs}| - |F_{calc}|)^2$ with the weight, w, being defined as:

$$w = \frac{1.0000}{(\sigma^2(F_{obs}) + 0.030229 * F_{obs}^2)}$$

In the final cycle of the full-matrix least-squares refinemnt, the ratio of maximum least-squares parameter shift per estimated standard deviation, $\Delta\sigma^{-1}$, was 0.05. A final difference electron density map showed the largest peak to be 0.35 eÅ^3, with the deepest trough being -0.65 eÅ^3. Data reduction and structure solution were performed with the SDP-PLUS[42] software package operating on a DEC PDP11/73. Structure refinement calculations were performed on a DEC VAX3300 using the program SHELX-76[43]. Atomic scattering factors and anomalous dispersion coefficients were from Cromer and Mann(1968)[44] and Cromer and Libermann(1970)[45] respectively.

All crystal data and parameters associated with the data collection are summarised in Table 2.12, those associated with data processing in Table 2.13. Parameters associated with structure solution and refinement are summarised in Table 2.14. Atomic coordinates for all non-hydrogen atoms are given in Table 2.15 (for the atomic numbering scheme refer to figure 2..3.1, page18). Anisotropic thermal parameters are listed in Table 2.16. Table 2.17 lists hydrogen atom coordinates and isotropic thermal parameters. Observed and calculated structure factors are presented on microfiche at the end of this thesis.

Table 2.12 Data Collection Parameter Summary For [Ag(PPh3)3(4-Brpcyd)]

Compound	[Ag(PPh$_3$)$_3$(4-Br pcyd)]
Formula	$AgBrP_3N_2C_{61}H_{49}$
Formula weight (a.m.u)	1090.80
Crystal size (mm)	0.24 x 0.28 x 0.48
Space group	$P\bar{1}$
a (Å)	9.927(2)
b (Å)	13.755(2)
c (Å)	20.256(2)
α (°)	102.67(1)
β (°)	94.61(1)
γ (°)	106.32(1)
V (Å^3)	2559.5
Z	2
λ (Mo-Kα) (Å)	0.71073
μ (Mo-Kα) (cm^{-1})	13.49
F(000)	1110
Number and θ range (°) of reflections used for determining lattice parameters	24,16.97 - 17.90
Temperature of measurement (°K)	290
Scan mode	$\omega/2\theta$
ω scan angle (°)	1.00 + 0.34*tanθ
Detector horizontal aperture width (mm)	1.50 + 1.00*tanθ
Detector vertical aperture width (mm)	4
Incident beam collimator diameter (mm)	0.8
Prescan scan speed (° min^{-1})	8.24
Prescan acceptance σ(I)/(I)	0.5
Requested counting σ(I)/(I)	0.015
Maximum scan time (sec)	60
Maximum value of θ reached in intensity measurement (°)	22
Range of *h*, *k* and *l*	0 ->12, -16 -> 16, -25 -> 25
Standard reflections used to monitor intensity variation	3 9 -4, 6 -2 11, -4 -1 16
Requested σ(I)/(I) for standard intensity measurements	0.012
Interval between standard intensity measurements (sec)	7200
Maximum permissable deviation between observed and calculated positions of standard orientation reflections (°)	0.10

Table 2.13 Data Processing Parameter Summary For [$Ag(Ph_3P)_3$(4-Brpcyd)]

Total number of reflections measured	9496
Number of reflections considered unobserved from prescan data	369
Total x-ray exposure time (hrs)	57.9
Average standard intensity variation (%)	-0.1
Method used for absorption correction	Empirical
Minimum transmission value (%)	85.7
Maximum transmission value (%)	99.9
Minimum absorption correction	0.926
Maximum absorption correction	1.000
Number of unique reflections measured	8931
Number of equivalent reflections averaged	761
Value of merging R, based on intensity of observed reflections	0.022

Table 2.14 Structure Solution and Refinement Parameter Summary For [Ag(Ph3P)3(4-Brpcyd)]

Method used to solve structure	Patterson
Criterion for recognising unobserved reflections during refinement	$F_{obs}^2 > 3\sigma(Fobs^2)$
Number of reflections used in refinement	5614
Method of locating Hydrogen atoms (C-H = 0.96Å)	Calculated positions
Weighting scheme§;k,g	1.0000, 0.030229
Parameters refined	493
Value of R	0.035
Value of R_w	0.040
Maximum and minimum height in final difference electron density map ($eÅ^{-3}$)	0.35, -0.65
Computer programs used	SHELX-76,SDP-PLUS package

§ weight = $k/\sigma^2(Fobs) + g*(Fobs^2)$

Table 2.15 Fractional Atomic Coordinates for the Non-Hydrogen Atoms of [Ag(Ph$_3$P)$_3$(4-Brpcyd)] (estimated standard deviations in parentheses)

Atom	x/a	y/b	z/c
Ag	0.2900(0)	0.1476(0)	0.2681(0)
P(1)	0.3617(1)	0.0715(1)	0.1551(0)
P(2)	0.3378(1)	0.3448(1)	0.2809(1)
P(3)	0.3776(1)	0.0929(1)	0.3726(1)
Br	-0.3359(1)	-0.5220(1)	0.0701(0)
N(1)	0.0539(4)	0.0594(4)	0.2592(3)
N(2)	-0.1691(4)	-0.0776(4)	0.2502(3)
C(1)	-0.0473(5)	-0.0094(4)	0.2537(3)
C(2)	-0.2009(3)	-0.1795(2)	0.2079(2)
C(3)	-0.0993(3)	-0.2221(2)	0.1806(2)
C(4)	-0.1407(3)	-0.3242(2)	0.1392(2)
C(5)	-0.2838(3)	-0.3835(2)	0.1250(2)
C(6)	-0.3854(3)	-0.3409(2)	0.1522(2)
C(7)	-0.3440(3)	-0.2389(2)	0.1937(2)
C(111)	0.3140(3)	-0.0707(1)	0.1222(1)
C(112)	0.2978(3)	-0.1172(1)	0.0523(1)
C(113)	0.2682(3)	-0.2254(1)	0.0293(1)
C(114)	0.2548(3)	-0.2871(1)	0.0761(1)
C(115)	0.2710(3)	-0.2406(1)	0.1459(1)
C(116)	0.3006(3)	-0.1324(1)	0.1690(1)
C(121)	0.5515(2)	0.1161(2)	0.1516(2)
C(122)	0.6338(2)	0.0483(2)	0.1436(2)
C(123)	0.7807(2)	0.0881(2)	0.1477(2)
C(124)	0.8454(2)	0.1958(2)	0.1599(2)
C(125)	0.7631(2)	0.2636(2)	0.1678(2)
C(126)	0.6162(2)	0.2237(2)	0.1637(2)
C(131)	0.2799(3)	0.1110(2)	0.0857(1)
C(132)	0.1380(3)	0.1063(2)	0.0874(1)
C(133)	0.0629(3)	0.1303(2)	0.0353(1)
C(134)	0.1297(3)	0.1592(2)	-0.0186
C(135)	0.2716(3)	0.1639(2)	-0.0203(1)
C(136)	0.3467(3)	0.1399(2)	0.0318(1)
C(211)	0.2603(3)	0.3936(2)	0.2140(1)
C(212)	0.1531(3)	0.4399(2)	0.2252(1)
C(213)	0.0893(3)	0.4695(2)	0.1723(1)
C(214)	0.1328(3)	0.4530(2)	0.1081(1)
C(215)	0.2401(3)	0.4067(2)	0.0968(1)
C(216)	0.3038(3)	0.3770(2)	0.1498(1)
C(221)	0.5287(2)	0.4126(2)	0.2917(1)
C(222)	0.5866(2)	0.5036(2)	0.2706(1)
C(223)	0.7332(2)	0.5516(2)	0.2827(1)
C(224)	0.8220(2)	0.5086(2)	0.3158(1)
C(225)	0.7641(2)	0.4176(2)	0.3368(1)
C(226)	0.6174(2)	0.3697(2)	0.3248(1)
C(231)	0.2856(3)	0.4129(2)	0.3577(1)
C(232)	0.3697(3)	0.5110(2)	0.3974(1)

(Table continued over page)

C(233)	0.3227(3)	0.5610(2)	0.4545(1)
C(234)	0.1916(3)	0.5131(2)	0.4718(1)
C(235)	0.1074(3)	0.4150(2)	0.4321(1)
C(236)	0.1544(3)	0.3650(2)	0.3750(1)
C(311)	0.3252(3)	-0.0499(2)	0.3584(2)
C(312)	0.1805(3)	-0.1046(2)	0.3428(2)
C(313)	0.1347(3)	-0.2136(2)	0.3288(2)
C(314)	0.2337(3)	-0.2680(2)	0.3303(2)
C(315)	0.3785(3)	-0.2134(2)	0.3460(2)
C(316)	0.4243(3)	-0.1043(2)	0.3600(1)
C(321)	0.3155(3)	0.1363(2)	0.4532(1)
C(322)	0.2693(3)	0.0698(2)	0.4953(1)
C(323)	0.2251(3)	0.1075(2)	0.5568(1)
C(324)	0.2270(3)	0.2117(2)	0.5762(1)
C(325)	0.2732(3)	0.2782(2)	0.5341(1)
C(326)	0.3175(3)	0.2405(2)	0.4726(1)
C(331)	0.5701(2)	0.1307(2)	0.3953(1)
C(332)	0.6393(2)	0.1616(2)	0.4627(1)
C(333)	0.7862(2)	0.1832(2)	0.4759(1)
C(334)	0.8640(2)	0.1740(2)	0.4218(1)
C(335)	0.7974(2)	0.1431(2)	0.3544(1)
C(336)	0.6479(2)	0.1215(2)	0.3412(1)

Table 2.16 Anisotropic Thermal Parameters for the Non-Hydrogen Atoms of [Ag(Ph$_3$P)$_3$(4-Brpcyd)] (estimated standard deviations in parentheses)

Atom	U11	U22	U33	U23	U13	U12
Ag	0.0415(2)	0.0351(2)	0.0372(2)	0.0087(1)	0.0086(1)	0.0095(1)
P(1)	0.0396(5)	0.0408(6)	0.0338(5)	0.0061(4)	0.0079(4)	0.0134(4)
P(2)	0.0462(6)	0.0290(5)	0.0451(6)	0.0089(4)	0.0098(4)	0.0107(4)
P(3)	0.0515(6)	0.0380(5)	0.0374(5)	0.0121(4)	0.0058(4)	0.0127(5)
Br	0.1513(7)	0.0716(4)	0.0880(5)	0.0090(4)	0.0280(5)	0.0253(4)
N(1)	0.042(2)	0.066(3)	0.099(4)	0.028(3)	0.013(2)	0.007(2)
N(2)	0.053(2)	0.060(3)	0.117(4)	0.019(3)	0.029(3)	0.006(2)
C(1)	0.049(3)	0.064(3)	0.085(4)	0.028(3)	0.016(2)	0.019(3)
C(2)	0.059(3)	0.061(3)	0.075(3)	0.031(3)	0.020(2)	0.019(2)
C(3)	0.057(3)	0.072(3)	0.071(3)	0.032(3)	0.018(2)	0.025(3)
C(4)	0.090(4)	0.076(3)	0.068(3)	0.034(3)	0.030(3)	0.043(3)
C(5)	0.096(4)	0.053(3)	0.062(3)	0.022(3)	0.015(3)	0.018(3)
C(6)	0.063(3)	0.054(3)	0.081(4)	0.026(3)	0.016(3)	0.002(2)
C(7)	0.050(3)	0.059(3)	0.094(4)	0.027(3)	0.021(3)	0.011(2)
C(111)	0.044(2)	0.039(2)	0.041(2)	0.007(2)	0.010(2)	0.014(2)
C(112)	0.076(3)	0.054(3)	0.044(3)	0.011(2)	0.009(2)	0.028(2)
C(113)	0.100(4)	0.050(3)	0.052(3)	-0.003(2)	0.015(3)	0.017(3)
C(114)	0.088(4)	0.034(2)	0.088(4)	0.008(3)	0.022(3)	0.016(2)
C(115)	0.100(4)	0.046(3)	0.072(3)	0.025(3)	0.026(3)	0.020(3)
C(116)	0.074(3)	0.059(3)	0.043(2)	0.011(2)	0.014(2)	0.020(2)
C(121)	0.046(2)	0.050(2)	0.033(2)	0.004(2)	0.008(2)	0.016(2)
C(122)	0.047(2)	0.054(3)	0.071(3)	0.019(2)	0.011(2)	0.016(2)
C(123)	0.052(3)	0.077(4)	0.083(4)	0.020(3)	0.011(3)	0.030(3)
C(124)	0.042(2)	0.079(4)	0.074(4)	-0.002(3)	0.006(2)	0.006(2)
C(125)	0.061(3)	0.058(3)	0.079(4)	-0.005(3)	0.021(3)	0.002(2)
C(126)	0.048(3)	0.048(3)	0.085(4)	-0.001(2)	0.013(2)	0.009(2)
C(131)	0.062(2)	0.043(2)	0.037(2)	0.008(2)	0.006(2)	0.018(2)
C(132)	0.058(3)	0.065(3)	0.046(3)	0.016(2)	0.002(2)	0.023(2)
C(133)	0.074(3)	0.078(4)	0.064(3)	0.022(3)	-0.004(3)	0.025(3)
C(134)	0.102(5)	0.087(4)	0.060(3)	0.023(3)	-0.009(3)	0.040(4)
C(135)	0.108(5)	0.075(4)	0.047(3)	0.029(3)	0.024(3)	0.031(3)
C(136)	0.082(3)	0.071(3)	0.049(3)	0.020(3)	0.027(2)	0.035(3)
C(211)	0.056(2)	0.030(2)	0.049(2)	0.013(2)	0.001(2)	0.006(2)
C(212)	0.062(3)	0.063(3)	0.078(4)	0.027(3)	0.011(3)	0.025(3)
C(213)	0.078(4)	0.087(4)	0.117(6)	0.061(4)	0.002(4)	0.033(3)
C(214)	0.095(4)	0.058(3)	0.098(5)	0.043(3)	-0.023(4)	0.001(3)
C(215)	0.112(5)	0.059(3)	0.054(3)	0.021(3)	-0.002(3)	0.008(3)
C(216)	0.087(4)	0.051(3)	0.056(3)	0.014(2)	0.008(3)	0.025(3)
C(221)	0.053(2)	0.037(2)	0.039(2)	0.005(2)	0.010(2)	0.014(2)
C(222)	0.050(2)	0.047(3)	0.060(3)	0.018(2)	0.011(2)	0.003(2)
C(223)	0.062(3)	0.065(3)	0.058(3)	0.017(2)	0.013(2)	0.002(2)
C(224)	0.042(3)	0.084(4)	0.065(3)	0.007(3)	0.007(2)	-0.004(3)
C(225)	0.051(3)	0.078(4)	0.083(4)	0.017(3)	-0.002(3)	0.021(3)
C(226)	0.055(3)	0.057(3)	0.067(3)	0.020(2)	0.006(2)	0.014(2)
C(231)	0.053(2)	0.039(2)	0.049(2)	0.011(2)	0.011(2)	0.017(2)
C(232)	0.067(3)	0.053(3)	0.080(4)	-0.014(3)	0.029(3)	-0.001(2)

(Table continued over page)

C(233)	0.088(4)	0.070(4)	0.113(5)	-0.037(4)	0.028(4)	0.010(3)
C(234)	0.089(4)	0.088(4)	0.080(4)	-0.003(3)	0.036(3)	0.039(4)
C(235)	0.062(3)	0.092(4)	0.072(4)	0.019(3)	0.028(3)	0.033(3)
C(236)	0.051(3)	0.057(3)	0.061(3)	0.012(2)	0.017(2)	0.012(2)
C(311)	0.060(2)	0.040(2)	0.037(2)	0.012(2)	0.004(2)	0.010(2)
C(312)	0.060(3)	0.060(3)	0.059(3)	0.023(2)	0.003(2)	0.009(2)
C(313)	0.080(4)	0.051(3)	0.071(4)	0.021(3)	-0.006(3)	-0.013(3)
C(314)	0.109(5)	0.037(3)	0.065(3)	0.007(2)	0.002(3)	-0.001(3)
C(315)	0.111(5)	0.056(3)	0.075(4)	0.013(3)	0.012(3)	0.038(3)
C(316)	0.069(3)	0.040(2)	0.061(3)	0.012(2)	0.006(2)	0.015(2)
C(321)	0.052(2)	0.041(2)	0.037(2)	0.010(2)	0.006(2)	0.014(2)
C(322)	0.103(4)	0.062(3)	0.053(3)	0.022(2)	0.037(3)	0.032(3)
C(323)	0.108(5)	0.085(4)	0.062(3)	0.023(3)	0.043(3)	0.030(4)
C(324)	0.087(4)	0.083(4)	0.064(3)	0.004(3)	0.029(3)	0.034(3)
C(325)	0.091(4)	0.061(3)	0.076(4)	0.003(3)	0.020(3)	0.034(3)
C(326)	0.072(3)	0.054(3)	0.060(3)	0.013(2)	0.009(2)	0.023(2)
C(331)	0.052(2)	0.034(2)	0.042(2)	0.013(2)	0.012(2)	0.013(2)
C(332)	0.060(3)	0.046(2)	0.042(2)	0.014(2)	0.002(2)	0.009(2)
C(333)	0.067(3)	0.062(3)	0.063(3)	0.016(3)	-0.013(3)	0.009(3)
C(334)	0.049(3)	0.063(3)	0.092(4)	0.027(3)	0.004(3)	0.012(2)
C(335)	0.059(3)	0.062(3)	0.07(3)	0.016(3)	0.022(3)	0.019(2)
C(336)	0.072(3)	0.062(3)	0.047(3)	0.012(2)	0.014(2)	0.021(2)

Table 2.17 Hydrogen Atom Coordinates and Isotropic Thermal Parameters for [Ag(Ph_3P)$_3$(4-Brpcyd)]

Atom	x/a	y/b	z/c	U
H(3)	-.0008	-0.1812	0.1904	0.05
H(4)	-0.0708	-0.3535	0.1205	0.05
H(6)	-0.4839	-0.3818	0.1424	0.05
H(7)	-0.4139	-0.2096	0.2124	0.05
H(112)	0.3067	-0.0748	0.0201	0.06
H(113)	0.2567	-0.2574	-0.0189	0.06
H(114)	0.2344	-0.3615	0.0601	0.06
H(115)	0.2621	-0.2830	0.1781	0.06
H(116)	0.3121	-0.1004	0.2171	0.06
H(122)	0.5893	-0.0258	0.1353	0.06
H(123)	0.8374	0.0416	0.1423	0.06
H(124)	0.9465	0.2233	0.1627	0.06
H(125)	0.8076	0.3377	0.1761	0.06
H(126)	0.5595	0.2704	0.1691	0.06
H(132)	0.0922	0.0866	0.1246	0.07
H(133)	-0.0346	0.1275	0.0367	0.07
H(134)	0.0780	0.1761	-0.0543	0.07
H(135)	0.3174	0.1839	-0.0574	0.07
H(136)	0.4442	0.1430	0.0305	0.07
H(212)	0.3042	0.3732	0.2505	0.06
H(213)	0.0156	0.5014	0.1800	0.06
H(214)	0.0890	0.4733	0.0716	0.06
H(215)	0.2700	0.3952	0.0526	0.06
H(216)	0.3776	0.3451	0.1420	0.06
H(222)	0.5254	0.5331	0.2478	0.06
H(223)	0.7729	0.6142	0.2682	0.06
H(224)	0.9228	0.5418	0.3240	0.06
H(225)	0.8253	0.3883	0.3596	0.06
H(226)	0.5777	0.3071	0.3392	0.06
H(232)	0.4600	0.5440	0.3855	0.06
H(233)	0.3807	0.6285	0.4818	0.06
H(234)	0.1593	0.5475	0.5111	0.06
H(235)	0.0173	0.3820	0.4441	0.06
H(236)	0.0966	0.2975	0.3477	0.06
H(312)	0.1124	-0.0671	0.3416	0.07
H(313)	0.0350	-0.2512	0.3178	0.07
H(314)	0.2021	-0.3431	0.3205	0.07
H(315)	0.4466	-0.2509	0.3471	0.07
H(316)	0.5239	-0.668	0.3708	0.07
H(322)	0.2683	-0.0019	0.4821	0.06
H(323)	0.1933	0.0617	0.5859	0.06
H(324)	0.1961	0.2376	0.6184	0.06
H(325)	0.2738	0.3498	0.5472	0.06
H(326)	0.3489	0.2862	0.4435	0.06
H(332)	0.5858	0.1678	0.5000	0.06
H(333)	0.8338	0.2041	0.5223	0.06
H(334)	0.9651	0.1885	0.4308	0.06
H(335)	0.8483	0.1366	0.3171	0.06
H(336)	0.6003	0.1003	0.2948	0.06

2.11 The Crystal Structure Determination of [(4-methoxyphenylcyanamido-κN) tris(triphenylphosphine-κP)silver(I)], [$Ag(Ph_3P)_3$(4-MeOpcyd)]

2.11.1 Crystal Preparation and Data Collection

The crystal was grown by slow evaporation of a dichloromethane solution to which warm n-butanol had been added.

Data were collected using the general method described in section 2.10.3. All crystal data and parameters associated with data collection are summarised in Table 2.18.

2.11.2 Data Processing and Structure solution

Data were processed as described in section 2.10.4.

A possible Ag site at (x,y,z) = (0.2217,0.3076,0.2979) corresponding to the Patterson vector (0.4434,0.6152,0.5957) was identified from the Patterson map and a structure factor calculation based on this position gave a residual, R, of 0.39.

Calculation of an electron density map, based on the phasing contribution of the silver atom, revealed the positions of the three phosphorus atoms. A series of electron density maps and full-matrix least-squares calculations revealed all non-hydrogen atom positions and gave a residual of 0.14.

In subsequent refinement, all phenyl rings were refined as rigid groups (C-C = 1.395Å). Hydrogen atoms were placed in calculated positions (C-H = 0.96Å) and were constrained to ride on their associated carbon atoms.The isotropic thermal parametersof the hydrogen atoms in individual phenyl rings were constrained to be equal and refined as such. Anisotropic thermal motion was assumed for all non-hydrogen atoms in the final stages of refinement. Final R-factors of R = 0.050 and R_w = 0.052 were obtained. Parameters associated with data processing and with structure solution and refinement are summarised in Tables 2.19 and 2.20 respectively. Atomic coordinates for all non-hydrogen atoms are given in Table 2.21 (for the atomic numbering scheme refer to

figure 2.4.1). Anisotropic thermal parameters are listed in Table 2.22. Table 2.23 lists hydrogen atom coordinates and isotropic thermal parameters. Observed and calculated structure factors are given on microfiche at the end of this thesis.

Table 2.18 Data Collection Parameter Summary For [Ag(PPh3)3(4-MeO pcyd)]

Compound	[Ag(PPh3)3(4-MeO pcyd)]
Formula	$AgP_3N_2OC_{62}H_{52}$
Formula weight (a.m.u)	1041.92
Crystal size (mm)	0.20x 0.22 x 0.40
Space group	P $\bar{1}$
a (Å)	13.7557(4)
b (Å)	14.1164(2)
c (Å)	14.1980(3)
α (°)	87.87(2)
β (°)	103.68(2)
γ (°)	101.87(2)
V (Å^3)	2621.3
Z	2
λ (Mo-Kα) (Å)	0.71073
μ (Mo-Kα) (cm^{-1})	5.12
F(000)	1074
Number and θ range (°) of reflections used for determining lattice parameters	23,13.00 - 15.00
Temperature of measurement (°K)	290
Scan mode	ω/2θ
ω scan angle (°)	0.80 + 0.34*tanθ
Detector horizontal aperture width (mm)	1.20 + 0.80*tanθ
Detector vertical aperture width (mm)	4
Incident beam collimator diameter (mm)	0.8
Prescan scan speed (° min^{-1})	8.24
Prescan acceptance σ(I)/(I)	0.5
Requested counting σ(I)/(I)	0.022
Maximum scan time (sec)	60
Maximum value of θ reached in intensity measurement (°)	25
Range of *h*, *k* and *l*	0 ->18, -18 -> 18, -18 -> 18
Standard reflections used to monitor intensity variation	4 3 -8, 8 0 2, -2 9 -1
Requested σ(I)/(I) for standard intensity measurements	0.018
Interval between standard intensity measurements (sec)	7200
Maximum permissable deviation between observed and calculated positions of standard orientation reflections (°)	0.10

Table 2.19 Data Processing Parameter Summary For [Ag(Ph3P)3(4-MeOpcyd)]

Total number of reflections measured	9704
Number of reflections considered unobserved from prescan data	587
Total x-ray exposure time (hrs)	118.0
Average standard intensity variation (%)	-1.6
Correction applied for intensity decay of standard reflections	Anisotropic
Method used for absorption correction	Empirical
Minimum transmission value (%)	93.7
Maximum transmission value (%)	99.9
Minimum absorption correction	0.968
Maximum absorption correction	1.000
Number of unique reflections measured	9194
Number of equivalent reflections averaged	433
Value of merging R, based on intensity of observed reflections	0.027

Table 2.20 Structure Solution and Refinement Parameter Summary For [Ag(Ph3P)3(4-MeOpcyd)]

Method used to solve structure	Patterson
Criterion for recognising unobserved reflections during refinement	$F_{obs}^2 > 3\sigma(Fobs^2)$
Number of reflections used in refinement	3767
Method of locating Hydrogen atoms	Calculated positions
Weighting scheme§;k,g	1.0000, 0.002222
Parameters refined	254
Value of R	0.050
Value of R_w	0.052
Maximum and minimum height in final difference electron density map (eÅ-3)	0.62, -0.65
Computer programs used	SHELX-76,SDP-PLUS package

§ weight = $k/\sigma^2(Fobs) + g^*(Fobs^2)$

Table 2.21 Fractional Atomic Coordinates for the Non-Hydrogen Atoms of[Ag(Ph_3P)$_3$(4-MeOpcyd)] (estimated standard deviations in parentheses)

Atom	x/a	y/b	z/c
Ag	0.2292(0)	0.3123(0)	0.2983(0)
P(1)	0.2308(2)	0.4824(1)	0.2358(1)
P(2)	0.1853(2)	0.2838(1)	0.4627(1)
P(3)	0.1370(2)	0.1753(1)	0.1743(1)
O(1)	0.5244(9)	-0.1213(8)	0.1676(8)
N(1)	0.5226(7)	0.2610(7)	0.2520(8)
N(2)	0.3983(6)	0.3030(6)	0.3277(6)
C(1)	0.4477(9)	0.2814(7)	0.2959(8)
C(2)	o.5226(6)	0.1611(4)	0.2393(5)
C(3)	0.4614(6)	0.0849(4)	0.2768(5)
C(4)	0.4604(6)	-0.0105(4)	0.2538(5)
C(5)	0.5206(6)	-0.0298(4)	0.1933(5)
C(6)	0.5818(6)	0.0463(4)	0.1588(5)
C(7)	0.5829(6)	0.1418(4)	0.1788(5)
C(8)	0.500(1)	-0.1955(9)	0.219(1)
C(111)	0.2864(4)	0.5128(4)	0.1313(3)
C(112)	0.3177(4)	0.6084(4)	0.1049(3)
C(113)	0.3655(4)	0.6282(4)	0.0280(3)
C(114)	0.3822(4)	0.5524(4)	-0.0255(3)
C(115)	0.3509(4)	0.4568(4)	0.0039(3)
C(116)	0.3030(4)	0.4370(4)	0.0808(3)
C(121)	0.3074(4)	0.5782(3)	0.3206(3)
C(122)	0.2725(4)	0.6610(3)	0.3362(3)
C(123)	0.3338(4)	0.7312(3)	0.4031(3)
C(124)	0.4301(4)	0.7187(3)	0.4544(3)
C(125)	0.4650(4)	0.6360(3)	0.4388(3)
C(126)	0.4037(4)	0.5657(3)	0.3719(3)
C(131)	0.1049(3)	0.5150(4)	0.2048(4)
C(132)	0.0686(3)	0.5648(4)	0.1215(4)
C(133)	-0.0284(3)	0.5867(4)	0.1044(4)
C(134)	-0.0891(3)	0.5588(4)	0.1706(4)
C(135)	-0.0528(3)	0.5091(4)	0.2540(4)
C(136)	0.0442(3)	0.4871(4)	0.2711(4)
C(211)	0.2535(4)	0.3658(3)	0.5635(3)
C(212)	0.2879(4)	0.3330(3)	0.6570(3)
C(213)	0.3428(4)	0.3988(3)	0.7309(3)
C(214)	0.3634(4)	0.4976(3)	0.7114(3)
C(215)	0.3290(4)	0.5305(3)	0.6180(3)
C(216)	0.2740(4)	0.4646(3)	0.5441(3)
C(221)	0.2066(5)	0.1669(4)	0.5112(5)
C(222)	0.2933(5)	0.1379(4)	0.4974(5)
C(223)	0.3185(5)	0.0522(4)	0.5384(5)
C(224)	0.2570(5)	-0.0044(4)	0.5932(5)
C(225)	0.1703(5)	0.0246(4)	0.6069(5)
C(226)	0.1451(5)	0.1102(4)	0.5659(5)
C(231)	0.0507(4)	0.2828(4)	0.4566(4)

(Table continued over page)

C(232)	-0.0197(4)	0.2421(4)	0.3732(4)
C(233)	-0.1228(4)	0.2449(4)	0.3602(4)
C(234)	-0.1556(4)	0.2884(4)	0.4304(4)
C(235)	-0.0852(4)	0.3290(4)	0.5137(4)
C(236)	0.0179(4)	0.3263(4)	0.5268(4)
C(311)	0.1354(4)	0.0505(3)	0.2152(4)
C(312)	0.1094(4)	0.0259(3)	0.3032(4)
C(313)	0.1023(4)	-0.0691(3)	0.3359(4)
C(314)	0.1219(4)	-0.1395(3)	0.2806(4)
C(315)	0.1482(4)	-0.1149(3)	0.1925(4)
C(316)	0.1549(4)	-0.0199(3)	0.1598(4)
C(321)	0.1830(4)	0.1791(4)	0.0631(3)
C(322)	0.2864(4)	0.1791(4)	0.0738(3)
C(323)	0.3262(4)	0.1795(4)	-0.0080(3)
C(324)	0.2625(4)	0.1799(4)	-0.1004(3)
C(325)	0.1591(4)	0.1799(4)	-0.1110(3)
C(326)	0.1193(4)	0.1795(4)	-0.0292(3)
C(331)	0.0012(3)	0.1759(4)	0.1300(4)
C(332)	-0.0276(3)	0.2656(4)	0.1188(4)
C(333)	-0.1299(3)	0.2705(4)	0.0827(4)
C(334)	-0.2035(3)	0.1857(4)	0.0578(4)
C(335)	-0.1748(3)	0.0960(4)	0.0689(4)
C(336)	-0.0724(3)	0.0911(4)	0.1051(4)

Table 2.22 Anisotropic Thermal Parameters for the Non-Hydrogen Atoms of[$Ag(Ph_3P)_3$(4-MeOpcyd)] (estimated standard deviations in parentheses)

Atom	U11	U22	U33	U23	U13	U12
Ag	0.0546(4)	0.0531(4)	0.0531(4)	-0.0043(3)	0.0184(3)	0.0182(3)
P(1)	0.054(1)	0.051(1)	0.051(1)	0.000(1)	0.018(1)	0.018(1)
P(2)	0.069(2)	0.055(1)	0.057(1)	0.002(1)	0.027(1)	0.015(1)
P(3)	0.060(1)	0.057(1)	0.056(1)	-0.014(1)	0.012(1)	0.015(1)
O(1)	0.28(1)	0.119(8)	0.22(1)	0.100(7)	0.162(9)	0.084(8)
N(1)	0.094(7)	0.090(7)	0.17(1)	-0.019(6)	0.067(7)	0.016(5)
N(2)	0.053(5)	0.098(6)	0.081(6)	-0.015(4)	0.014(4)	0.015(4)
C(1)	0.082(8)	0.064(7)	0.071(8)	-0.11(6)	-0.006(6)	0.011(6)
C(2)	0.074(7)	0.102(8)	0.092(7)	-0.006(6)	0.032(6)	0.028(6)
C(3)	0.100(8)	0.111(9)	0.097(8)	-0.006(7)	0.045(7)	0.035(7)
C(4)	0.14(1)	0.89(8)	0.128(9)	0.024(7)	0.081(8)	0.043(7)
C(5)	0.18(1)	0.091(8)	0.15(1)	0.016(7)	0.097(9)	0.072(8)
C(6)	0.21(1)	0.12(1)	0.20(1)	0.05(1)	0.16(1)	0.09(1)
C(7)	0.15(1)	0.12(1)	0.16(1)	0.031(8)	0.12(1)	0.049(9)
C(8)	0.18(1)	0.08(1)	0.25(2)	-0.02(1)	0.10(1)	-0.03(1)
C(111)	0.049(5)	0.085(6)	0.047(5)	-0.007(5)	0.013(4)	0.022(5)
C(112)	0.096(7)	0.094(8)	0.073(6)	0.031(5)	0.057(5)	0.045(6)
C(113)	0.098(8)	0.131(9)	0.097(8)	0.048(7)	0.048(7)	0.045(7)
C(114)	0.096(8)	0.17(1)	0.070(7)	0.008(9)	0.045(6)	0.026(9)
C(115)	0.12(1)	0.15(1)	0.098(9)	-0.055(8)	0.059(7)	0.008(9)
C(116)	0.103(8)	0.088(8)	0.080(7)	-0.026(6)	0.042(6)	0.009(6)
C(121)	0.056(5)	0.059(5)	0.045(5)	0.16(4)	0.019(4)	0.019(4)
C(122)	0.057(5)	0.060(5)	0.062(5)	-0.006(4)	0.015(4)	0.016(4)
C(123)	0.066(6)	0.065(6)	0.077(6)	-0.013(5)	0.018(5)	0.015(5)
C(124)	0.072(7)	0.074(7)	0.067(6)	-0.020(5)	0.006(5)	-0.009(5)
C(125)	0.054(6)	0.100(8)	0.072(6)	0.000(5)	-0.002(5)	0.011(6)
C(126)	0.065(6)	0.067(6)	0.071(6)	-0.008(5)	0.015(5)	0.019(5)
C(131)	0.047(4)	0.049(5)	0.054(4)	-0.006(4)	0.011(4)	0.015(4)
C(132)	0.059(6)	0.103(7)	0.081(7)	0.021(5)	0.020(5)	0.033(5)
C(133)	0.082(7)	0.132(9)	0.090(7)	0.028(7)	0.008(6)	0.060(7)
C(134)	0.063(6)	0.104(8)	0.12(1)	-0.008(7)	0.014(7)	0.041(6)
C(135)	0.067(6)	0.100(7)	0.094(7)	0.001(6)	0.037(5)	0.034(5)
C(136)	0.060(5)	0.075(6)	0.063(6)	0.007(5)	0.023(5)	0.018(5)
C(211)	0.073(6)	0.060(5)	0.052(5)	0.004(4)	0.032(4)	0.014(4)
C(212)	0.17(1)	0.066(6)	0.056(6)	0.006(5)	0.010(7)	0.010(7)
C(213)	0.23(1)	0.077(7)	0.039(6)	0.004(5)	0.004(7)	0.016(8)
C(214)	0.111(8)	0.098(8)	0.061(6)	-0.024(5)	0.019(6)	0.014(6)
C(215)	0.137(9)	0.063(6)	0.086(7)	-0.003(6)	0.035(7)	0.005(6)
C(216)	0.117(8)	0.048(5)	0.061(6)	0.011(5)	0.018(5)	0.005(5)
C(221)	0.091(7)	0.059(6)	0.075(6)	-0.000(5)	0.029(5)	0.008(5)
C(222)	0.074(7)	0.066(6)	0.123(8)	0.014(6)	0.025(6)	0.023(5)
C(223)	0.088(8)	0.075(8)	0.21(1)	0.019(8)	0.100(9)	0.031(6)
C(224)	0.14(1)	0.073(8)	0.18(1)	0.055(9)	0.01(1)	0.029(9)
C(225)	0.15(1)	0.079(9)	0.20(1)	0.062(9)	0.06(1)	0.023(8)
C(226)	0.103(8)	0.084(7)	0.14(1)	0.025(7)	0.058(8)	0.023(6)
C(231)	0.069(6)	0.059(5)	0.067(5)	0.009(4)	0.042(5)	0.014(4)

(Table continued over page)

C(232)	0.068(6)	0.082(6)	0.078(6)	0.000(5)	0.028(5)	0.023(5)
C(233)	0.081(7)	0.085(7)	0.105(8)	0.015(6)	0.100(6)	0.012(6)
C(234)	0.089(8)	0.124(9)	0.15(1)	0.020(8)	0.068(8)	0.054(7)
C(235)	0.11(1)	0.13(1)	0.13(1)	-0.024(8)	0.072(8)	0.029(8)
C(236)	0.095(8)	0.113(8)	0.092(7)	-0.023(6)	0.047(6)	0.020(6)
C(311)	0.053(5)	0.050(5)	0.072(6)	-0.011(4)	0.008(4)	0.009(4)
C(312)	0.109(8)	0.058(6)	0.081(6)	-0.003(5)	0.041(6)	0.013(5)
C(313)	0.108(8)	0.084(7)	0.099(8)	0.012(6)	0.054(6)	0.015(6)
C(314)	0.086(7)	0.059(6)	0.15(1)	0.015(7)	0.024(7)	0.031(5)
C(315)	0.14(1)	0.068(7)	0.13(1)	-0.002(6)	0.037(8)	0.052(7)
C(316)	0.132(9)	0.065(6)	0.092(7)	-0.003(5)	0.038(6)	0.046(6)
C(321)	0.063(6)	0.056(5)	0.055(5)	-0.021(4)	0.011(4)	0.014(4)
C(322)	0.060(6)	0.103(7)	0.060(6)	-0.019(5)	0.010(5)	0.023(5)
C(323)	0.080(7)	0.112(8)	0.092(7)	-0.015(6)	0.037(6)	0.027(6)
C(324)	0.099(8)	0.092(7)	0.074(7)	-0.010(5)	0.044(6)	0.021(6)
C(325)	0.101(8)	0.094(7)	0.059(6)	-0.000(5)	0.016(6)	0.023(6)
C(326)	0.076(6)	0.071(6)	0.068(6)	-0.006(4)	0.019(5)	0.018(5)
C(331)	0.059(5)	0.063(5)	0.047(4)	-0.015(4)	0.010(4)	0.017(4)
C(332)	0.079(6)	0.055(5)	0.060(5)	-0.008(4)	0.013(5)	0.012(5)
C(333)	0.076(7)	0.073(6)	0.086(6)	-0.000(5)	0.020(5)	0.032(6)
C(334)	0.052(6)	0.113(8)	0.088(7)	-0.004(6)	0.018(5)	0.028(6)
C(335)	0.058(6)	0.072(7)	0.129(8)	-0.016(6)	0.030(6)	0.008(5)
C(336)	0.061(6)	0.064(6)	0.093(7)	-0.025(5)	0.013(5)	0.012(5)

Table 2.23 Hydrogen Atom Coordinates and Isotropic Thermal Parameters for [Ag(Ph$_3$P)$_3$(4-MeOpcyd)]

Atom	x/a	y/b	z/c	U
H(8a)	0.5121	-0.2530	0.1933	0.06
H(8b)	0.4302	-0.2507	0.2235	0.06
H(8c)	0.5445	-0.1807	0.2817	0.06
H(3)	0.4200	0.0982	0.3185	0.06
H(4)	0.4183	-0.0629	0.2796	0.06
H(6)	0.6233	0.0330	0.1141	0.06
H(7)	0.6250	0.1942	0.1530	0.06
H(112)	0.3062	0.6605	0.1397	0.06
H(113)	0.3870	0.6940	0.0098	0.06
H(114)	0.4151	0.5661	-0.0754	0.06
H(115)	0.3624	0.4047	-0.0309	0.06
H(116)	0.2815	0.3712	0.0989	0.06
H(122)	0.2062	0.6696	0.3009	0.06
H(123)	0.3098	0.7882	0.4139	0.06
H(124)	0.4723	0.7671	0.5005	0.06
H(125)	0.5313	0.6274	0.4742	0.06
H(126)	0.4277	0.5087	0.3612	0.06
H(132)	0.1104	0.5839	0.0759	0.06
H(133)	-0.0534	0.6209	0.0470	0.06
H(134)	-0.1559	0.5739	0.1589	0.06
H(135)	-0.0946	0.4899	0.2996	0.06
H(136)	0.0691	0.4529	0.3289	0.06
H(212)	0.2737	0.2650	0.6704	0.06
H(213)	0.3665	0.3762	0.7952	0.06
H(214)	0.4012	0.5429	0.7623	0.06
H(215)	0.3431	0.5984	0.6064	0.06
H(216)	0.2504	0.4872	0.4798	0.06
H(222)	0.3357	0.1769	0.4598	0.06
H(223)	0.3782	0.0323	0.5290	0.06
H(224)	0.2743	-0.0634	0.6214	0.06
H(225)	0.1279	-0.0144	0.6445	0.06
H(226)	0.0854	0.1302	0.5753	0.06
H(232)	0.0029	0.2122	0.3249	0.06
H(233)	-0.1722	0.2169	0.3028	0.06
H(234)	-0.2265	0.2903	0.4214	0.06
H(235)	-0.1078	0.3589	0.5621	0.06
H(236)	0.0663	0.3543	0.5841	0.06
H(312)	0.0956	0.0743	0.3414	0.06
H(313)	0.0842	-0.0861	0.3966	0.06
H(314)	0.1172	-0.2049	0.3031	0.06
H(315)	0.1617	-0.1633	0.1544	0.06
H(316)	0.1731	-0.0029	0.0992	0.06
H(322)	0.3303	0.1788	0.1373	0.06
H(323)	0.3974	0.1795	-0.0007	0.06
H(324)	0.2899	0.1802	-0.1567	0.06
H(325)	0.1153	0.1802	-0.1746	0.06
H(326)	0.0481	0.1759	-0.0366	0.06

(Table continued over page)

H(332)	0.0231	0.3239	0.1360	0.06
H(333)	-0.1497	0.3322	0.0750	0.06
H(334)	-0.2740	0.1891	0.0329	0.06
H(335)	-0.2254	0.0377	0.0518	0.06
H(336)	-0.526	0.0294	0.1128	0.06

CHAPTER THREE

A Summary of Phenylcyanamido Complexation to Transition Metals

It is interesting to consider the geometries of the two phenylcyanamido canonical forms as follows:

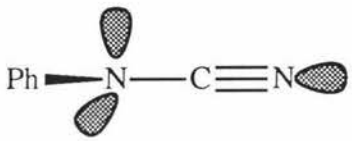

(I)

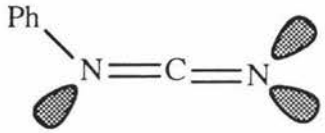

(II)

In form (**I**), the overlap of the sp lone pair on the nitrilo nitrogen with an unfilled σ-type metal orbital can result on coordination in a linear M-N-C arrangement. This will ideally give angles of 180° about the nitrilo nitrogen and 109° about the sp^3 hybridised amido nitrogen respectively. In contrast, form (**II**) possesses two sp^2 trigonal nitrogen atoms with theoretical bond angles of 120° about both the nitrilo and amido nitrogen atoms. Thus consideration of the Ph-N(2)-C(1)-N(1)-M bond distances and angles should provide information on the nature of the bonding in anionic phenylcyanamide complexes that have been structurally characterised. Bond parameter values are summarised in Tables 3.1 and 3.2 respectively.

The X-ray structures of copper(I) and (II) complexes with phenylcyanamido ligands reveal that the anion may coordinate to a metal in three ways:

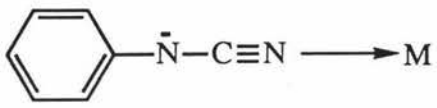

(IIIa)

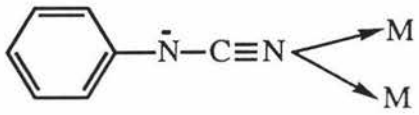

(IIIb)

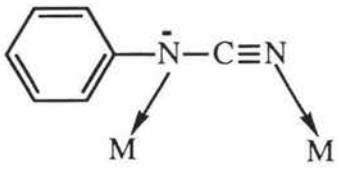

(IIIc)

The mean N(1)-C(1) bond distance in those copper complexes involving a terminally coordinated phenylcyanamido ligand (mode **IIIa**) is 1.153(10) Å which is consistent with that of a CN triple bond (1.158(2) Å [36]).The N(2)-C(1) bond distances have a mean value of 1.277(10) Å which approaches the expected value for a CN double bond (1.287 Å [19]), whereas the mean N(2)-C(2) bond length is 1.388(10) Å and is significantly shorter than a CN single bond (1.472(5) Å [36]). As discussed in Section 2.3, although the shortened N(2)-C(2) bond distance can be attributed to delocalisation of the negative charge into the phenyl ring, in the case of the N(2)-C(1) bond distance, this phenomenon of shortened bonds adjacent to a CN triple bond is not fully understood [31-35].

The N(1)-C(1)-N(2) bond angles are slightly non-linear (mean = 172.9°), possibly due to steric repulsions induced by the phenyl ring of the ligand with the phosphine phenyl rings. The cyanamido (NCN) moieties are generally slightly non-coplanar to their respective phenyl ring. The average C(2)-N(2)-C(1) bond angle of 119.9(7)° is very close to the ideal trigonal value of 120°.

Those complexes involving a μ-1,3-bridging phenylcyanamido ligand (mode **IIIc**) have mean N(1)-C(1), N(2)-C(1), and N(2)-C(2) bond distances of 1.161(5), 1.295(5) and 1.406(5) Å respectively, which are consistent with the above results of values that approach those of a CN triple bond, a CN double bond and a shortened single bond respectively.

As above, the N(1)-C(1)-N(2) angle approaches linearity (mean = 174.0(7)°), whereas the C(2)-N(2)-C(1) bond angle is approximately trigonal (mean = 118.2(4)°).

In the complex $[\{Cu(phen)(3\text{-}Clpcyd)(CH_3CO_2)\}_2]\cdot 2H_2O$, the 3-Clpcyd$^-$ ligand is coordinated *via* the μ-1,1-bridging mode (**IIIb**). This complex has the longest N(1)-C(1) bond length at 1.196(8) Å, although, statistically, this is not significantly longer than the others and is still consistent with a CN triple bond. The N(2)-C(1) and N(2)-C(2) bond distances are 1.269(9) and 1.402(9) Å respectively, with the respective N(1)-C(1)-N(2) and C(2)-N(2)-C(1) bond angles being 172.2(7) and 120.2(6)°.The M-N(1)-C(1) bond angles range from 141.4(7) to 170.7(5)°, whereas the M'-N(2)-C(1) bond angles are 105.6(6) and 112.9(4)°.

Despite the various coordination modes involved, all these complexes possess similar trends: all have N(1)-C(1) bond lengths consistent with a CN triple bond, N(2)-C(1) bond lengths consistent with a CN double bond, and a N(2)-C(2) bond length which has some partial double bond character. The bond angles about the amido nitrogen are trigonal, whereas the angles about the nitrilo nitrogen vary greatly between the trigonal and linear angles, showing the geometrical flexibility of phenylcyanamide coordination. These findings would suggest that in general, the ligands are closer to the phenylcyanamido representation (**I**) , than the carbodiimide form (**II**) although the latter must make an important contribution to the bonding description.

It has been proposed that when phenylcyanamido anions coordinate to ruthenium(III), a more polarising metal ion and a stronger π-acid than copper(II), then the contribution of the carbodiimide form (II) to the bonding description will be greater than in the case of copper(II), with a Ru(III)-N(1)-C(1) bond angle approaching 180° [14]. Electronic spectra suggest a significant π-bonding contribution is being observed [12]. The complex $[Ru(NH_3)_5(2,3\text{-}Cl_2pcyd)]\ [SO_4]\cdot EtOH$ has longer N(1)-C(1), N(2)-C(1), N(2)-C(2) bond distances than the previously described copper complexes, at 1.173(20), 1.308(20) and 1.417(18) Å respectively, although they are not significantly different from their respective values in the series of copper(I) and (II) phenylcyanamido complexes. The N(1)-C(1) bond length is still consistent with a CN triple bond, N(2)-C(1) is not significantly different from a CN double bond and N(2)-C(2) is shorter than a CN single bond in length due to

the delocalisation of the negative charge into the phenyl ring which is stabilised by the NCN group and phenyl ring being coplanar. The bond angle Ru-N(1)-C(1) is approximately linear at 171.4(10)°, whereas, in general, the Cu-N(1)-C(1) bond angle for those complexes involving a terminal "end-on" phenylcyanamido ligand is more acute (mean = 156.2(7)°). This could indicate some π-interaction between the phenylcyanamide anion and the ruthenium(III) atom. Although it has been proposed that the carbodiimide form best describes the electronic structure of the 2,3-dichlorophenylcyanamido ligand in this complex the above observations about the NCN bond distances and angles of the complex $[Ru(NH_3)_5(2,3\text{-}Cl_2pcyd)]$ do not individually represent significant differences from those observed in the previously discussed copper complexes.

The two X-ray crystal structures described previously in this work show phenylcyanamide anions terminally coordinated to silver(I). The complex $[Ag(Ph_3P)_3(4\text{-}Brpcyd)]$ has N(1)-C(1), N(2)-C(1) and N(2)-C(2) bond distances of 1.149(6) , 1.290(6) and 1.407(5) Å respectively, which are comparable with the values for copper(I) and copper(II) complexes involving terminally coordinated phenylcyanamido ligands (mean N(1)-C(1) = 1.153(10), mean N(2)-C(1) = 1.277(10) and mean N(2)-C(2) = 1.388(10) Å respectively). Likewise the bond angles are comparable with those observed in the previously discussed copper complexes, and thus the 4-Brpcyd$^-$ ligand in the silver complex can best be described by the phenylcyanamido canonical form **(I)**. Interestingly, in comparison with all the structurally characterised phenylcyanamido complexes, $[Ag(Ph_3P)_3(4\text{-}MeOpcyd)]$ has a significantly shorter N(1)-C(1) bond distance at 1.001(16) Å, a significantly longer N(2)-C(1) bond length of 1.404(18) Å and the longest N(2)-C(2) bond distance of 1.428(11) Å (significantly longer than the corresponding value in the copper complexes and comparable with that of the previously described ruthenium(III) complex). Whereas in all the other structures the N(2)-C(1) bond length is consistent with a CN double bond, the N(2)-C(1) distance in this structure has characteristics of a shortened single bond with only partial double bond character. The N(1)-C(1)-N(2) bond angle approaches linearity at 174.1(11)°, the amido nitrogen has the most accute angle (C(1)-N(2)-C(2) = 116.5(8)°), and the M-N(1)-C(1) bond angle is the smallest at 140.7(8)°. Apart from the complex $[\{Cu(Ph_3P)_2(4\text{-}Mepcyd)\}_2]$, this is the only

structurally characterised phenylcyanamido complex in which the phenylcyanamide anion contains an electron donating substituent on the phenyl ring. The methoxy group has a destabilising effect on the delocalisation of the negative charge into the phenyl ring, thus the longer N(2)-C(2) bond distance (although it is still consistent with a single bond with partial double bond character), and promotes extra electron density onto the nitrilo nitrogen to give the short N(1)-C(1) bond. Thus, although the majority of those complexes structurally characterised can be described as having a major contribution of resonance form **(I)** relative to form **(II)** in their bonding description, the 4-methoxyphenylcyanamido ligand in $[Ag(Ph_3P)_3(4\text{-}MeOpcyd)]$ exhibits a hybridisation which enhances further the contribution of canonical form **(I)** over form **(II)**.

The effect on ring substituents on the ligand electronic structure and coordination mode requires further research, including extending the series of silver(I), copper(I), copper(II), cobalt(III) and iron(III) complexes to involve a wide range of phenylcyanamido ligands in which various electron-donating or electron-withdrawing groups have been substituted in various positions on the phenyl ring. Also, further synthetic work to study the pseudohalide-like properties of the phenylcyanamides would be of interest.

Table 3.1 Ph-N(2)-C(1)-N(1)-M Bond Distances for Structurally Characterised Phenylcyanamido Complexes

Complex	Mode	Ph-N(2)	N(2)-C(1)	N(1)-C(1)	N(1)-M	N(2)-M'
$[Ru(NH_3)_5(2,3\text{-}Cl_2pcyd)]$	IIIa	1.417(18)	1.308(20)	1.173(20)	1.980(12)	
$[Cu(bipy)_2(2,3\text{-}Cl_2pcyd)]$ [PF6]	IIIa	1.382(8)	1.262(9)	1.159(9)	1.944(6)	
$[(Cu(bipy)(2,3\text{-}Cl_2pcyd)_2]$	IIIa	1.393(11)	1.274(11)	1.150(11)	1.928(7)	
		1.391(11)	1.255(11)	1.158(11)	1.950(6)	
		1.387(12)*	1.281(11)*	1.158(12)*	1.951(7)*	
		1.392(11)*	1.272(12)*	1.135(12)*	1.933(7)*	
$[Cu_2(dppe)_3(4\text{-}Clpcyd)_2]\cdot 2Me_2CO$	IIIa	1.385(7)	1.319(8)	1.156(8)	1.967(5)	
$[Ag(Ph_3P)_3(4\text{-}Brpcyd)]$	IIIa	1.407(5)	1.290(6)	1.149(6)	2.288(4)	
$[Ag(Ph_3P)_3(4\text{-}MeOpcyd)]$	IIIa	1.428(11)	1.404(18)	1.001(16)	2.295(8)	
$[\{Cu(bipy)(pcyd)\}_2]$	IIIa	‡				
	IIIc	1.409(7)	1.293(7)	1.169(7)	1.938(5)	2.355(6)
$[\{Cu(Ph_3P)_2(4\text{-}Mepcyd)\}_2]$	IIIc	1.402(3)	1.296(4)	1.152(4)	2.045(2)	2.095(2)
						N(1)-M'
$[\{Cu(phen)(3\text{-}Clpcyd)(CH_3CO_2)\}_2]\cdot 2H_2O$	IIIb	1.402(9)	1.269(9)	1.196(8)	1.950(6)	2.454(6)

* Two inequivalent configurations of $[Cu(bipy)(2,3\text{-}Cl_2pcyd)_2]$ wre observed due to crystal packing forces.

‡ Involves a disordered terminal phenylcyanamido ligand and thus the data is not considered accurate

Table 3.2 Ph-N(2)-C(1)-N(1)-M Bond Angles For Structurally Characterised Phenylcyanamido Complexes

Complex	Mode	N(1)-C(1)-N(2)	Ph-N(2)-C(1)	M-N(1)-C(1)	M'-N(2)-C(1)	M'-N(1)-C(1)
$[Ru(NH_3)_5(2,3\text{-}Cl_2pcyd)]$	IIIa	172.5(22)	118.9(12)	171.4(10)		
$[Cu(bipy)_2(2,3\text{-}Cl_2pcyd)]\ [PF_6]$	IIIa	174.0(7)	119.5(6)	158.6(6)		
$[Cu(bipy)(2,3\text{-}Cl_2pcyd)_2]$	IIIa	170.3(9)	1222.0(7)	155.5(7)		
		173.8(10)	118.9(7)	145.7(7)		
		176.2(11)*	119.8(8)*	141.4(7)*		
		173.1(10)*	120.6(8)*	165.3(9)*		
$[Cu_2(dppe)_3(4\text{-}Clpcyd)_2]\cdot 2Me_2CO$	IIIa	173.5(6)	118.6(5)	170.7(5)		
$[Ag(Ph_3P)_3(4\text{-}Brpcyd)]$	IIIa	172.5(6)	120.2(4)	159.1(4)		
$[Ag(Ph_3P)_3(4\text{-}MeOpcyd)]$	IIIa	174.1(11)	116.5(8)	140.7(8)		
$[\{Cu(bipy)(pcyd)\}_2]$	IIIa	‡				
	IIIc	172.7(7)	118.3(5)	151.0(5)	105.6(6)	
$[\{Cu(Ph_3P)_2(4\text{-}Mepcyd)\}_2]$	IIIc	175.2(3)	118.0(2)	156.8(2)	112.9(4)	
$[\{Cu(phen)(3\text{-}Clpcyd)(CH_3CO_2)\}_2]\cdot 2H_2O$	IIIb	172.2(7)	120.2(6)	149.1(5)		113.9(5)

* Two inequivalent configurations of[Cu(bipy)(2,3-CL2pcyd)2] were observed due to crystal packing forces.

‡ Involves a disordered terminal phenylcyanamido ligand and thus the bond data is not considered accurate.

REFERENCES FOR SECTION ONE

1. K. Caneiro, M. Olsen, F.B. Rasmussen and C.S. Jacobsen, **Phys. Rev. Lett.**, **46**(13), 852 (1981)
2. J. Williams, T.J. Emge, H.H. Wang, M.A. Beno, P.T. Copps, L.N. Hall, K.D. Carlson and G.W. Crabtree, **Inorg. Chem.**, **23**, 2558 (1984)
3. E. Amberger, H. Fuchs and K. Polborn, **Angew. Chem. Int. Ed. Engl.**, 24(11), 968 (1985)
4. A. Aumuller, P. Erk, G. Klebe, S. Hunig, J.U. von Schutz and H.P. Werner, **Angew. Chem. Int. Ed. Engl.**, **25**(8), 740 (1986)
5. P. Erk, S. Hunig, J.U. von Schutz, H.P. Werner and H.C. Wolf, **Angew. Chem. Int. Ed. Engl.**, **27**(2), 740 (1988)
6. F. Kurzer, J. Chem. Soc., 1949, 3033; R.L. Frank and P.V. Smith, **Org. Synth.**, Coll. vol. **3**, 735 (1975); Gy. Simig, K. Lempart, J. Tamas and G. Gzira, **Tetrahedron**, **31**, 1195 (1975)
7. M.L. Brader, E.W. Ainscough, E.N. Baker, A.M. Brodie and S.L. Ingham, **J. Chem. Soc. Dalton Trans.**, 2785 (1990)
8. M.L. Brader, E.W. Ainscough, E.N. Baker and A.M. Brodie, **Polyhedron**, **8**(17), 2219 (1989)
9. E.W. Ainscough, E.N. Baker, M.L. Brader, A.M. Brodie, S.L. Ingham, J.M. Waters, J.V. Hanna and P.C. Healy, **J. Chem. Soc. Dalton Trans.**, 1243 (1991)
10. R.J. Crutchley and M.L.Naklicki, **Inorg. Chem.**, **28**,1955 (1989)
11. M.L. Naklicki and R.J. Crutchley, **Inorg. Chem.**, **28**,4226 (1989)
12. R.J. Crutchley, K.M. McCaw, F.L. Lee and E.J. Gabe, **Inorg. Chem.**, **29**, 2576 (1990)
13. M.A.S. Aquino, A.E.Bostock and R.J.Crutchley, **Inorg. Chem.**, **29**, 3641 (1990)

14. R.J. Crutchley, R. Hynes and E.J. Gabe, **Inorg. Chem.**, **29**, 4921 (1990)

15. B.R. Hollebone and R.S. Nyholm, **J. Chem. Soc. (A)**,332 (1971)

16. M.L. Brader, PhD Thesis, Massey University (1988)

17. E.L. Muetterties and C.W. Alegranti, **J. Am. Chem. Soc., 94**, 6386 (1972)

18. D.V. Sanghani, P.J. Smith, D.W. Allen and B.F. Taylor, **Inorg. Chim. Acta., 59**, 203 (1982)

19. L. Pauling, **"The Nature of the Chemical Bond"**, 3rd ed, Cornell University Press: Ithaca, NY, pp 224,256 (1960)

20. B-K. Teo and J.C. Calabrese, **Inorg. Chem., 15**, 2467 (1976)

21. M.R. Churchill, J. Donahue and F.J. Rotella, **Inorg. Chem., 15**, 2752 (1976)

22. A. Cassel, **Acta Cryst., B35**, 174 (1979)

23. J. Howatson and B. Morosin, **Cryst. Struct. Commun., 2**, 51 (1973)

24. D. Coucouvanis, N.C. Baenziger and S.M. Johnson, **Inorg. Chem., 13**, 1191 (1974)

25. A. Cassel, **Acta Cryst., B37**, 229 (1981)

26. P.F. Barron, J.C. Dyason, P.C. Healy, L.M. Englehardt, B.W. Skelton and A.H. White, **J. Chem. Soc. Dalton Trans.**, 1965 (1986)

27. F.A. Cotton and R.L. Luck, **Acta Cryst., C45**, 1222 (1989)

28. M.I. Bruce, J.D. Walsh, B.W. Skelton and A.H. White, **J. Chem. Soc. Dalton Trans.**, 956 (1981)

29. R.L. Bodner and A.I. Popov, **Inorg. Chem., 11**, 1410 (1972)

30. R.H.P. Francisco, Y.P. Mascarenhas and J.R. Lechat, **Acta Cryst., B35**, 2712 (1979)

31. Y.M. Chow, **Inorg. Chem., 9**, 794 (1970)

32. K. Emerson, **Acta Cryst., 21**, 970 (1966)

33. L. Piere, R. Nelson and C. Thomas, **J. Chem. Phys., 43**, 3423 (1965)

34. Z.V. Zvonkova and A.N. Khvatkina, **Sov. Phys. Cryst., 6, 147 (1961)**

35. S.M. Ohlberg and P.A. Vaughan, **J. Am. Chem. Soc., 76**, 2649 (1954)

36. "International Tables for X-Ray Crystallography", Kynoch Press, Birmingham, 1962,

Vol III,p.276

37. D.D. Perrin and W.L.F. Armarego, "Purification of Laboratory Chemicals"., Pergamon Press, Aust., 3rd Ed.
38. R.L. Frank and P.V. Smith, **Org. Synth., Collective volume., 3**, 735
39. F. Kurzer, **J. Chem. Soc, 44**, 3033 (1949)
40. G.Y. Simig, K. Lempart, J. Tama's and G. Czira, **Tetrahedron., 31**, 1195 (1975)
41. V.A. Pankratov, V.V. Korshak, S.V. Vinogradova, N.P. Antsiferova and D.F. Kutepov, **Ser. Khim., 10**, 2315 (1975)
42. B.A. Frenz, "Computing in Crystallography", Delft University, Delft, Holland, 1978
43. G.M. Sheldrick, SHELX76, Program for Crystal Structure Determination and Refinement, University of Cambridge, England, 1976
44. D.T. Cromer and J.B. Mann, **Acta Cryst., A24**, 321 (1968)
45. D.T. Cromer and D. Liebermann,**J. Chem. Phys., 53**, 1891 (1970)

SECTION TWO
β-KETOPHENOLATO COMPLEXES OF URANYL(VI)

CHAPTER FOUR

INTRODUCTION

4.1 Dinuclear Complexation

The polyketones and functionally substituted β-diketones are a versatile class of ligands capable of acting as binucleating ligands, i.e. forming a series of transition metal complexes in which two metal ions can be secured in close proximity to each other. If the metal ions are the same then homodinuclear complexes are formed, whereas two different metal ions yield heterodinuclear complexes.

The primary interest in dinuclear complexes occurs in the field of bio-inorganic chemistry, in particular attempting to model some feature of a metalloenzyme or metalloprotein. These models may be *speculative*, where the structure of the active site - the metal ion coordination geometry and "ligand" types - are unknown and the aim is to reproduce some spectroscopic property, or *corroborative* in which the structure of the active site is known and so the model compound is designed accordingly[1]. In some cases a *functional* model can be achieved whereby the mode of action is also reproduced[2].

Much of this modelling work has been carried out in attempts to mimic the oxygen binding and mono-oxygenase activity of the homodinuclear copper proteins, namely the hemocyanins and the tyrosinases[3].

Further interest in di- and polynuclear complexation arises from the potential of pairs or clusters of metal ions that are electronically and magnetically "linked" to mediate industrially important chemical reactions more efficently than isolated metal centres[4].

The β-diketones have been applied to the area of dinuclear complexation in two major ways, the first of these being as precursors in the preparation of compartmental ligands and the second being their utilisation as.dinucleating ligands themselves.

4.2 Compartmental Ligands

Compartmental ligands are prepared by the condensation of a β-triketone, ketophenol or keto carboxylic acid with α,ω-diamines to produce a Schiff base having adjacent, dissimilar coordination compartments- i.e. N_2O_2 and O_2O_2 donor sets.

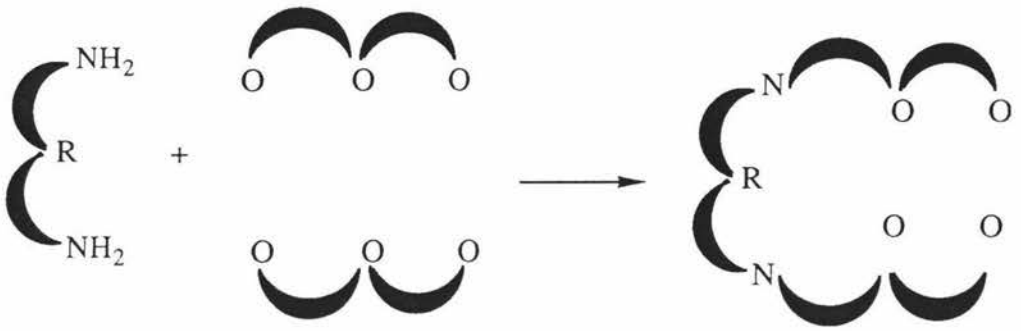

= 1,3,5-triketone, β-ketophenol or β-ketocarboxylic acid

There is an extensive number of homo- and heterodinuclear complexes involving these compartmental ligands, with several reviews published over the last decade [5-7].

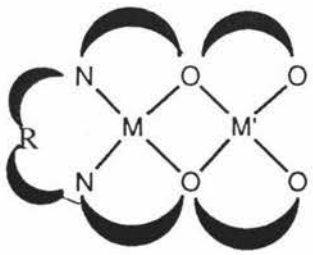

R = $-(CH_2)_2-$

M = Cu(II), Ni(II)

M' = Cu(II), Co(II), Mn(II), Zn(II) VO(IV), Fe(III) [8,9,10].

Not only can the β-diketonates be employed to synthesise compartmental ligands but they can also be utilised as dinucleating ligands in their own right.

4.3 β-diketones as Dinucleating Ligands

Although a number of bonding modes are known for the β-diketonates, e.g. carbon bonded (with elements like sulphur, selenium, mercury and gold) and both carbon and oxygen bonded

(with metals such as platinum and palladium), the chemistry of β-diketonate complexes of the transition and main group elements is dominated by oxygen bonded chelates (**1**) [11].

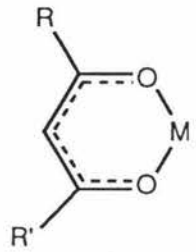

(**1**)

A variety of homodinuclear and heterodinuclear complexes of the divalent and trivalent first row transition metals has been reported.

Several homodinuclear copper(II) complexes of 1,3,5-triketonato ligands have been prepared and their redox, magnetic and spectroscopic properties investigated, in order to mimic metalloenzymes containing type 3 copper atoms[12].

Iron(III) 1,3,5-triketonato complexes have been prepared and characterised as corroborative models for iron metalloproteins[13].

The β-ketophenol ligands utilised in this study, namely 1-(2-hydroxyphenyl)-1,3-butanedione (H_2L^1) (4) and 1-(2-hydroxyphenyl)-3-phenyl-1,3-propanedione (H_2L^2) (5), are potential dinucleating ligands.

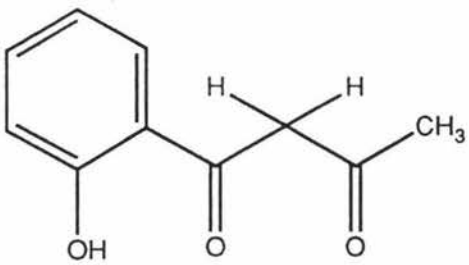

1-(2-hydroxyphenyl)-1,3-butanedione
H_2L^1
(**3**)

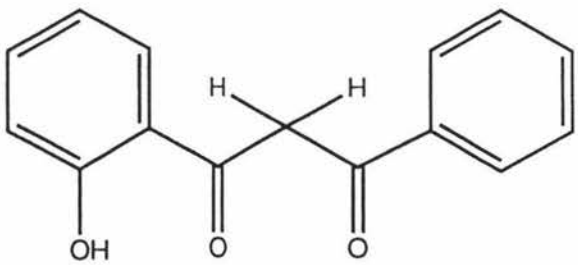

1-(2-hydroxyphenyl)-3-phenyl-1,3-propanedione
H_2L^2
(**4**)

The mononuclear complexes with the first row transition metals Cu(II), Ni(II), Mn(II), Zn(II), Al(III) and Cr(III) have been prepared by several workers independently and characterised principally by infrared and electronic spectroscopy[14-16].

The mononuclear complexes of the divalent metals can exhibit "positional" isomerism: the metal ion can coordinate in an "O_2O_2" site containing two phenolic oxygens and two carbonylic oxygens, or into the "O_4" site created by the bis(1,3-diketo) moiety (Fig.4.1).

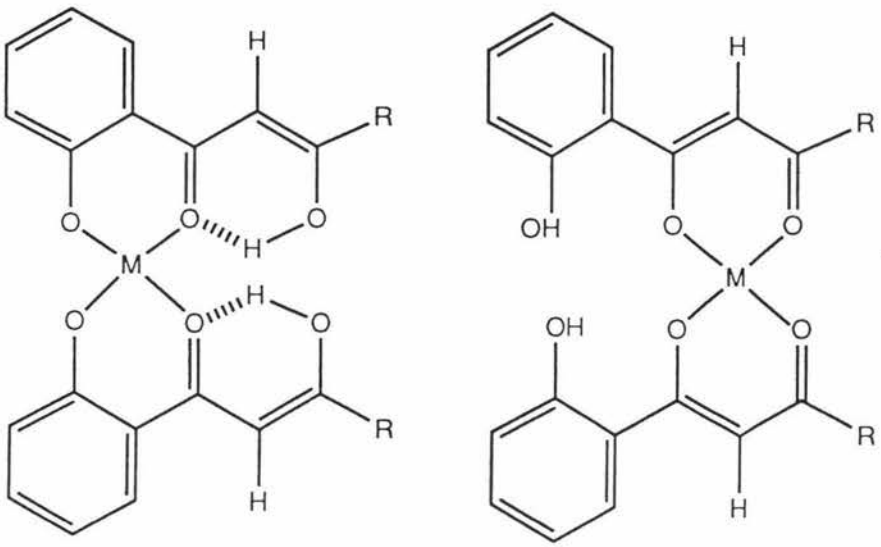

"O_2O_2" isomer "O_4" isomer

Fig. 4.1 The two possible "positional" isomers for mononuclear β-ketophenol complexes

Geometric isomerism is also possible as shown in Fig4.2. In the absence of X-ray structural information it has not been possible to identify the nature of the mononuclear species, i.e. which of the isomeric forms is present. Due to the similarity in the magnetic and spectroscopic properties of the copper(II) complexes with those of $Cu(acac)_2$ the structure proposed is that of the copper (II) ion in the "O_4" site with the ligands in a *trans* arrangement to prevent steric hindrance of the phenolic protons which may occur in the *cis* structure (Fig.4.3)[15,16].

Figure 4.2 Possible geometric isomers in β-ketophenol complexes

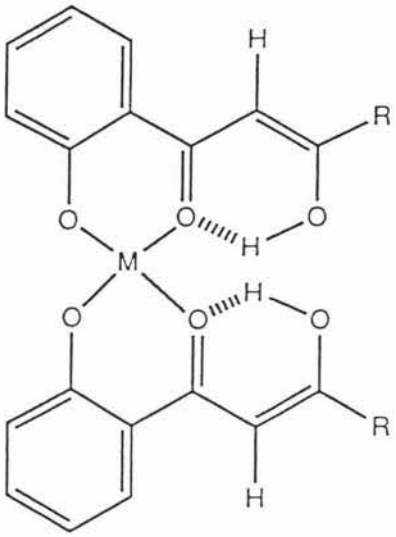

cis - "O_2O_2" isomer

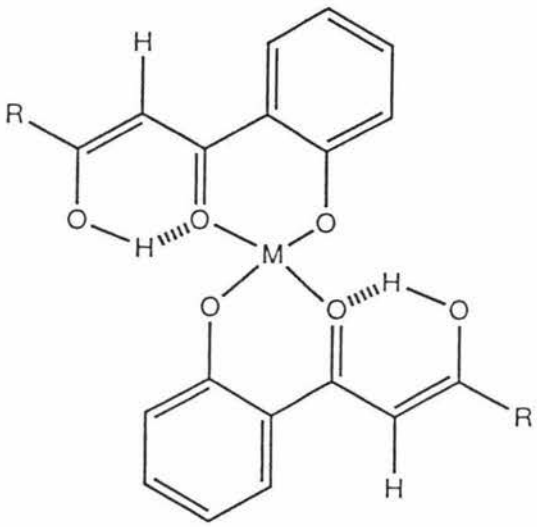

trans - "O_2O_2" isomer

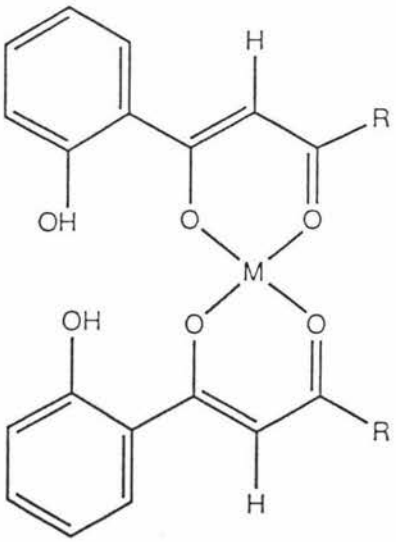

cis - "O_4" isomer

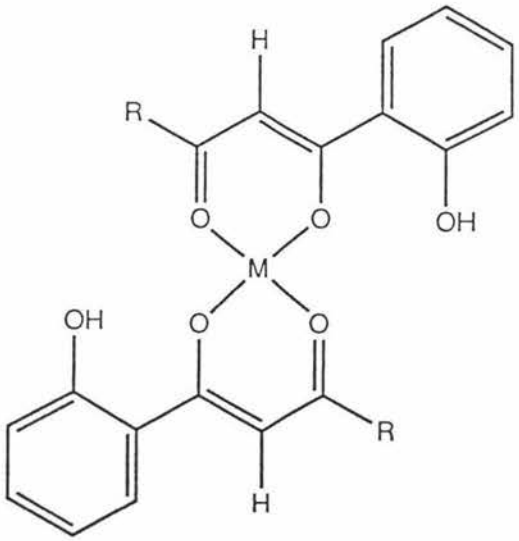

trans - "O_4" isomer

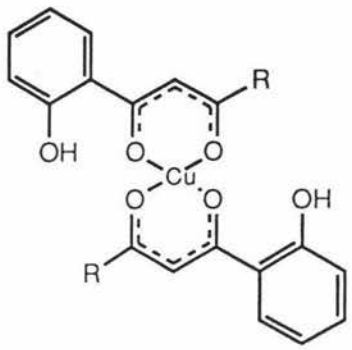

Fig. 4.3 Suggested structure for the mononuclear copper(II) complexes of H_2L^1 and H_2L^2.

Homodinuclear complexes of Cu(II), Ni(II) and Co(II) are readily formed and have magnetic moments indicative of antiferromagnetic coupling.

In order to model the oxidation of dihydroxy phenols by copper(II) metalloproteins the catalytic activity of these homodinuclear chelates towards the oxidation of 3,5-di-t-butylcatechol by molecular oxygen to quinone was investigated, with the copper(II) chelates, $[Cu_2(L^1)_2]$ and $[Cu_2(L^2)_2]$, showing enhanced activity with respect to their corresponding mononuclear chelates[16].

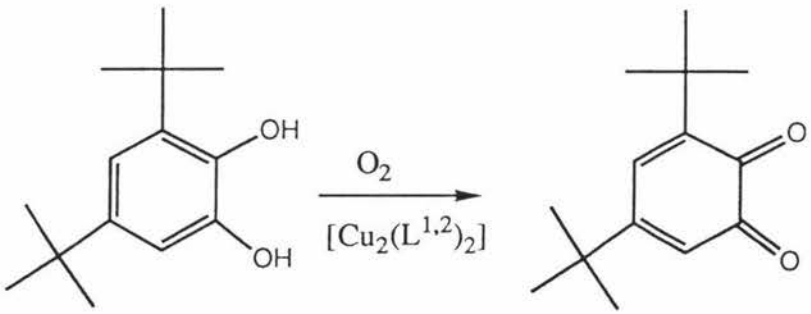

Three heterodinuclear complexes, namely $NiCu(L^1)_2]\cdot 2H_2O$ $[CoCu(L^2)_2]\cdot 2H_2O$ and $[NiCu(L^2)_2]\cdot 2H_2O$, have been reported and all have magnetic moments lower than the spin only values and similar to those found for analogous complexes in which magnetic exchange occurs[16].

4.4 Uranyl(VI) β-Diketonates

The number of known uranyl complexes is extensive, and virtually every kind of oxygen donor ligand as well as many nitrogen donors have been found in such complexes. There is considerable current research on the use of cyclic hexadentate and related ligands to form strong complexes with the uranyl ion, including the development of a new class of host molecules, the metalloclefts, and the use of uranyl crown ether complexes to assist the transport of neutral molecules such as urea through supported liquid membranes[17-19].

Numerous uranyl complexes with β-diketones and related dicarbonyl compounds have been reported, including some extensive infrared and electronic spectroscopy studies[20-24].

Although some complexes are obtained with the stoichiometric composition $[UO_2(\beta\text{-dike})_2]$ they are more usually obtained as $[UO_2(\beta\text{-dike})_2(L)]$, where L is a neutral monodentate ligand.

X-ray crystal structures of the latter complexes reveal the uranium coordination geometry is pentagonal bipyramidal, with the oxygen atoms of the linear uranyl ion in the axial positions and the pentagonal plane consisting of four oxygen donors from two β-diketonato ligands and a donor atom from the other ligand (Fig. 4.4) [25-30].

$[UO_2(acac)_2]$ (acac = acetylacetonate) is proposed to possess a dimeric structure involving acetylacetone oxygen atoms bridging the adjacent uranyl "monomer" (Fig. 4.5) [31], whereas $[UO_2(hfa)_2]_3$ (hfa = 1,1,1,5,5,5-hexafluoropentane-2,4-dionate) is trimeric in which half the uranyl oxygen atoms are bridging and half are terminal (Fig. 4.6)[32].

The uranyl complexes of benzoylpicolinoylmethane (Hpicmet) and nicotinoylmethane (Hnicmet), namely $[UO_2(picmet)_2]$ and $[UO_2(nicmet)_2]$, are proposed to be monomeric in structure (Fig. 4.7)[21].

A polymeric structure is proposed for the complex derived from the reaction of uranyl(VI) nitrate with 1,1'-bis(phenylpropane-1,3-dione)ferrocene (Fig. 4.8). No interaction between the uranium and the iron atoms was observed[33].

Poly-β-diketonates have been employed to prepare mononuclear, homodinuclear, heterotrinuclear and heterotetranuclear complexes with the uranyl ion UO_2^{2+} (Fig. 4.9) [34-38].

Trinuclear complexes of the symmetrical β-ketophenol ligand 1,3-bis(2-hydroxyphenyl)-1,3-propane dione (bhppH3) (**2**) with the general stoichiometry $[UO_2\text{-}M\text{-}UO_2(bhpp)_2]$, M is a first row divalent transition metal, have been prepared in which the metal introduced first coordinates in the most reactive coordination site (that of the β-diketone moiety), whereas in the homodinuclear Mn(III) complex both metals are unusually located in the less reactive outer compartments[39,40].

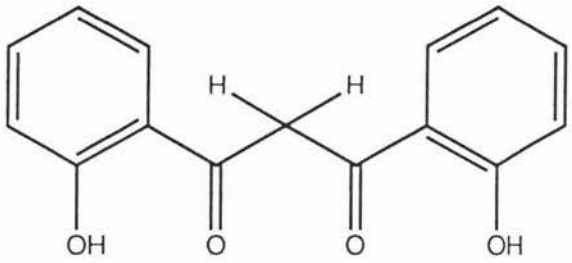

Bis(2-hydroxyphenyl)-1,3-propanedione
$bhppH_3$
(**2**)

The mononuclear vanadyl(IV) and uranyl(VI) complexes, involving the ligands used in this study H_2L^1 and H_2L^2, namely $[VO(HL^1)_2]$, $[VO(HL^2)_2OH]$, $[UO_2(HL^1)_2(H_2O)]$ and $[UO_2(HL^2)_2(H_2O)]$, have been reported, but whereas homodinuclear complexes of the type $[VO_2(L^1)_2]\cdot 2H_2O$ could be synthesised the corresponding uranyl(VI) homodinuclear chelates were unobtainable[41].

Attempts to prepare heterodinuclear complexes from the parent mononuclear vanadyl(IV) and uranyl(VI) chelates were unsuccessful[41].

Figure 4.4

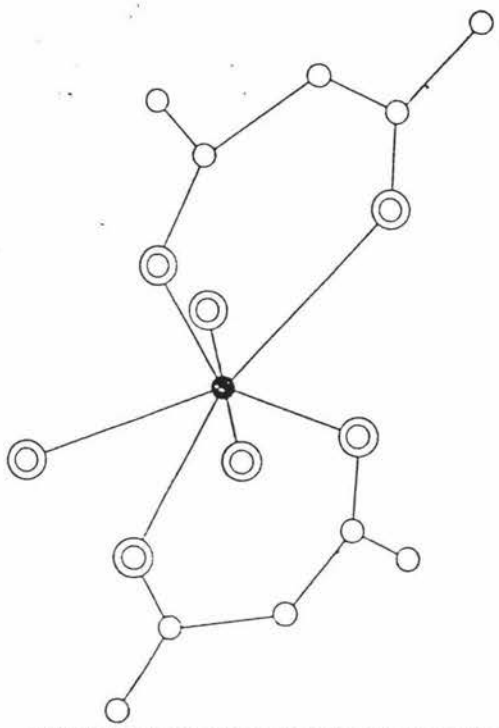

Molecular structure of uranyl-acetylacetonate monohydrate.
Black circle, uranium; double circles, oxygen; single circles, carbon

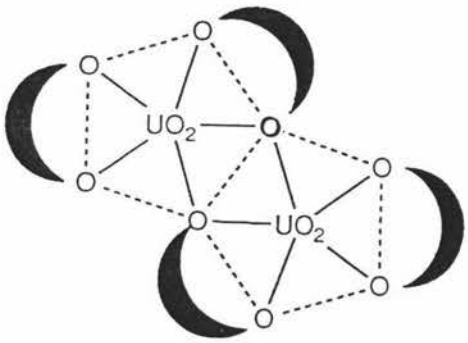

Figure 4.5 The proposed configuration of $[UO_2(acac)_2]$

Figure 4.6

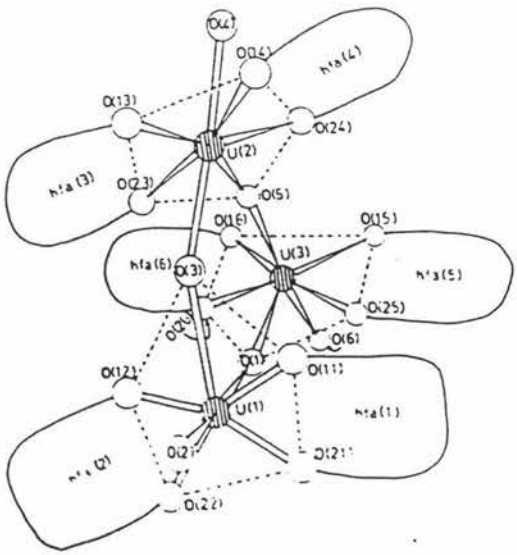

Schematic diagram of the $[UO_2(hfa)_2]_3$ trimeric molecule.

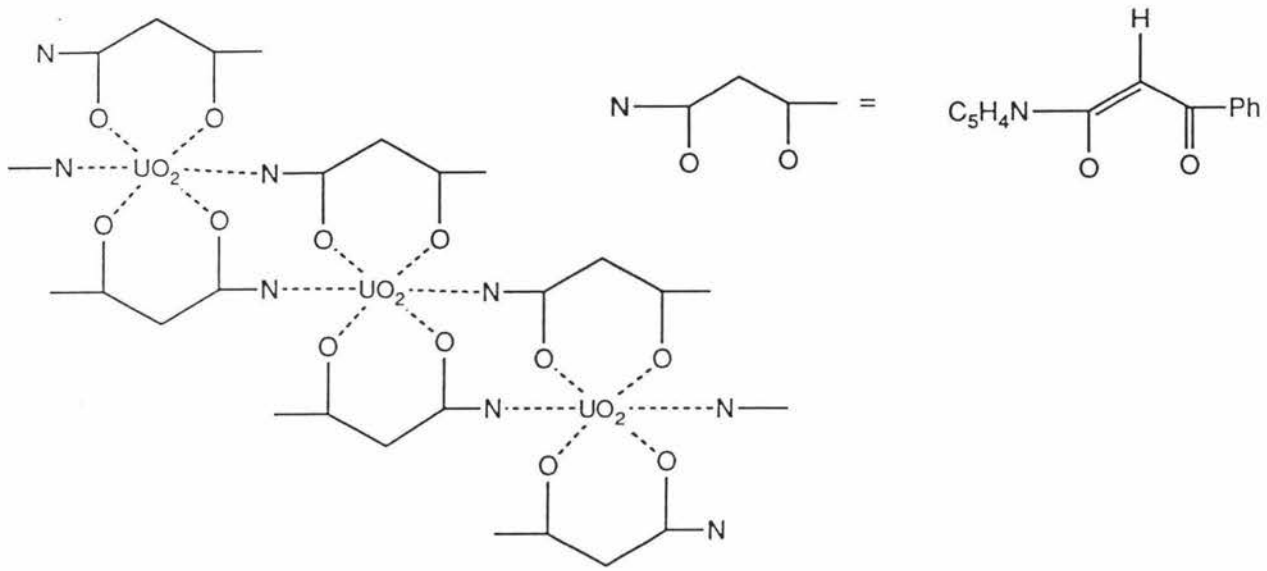

Figure 4.7 The polymeric structure of $[UO_2(picmet)_2]$

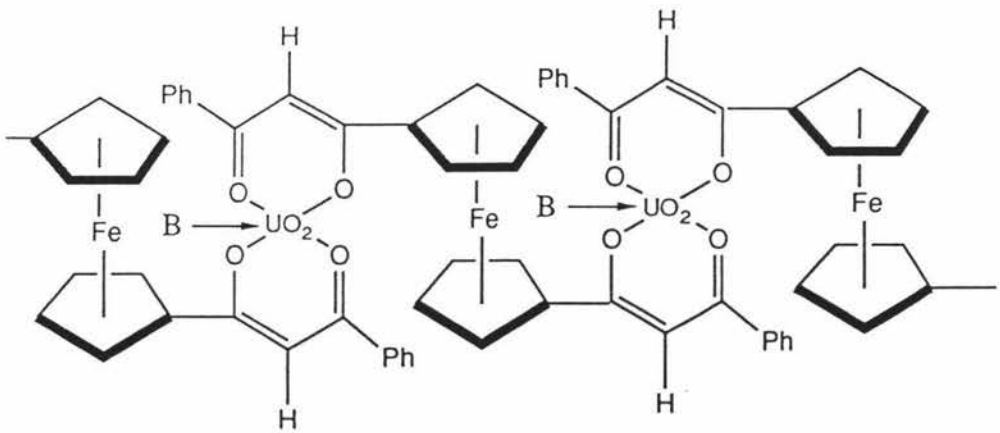

Figure 4.8 The polymeric structure of the uranyl complex of 1,1'-bis(phenylpropane-1,3-dione)ferrocene

Figure 4.9

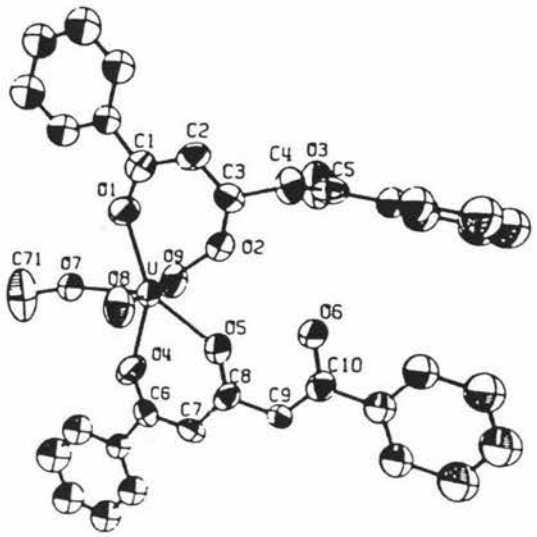

Structure of a triketonate uranyl complex, $UO_2(HDBA)_2 \cdot (CH_3OH)$.

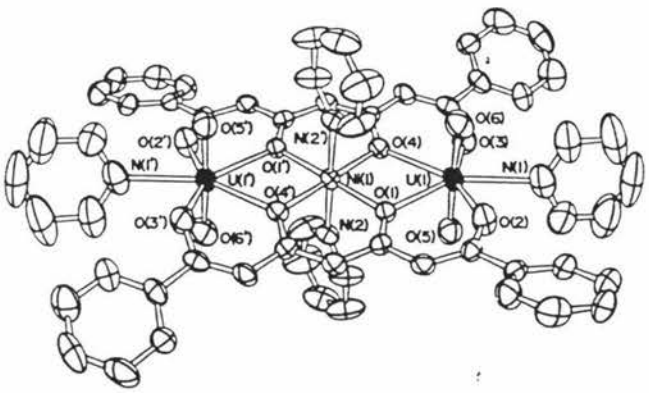

Structure of a tetraketonate uranyl complex, $Ni(UO_2)_2 \cdot (DBAA)_2(py)_4$.

4.5 This Present Study

In this study there were several aims:

(i) To determine the X-ray crystal structures of transition metal mononuclear chelates.

Since no complexes of the β-ketophenols have been structurally characterised and an understanding of the chemistry of the mononuclear complexes would assist an investigation of their dinucleating chemistry an attempt to crystallise the mononuclear chelates of H_2L^1 and H_2L^2 with the first row transition metals was carried out. The complex $[Ni(HL^2)_2]\cdot 2EtOH$ was the only such complex to crystallise using the various techniques employed. Unfortunately the crystals were very weakly diffracting and a X-ray structure determination could not be performed.

(ii) To prepare and characterise the mononuclear complexes with the uranyl(VI) ion.

Coordination numbers of 6,7 and 8 are known for the uranyl(VI) ion (UO_2^{2+}), although the seven coordinate pentagonal bipyramidal geometry is the most common. By replacing the transition metal ions in the mononuclear complexes with the larger and more coordinatively versatile uranyl(VI) ion a greater steric effect and different requirements for coordination geometry is introduced.

The mononuclear complexes $[UO_2(HL^1)_2(MeOH)]$ and $[UO_2(HL^2)_2(EtOH)]$ were prepared and characterised by infrared, electronic, ^1H NMR, and liquid secondary ion mass spectroscopy (LSIMS) .

These two complexes were crystallised and single crystal X-ray analyses of $[UO_2(HL^1)_2(EtOH)]$ and $[UO_2(HL^2)_2(EtOH)]\cdot EtOH$ are presented in Chapter Five.

(iii) To study the oxo-ligand adduct chemistry of the uranyl(VI) mononuclear complexes.

The ability to replace the solvent molecule in the above mentioned uranyl(VI) mononuclear chelates with more strongly coordinating unidentate neutral ligands was investigated. In chapter five the preparation, analytical data and IR spectroscopic results of the oxo-ligand

adducts $[UO_2(HL^1)_2(Ph_3AsO)]\cdot 2H_2O$, $[UO_2(HL^2)_2(Ph_3PO)]$ and $[UO_2(HL^2)_2(Ph_3AsO)]$ are presented.

(iv) To prepare and characterise the uranyl(VI) homodinuclear chelates.

Although the transition metal mononuclear complexes of β-triketones and ketophenols can readily be converted to the corresponding homodinuclear complexes with gentle heating or upon the addition of a mole equivalent of the appropriate metal, our attempts to prepare uranyl(VI) homodinuclear complexes were unsuccessful. Also the reaction of UO_2^{2+} with H_2L in a 1:1 ratio failed to produce the desired product.

(v) To prepare and characterise heterodinuclear complexes of the uranyl(VI) mononuclear precursors.

The preparation of heterodinuclear complexes from the uranyl(VI) mononuclear complexes was generally unsuccessful with metal substitution occurring, but in the following chapter the preparation and physicochemical properties of two uranyl(VI)-manganese(II) heterodinuclear complexes, namely $[UO_2Mn(L^1)_2(EtOH)]\cdot 1.5H_2O$ and $[UO_2Mn(L^2)_2(EtOH)]\cdot 2H_2O$, are described.

CHAPTER FIVE

URANYL(VI) COMPLEXES OF THE β-KETOPHENOL LIGANDS 1-(2-HYDROXYPHENYL)-1,3-BUTANEDIONE AND 1-(2-HYDROXYPHENYL)-3-PHENYL-1,3-PROPANEDIONE

5.1 Mononuclear Uranyl(VI) Complexes

5.1.1 Preparation of the Complexes

The reaction of the β-ketophenols H_2L^1 and H_2L^2 with uranyl(VI) acetate dihydrate in a 2:1 molar ratio affords complexes of the stoichiometry of $[UO_2(HL)_2(S)]$, where L = L^1 or L^2 and S = MeOH or EtOH. The oxo-ligand adducts, namely $[UO_2(HL^1)_2(Ph_3AsO)]\cdot 2H_2O$, $[UO_2(HL^2)_2(Ph_3PO)]$ and $[UO_2(HL^2)_2(Ph_3AsO)]$, are prepared by refluxing the appropriate oxo-ligand with the parent uranyl complex.The complexes prepared in this chapter are listed in Table 5.1 along with their elemental analyses, molar conductivities and infrared data.

5.1.2 Results and Discussion

5.1.2(a) Infrared Spectra

β-ketophenols are subject to keto-enol tautomerism and thus three possible tautomeric forms can be drawn for the ligands H_2L^1 and H_2L^2.

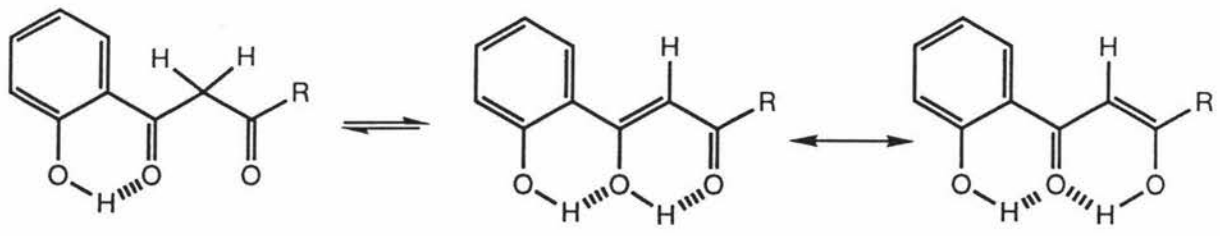

^{1}H NMR studies have shown that the free ligands exist at greater than 90% in the enol form in solution[42,43].

Table 5.1. Analytical, conductance and Infrared spectral data

	Analysis[a] (%)			Conductivity [d] ($S\ cm^2\ mol^{-1}$)	IR[e] (cm^{-1})			
	C	H	X	Λ	ν(C=O)	ν(C=C)	ν(O=U=O)	ν(X-O)
$[UO_2(HL^1)_2(MeOH)]$	38.8	3.2		5.3	1619,1520	1585	909	
	(38.4)	(3.4)						
$[UO_2(HL^2)_2(EtOH)]$	47.7	3.6		1.8	1618,1525	1587	914	
	(48.5)	(4.1)						
$[UO_2Mn(L^1)_2(EtOH)]\cdot 1.5H_2O$	35.4	3.4	6.3[b]	4.7	1616,1515	1579	903	
	(35.2)	(3.4)	(7.3)					
$[UO_2Mn(L^2)_2(EtOH)]\cdot 2H_2O$	43.6	3.3	6.4[b]	6.5	1620,1516	1590	910	
	(43.5)	(3.4)	(6.2)					
$[UO_2(HL^1)_2(Ph_3AsO)]\cdot 2H_2O$	46.8	3.5			1617,1516	1585	908	884[f]
	(46.5)	(3.8)						
$[UO_2(HL^2)_2(Ph_3PO)]$	55.8	3.4	3.2[c]		1618,1513	1587	913	1134[c]
	(56.1)	(3.6)	(3.0)					
$[UO_2(HL^2)_2(Ph_3AsO)]$	53.8	3.6			1617,1511	1587	908	869[f]
	(53.8)	(3.5)						

[a]Calculated values in parentheses.[b]X = Manganese. [c]X = Phosphorus. [d]In EtOH. [e]Recorded as Nujol mulls. [f]X = As

The solid infrared spectra of the free ligands show bands in the region 1600 - 1500 cm^{-1} (1680, 1615 and 1580 cm^{-1} for H_2L^1 ;1618, 1606 and 1571 $cm^{-1}$for H_2L^2) which are assigned to those of the hydrogen bonded carbonyl and the enolchelate vibration[14,15].

The relevant infrared data for the mononuclear complexes is presented in Table 5.1.

In some cases it is almost impossible to unambiguously assign the bands in the 1600 - 1400 cm^{-1} region in the metal chelate compounds of β-diketonates since the bond orders of the C=O and C=C bonds are similar and both absorb in the same region , and their relative positions are sensitive to change in the metal. For such a chelate ring as in these metal β-diketonate systems the coupling between various vibrational modes is considerable and the concept of group frequency is not generally applicable. For example, while some workers have empirically adopted the strongest band in this range as a carbonyl stretching mode, others have preferred the highest frequency band for this assignment[44,45].

Upon coordination two bands due to carbonyl and ethenylic bond vibrations are observed to be near 1620 and 1580 cm^{-1} respectively and a perturbed carbonyl absorption was noticed at ca. 1520 cm^{-1}.

Theoretical and empirical evidence unanimously support the assignment of the sharp intense band near 900 cm^{-1} in the spectra of all uranyl compounds to the asymmetric uranyl stretching frequency $\nu_{as}(O=U=O)$ [24,46,47].

The ligand orbitals of the β-diketone group are energetically and occupationally suitable for participation in both (U --> L) donor and (L --> U) acceptor π-interaction with the uranyl ion[48,49]. Electron withdrawing substituents will decrease the donor capacity of the carbonyl groups, as is evidenced by the high ν(C-O) values in copper(II) trifluoroacetylacetonates and likewise uranyl(VI) trifluoroacetylacetonates exhibit both high ν(C-O) and ν(O=U=O) frequency values[50].

Electron releasing β-ketoenolato substituents lead to a decrease in both ν(O=U=O) and ν(C-O).

The uranyl asymmetric stretching vibration for $[UO_2(HL^1)_2(MeOH)]$ and $[UO_2(HL^2)_2(EtOH)]$ (909 and 914 cm^{-1} respectively) is thus shifted to a lower frequency value with respect to that of $[UO_2(acac)_2(H_2O)]$ (922 cm^{-1}) [24].

In contrast, the carbonyl stretching frequencies are at higher values than those for the uranyl acetylacetonate complex. This effect has been observed for phenyl substituted copper(II) β-ketoenolates in a series involving various electron donating substituents, and is attributed to the significant contribution of the "benzenoid" canonical forms shown below.in the bonding description, however significant $U_{d\pi}$ -->$O_{p\pi}$ π-bonding will make these forms less likely since the oxygen has no vacant orbitals [51,52].

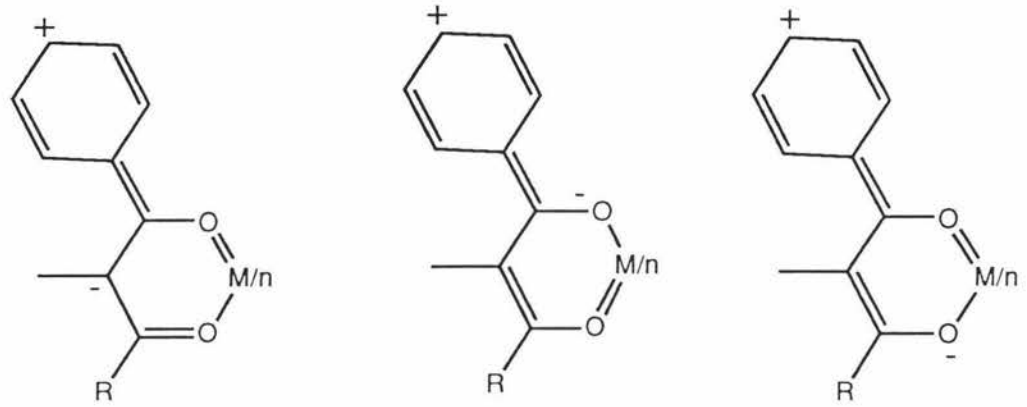

A study of ligation effects on ν(O=U=O) in a series of complexes $[UO_2(NO_3)_2(L)_2]$ revealed the shift in ν(O=U=O) induced by ligand L, may be expressed as

$$\Delta\nu = (\text{electrostatic effect}) - \sigma(L\text{-->}U) - \pi(L\text{-->}U) \pm \pi(U\text{-->}L) \qquad (1)$$

where a negative sign implies a shift to lower frequency and the adoption of a positive sign for the last term is generally more probable[53]. Equation (1) predicts that ν(O=U=O) will shift to lower frequency as the ligand field strength of L increases, except where U-->L π-bonding is of major importance and provides a positive contribution to Δν.

For the oxo-ligand adducts, $[UO_2(HL^1)_2(Ph_3AsO)]\cdot 2H_2O$, $[UO_2(HL^2)_2(Ph_3PO)]$ and $[UO_2(HL^2)_2(Ph_3AsO)]$, the uranyl frequency, ν(O=U=O), is slightly shifted to lower frequency values, whereas the carbonyl and ethylenic vibrational frequencies are generally invariant and similar to the values for the former parent uranyl complexes. These observations could imply that the transfer of negative charge from the oxo-ligand to the uranium which leads to increased electrostatic repulsion in the O=U=O bond and hence lowers ν(O=U=O) is partly relieved by U-O π-bonding interactions involving the β-diketonate ligands.

5.1.2(b) Mass Spectroscopy

Electron impact (EI) and liquid secondary ion (LSIMS) mass spectra of β-diketonate complexes involving the transition metals and lanthanides have been studied previously, with atom and group migrations from the ligand to the metal, according to theHard/Soft/Acid/Base nature of the metal, being observed in some cases. Also, the presence of cluster ions has been detected in the EI-MS of transition metal acetylacetonates[54-56]. There are few reports on the mass spectrometry of uranyl(VI) β-diketonates, the most striking feature of these reports being the appearence of the species $[(UO_2)_nO_m]^+$ (m = 0-5) [57-60].

Tables 5.2 and 5.3 present selected peaks and relative intensities for the five uranyl(VI) complexes in this study under the LSIMS conditions employed . The parent ion is not observed in the mass spectra of the two mononuclear complexes, $[UO_2(HL^1)_2(MeOH)]$ and $[UO_2(HL^2)_2(EtOH)]$. The most intense peak being formulated as $[MH^+-ROH]$. Other significant peaks correspond to the subsequent loss of the β-ketophenol ligands. Also, as observed in the EI-MS of the free ligands, a rearrangement of HL to yield a flavone-type compound occurs to give peaks corresponding to mixed ligand uranyl complexes.

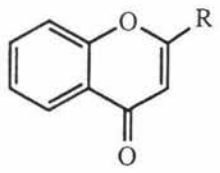

L^3: R = CH_3

L^4: R = Ph

In contrast, in the oxo-ligand adducts the parent ion is observed, owing to the stronger coordinating properties of the phosphine and arsine oxides relative to the alcohols, but the peak is not the most intense peak observed. The most intense peak corresponds to HL loss, and oxo-ligand migration is also observed.Under the conditions used no higher clusters were observed in any of the mass spectra [54-56].

Table 5.2 Selected Masses and their Designations for the LSIMS Spectra of $[UO_2(HL^1)_2(MeOH)]$ and $[UO_2(HL^2)_2(EtOH)]$

$[UO_2(HL^1)_2(MeOH)]$		$[UO_2(HL^2)_2(EtOH)]$	
m/z (% relative intensity)	Designation of Structure	m/z (% relative intensity)	Designation of Structure
785 (35)	$[UO_2(HL^1)_2(L^3)H]^+$	749 (100)	$[UO_2(HL^2)_2H]^+$
647 (37)	$[UO_2(HL^1)_2 + Na]^+$	714 (19)	$[UO_2(L^4)_2]^+$
625 (100)	$[UO_2(HL^1)_2H]^+$	509 (60)	$[UO_2(HL^2)H]^+$
606 (85)	$[UO_2(HL^1)(L^3)]^+$	497 (58)	$[UO_2(L^4)]^+$
447 (95)	$[UO_2(HL^1)]^+$	270 (60)	$[UO_2]^+$
432 (80)	$[UO_2(HL^1\text{-}CH_3)]^+$		
270 (85)	$[UO_2]^+$		
179 (100)	$[(H_2L^1)H]^+$		
161 (100)	$[(L^3)H]^+$		

Table 5.3 Selected Masses and Their Designations from the LSIMS Spectra of the uranyl(VI) (β-diketonate) oxo-ligand adducts.

$[UO_2(HL^1)_2(Ph_3AsO)]\cdot 2H_2O$		$[UO_2(HL^2)_2(Ph_3PO)]$	
m/z (% relative intensity)	Designated Structure	m/z (% relative intensity)	Designated Structure
1092 (12)	$[UO_2(HL^1)(Ph_3AsO)_2H]^+$	1066 (17)	$[UO_2(HL^2)(Ph_3PO)_2H]^+$
947 (7)	$[UO_2(HL^1)_2(Ph_3AsO)H]^+$	1028 (15)	$[UO_2(HL^2)_2(Ph_3PO)H]^+$
769 (100)	$[UO_2(HL^1)(Ph_3AsO)]^+$	787 (100)	$[UO_2(HL^2)(Ph_3PO)]^+$
592 (63)	$[UO_2(Ph_3AsO)]^+$	749 (24)	$[UO_2(HL^2)_2H]^+$
323 (100)	$[(Ph_3AsO)H]^+$	548 (67)	$[UO_2(Ph_3PO)]^+$
270 (20)	$[UO_2]^+$	279 (100)	$[(Ph_3PO)H]^+$
179 (20)	$[(H_2L^1)H]^+$	270 (36)	$[UO_2]^+$
		241 (63)	$[(H_2L^2)H]^+$

(Table continued over page)

Table 5.3 (continued)

$[UO_2(HL^2)_2(Ph_3AsO)]$	
m/z (% relative intensity)	Designated Structure
1153 (10)	$[UO_2(HL^2)(Ph_3AsO)_2]^+$
1072 (10)	$[UO_2(HL^2)_2(Ph_3AsO)H]^+$
831 (100)	$[UO_2(HL^2)(Ph_3AsO)]^+$
749 (5)	$[UO_2(HL^2)_2H]^+$
592 (50)	$[UO_2(Ph_3AsO)]^+$
323 (100)	$[(Ph_3AsO)H]^+$
270 (15)	$[UO_2]^+$
241 (25)	$[(H_2L^2)H]^+$

5.1.2(c) The Single Crystal X-Ray Structure of [(ethanol-κO)bis (1-(2-hydroxyphenyl)-1,3-butanedionato-κ^2O,O')dioxouranium(VI)], $[UO_2(HL^1)_2(EtOH)]$.

A thermal ellipsoid diagram for the title compound showing the atomic numbering scheme used is depicted in Figure 5.1. Figure 5.2 shows the packing of the molecules within the unit cell. Bond distance and angle data are given in Tables 5.4 and 5.5 respectively

The complex crystallises as a discrete monomer in which the uranium atom adopts a seven coordinate pentagonal bipyramidal geometry. The uranyl oxygens occupy the axial positions with a mean U-O(uranyl) bond distance of 1.765(16) Å and they approach linearity, demonstrated by the O(uranyl)-U-O(uranyl) bond angle of 175.3(1.2)°. Five oxygens make up the equatorial donors (four from two bidentate β-ketophenol ligands and the fifth from solvent ethanol acting as a ligand) to form a puckered pentagon. The uranyl ion is located in the "O_4" site, i.e. each ligand is behaving in a bidentate manner through the β-diketone moiety, and in this case the ligands are arranged *trans* with respect to each other (Figs 4.2 and 5.1). The mean U-O(ligand) bond distance is 2.371(7) Å and the average O(ligand)-U-O(ligand) bond angle is very close to that of the ideal pentagonal angle at 72.1(2)°. The U-O(uranyl) and U-O(ligand) bond distances are in accord with those observed in other similar complexes, e.g. mean U-O(uranyl) distances of 1.78(2), 1.71(2), 1.66(2), 1.74(3) Å and mean U-O(ligand) distances of 2.354(20), 2.390(10), 2.375(19) and 2.378(22) Å for the complexes $[UO_2(pd)_2(Ph_3PO)]\cdot C_6H_6$, $[UO_2(3\text{-}Clpd)_2(Ph_3PO)]$, $[UO_2(hfpd)_2(THF)]$ and α-$[UO_2(hfpd)_2\{PO(OMe)_3\}]$ respectively, where pd = pentane-2,4-dionato, 3-Clpd = 3-chloropentane-2,4-dionato and hfpd = 1,1,1,5,5,5-hexafluoropentanedionato and THF = tetrahydrofuran [26,27,29].

The bond distance and angle dimensions of the propanedione moieties in each of the β-ketophenol ligands are similar to those of transition metal and uranyl β-diketonates and are indicative of a delocalised system across the propanedione moiety[25-29,32,61,62]. The mean C-O bond distance is 1.279(20) Å which is intermediate between a C-O double bond

(1.23(1) Å) and a shortened C-O single bond (1.36(1) Å), whereas the average C-C bond of 1.380(20) Å has partial double bond character [63].

As mentioned previously, the pentagonal equatorial ring is puckered as a result of a slight mutual twisting of the β-ketophenol ligands with respect to each other. The two propanedione moieties (O(12), O(13), C(11), C(12) , C(13) and O(22), O(23), C(21), C(22), C(23)) are inclined with respect to the plane defined by atoms O(12), O(13), O(22) and O(23) to give an umbrella or boat-like configuration to this complex (planes 3 and 4 give dihedral angles of 12.1 and 4.7° to plane (2) respectively).

Planes of "best-fit" involving the uranyl coordination sphere of $[UO_2(HL^1)_2(EtOH)]$

Equation of Plane (1): -0.456x-0.320y -0.830z =0.0003			Equation of Plane (2): -0.447x-0.366y-0.816z = -0.045		
Atom	Deviation(Å)	Dev / esd	Atom	Deviation(Å)	Dev / esd
U	-0.000	0.31	O(12)	-0.015	1.46
O(3)	0.094	10.06	O(13)	0.010	0.93
O(12)	0.028	2.79	O(22)	-0.008	0.87
O(13)	-0.078	7.26	O(23)	0.019	1.65
O(22)	-0.078	8.22			
O(23)	0.074	6.26			

This tilting may be caused by intermolecular forces, or even by a preference for the near ideal bonding angles at the carbonyl oxygen atoms.

This observation of the tilting of the ligand planes with respect to the coordination plane has been observed in other pentagonal bipyramidal uranyl(VI) complexes such as $[UO_2(trop)_2(EtOH)]$ (trop = tropolonato), $[UO_2(saldien)]$ (saldien = N N'-3-azapentane-1,5-diyl bis (salicylidene- iminate)], $[UO_2(pmap)_2(H_2O)]$ (pmap = 1-phenyl-3-methyl-4-acetylpyrazolonato) and β-$[UO_2(hfpd)_2\{PO(OMe)_3\}]$ (hfpd = 1,1,1,5,5,5-hexafluoropentane-2,4-dionato) [28,30,64,65].

Planes of "best-fit" for the propanedione moieties of $[UO_2(HL^1)_2(EtOH)]$.

Equation of Plane (3): -0.608x-0.401y-0.685z = -0.4572			Equation of Plane (4): -0.385x-0.421y-0.821z = -0.174		
Atom	Deviation(Å)	Dev / esd	Atom	Deviation(Å)	Dev / esd
O(12)	0.0016	0.15	O(22)	0.0256	2.74
O(13)	-0.0010	0.09	O(23)	-0.0382	3.29
C(11)	-0.0019	0.21	C(21)	-0.0917	5.66
C(12)	0.0025	0.19	C(22)	0.0032	0.28
C(13)	0.0014	0.06	C(23)	0.0344	3.37

The propanedione moiety O(12), O(13), C(11), C(12) and C(13) is planar (plane (3) above)but when the uranium atom is also included in the plane the six membered chelate ring adopts a half-chair conformation (Fig. 5.3). The opposing propanedione moiety, O(22), O(23), C(21), C(22), C(23), is, however, slightly distorted. e.g. O(22) is significantly displaced from the plane defined by O(23), C(21), C(22), C(23). The inclusion of the uranium atom into the plane gives a skewed half-chair. The complete β-ketophenol ligands are not planar overall, with the phenolic ring of each ligand (O(11), C(111), C(112), C(113), C(114), C(115), C(116) or O(21), C(211), C(212), C(213), C(214), C(215), C(216)) being twisted with respect to the approximate plane defined by the propanedione moiety of that ligand (planes (3) and (4) respectively), but at the same time the two phenolic rings lie approximately parallel to one another.

Plane of "best-fit" showing the distortion of the propanedione moiety of ligand 2

Equation for Plane (5): -0.337x-0.486y-0.806z = -0.396

Atom	Deviation (Å)	Deviation / esd
O(23)*	-0.001	0.13
C(21)*	0.003	0.18
C(22)*	-0.003	0.28
C(23)*	0.003	0.24
O(22)	0.211	22.66
U	0.396	448.97

(* atoms defining the plane)

The phenolic oxygen of each ligand is intramolecularly hydrogen bonded to the adjacent carbonylic oxygen, with distances for O(11) · · · O(12) and O(21) · · · O(22) of 2.52 and 2.57 Å respectively. The tilting of the phenolic rings with respect to the ligand is thus most likely determined by steric effects and packing forces, due to some close intermolecular Ph - - - Ph contacts e.g. H(113) - - - H(213)' and H(116) - - - H(215)' at 2.26 and 2.42 Å respectively.

The ethanol ligand has bond lengths and angles which are regular and as expected.

Planes of "best-fit" for the phenolic rings in $[UO_2(HL^1)_2(EtOH)]$

Equation for plane (6): -0.684x-0.378y-0.624z = -0.717			Equation for plane (7): -0.676x-0.368y-0.638z = 0.962		
Atom	Deviation	Dev / esd	Atom	Deviation	Dev / esd
O(11)	-0.006	0.05	O(21)	-0.031	1.74
C(111)	0.005	0.51	C(211)	0.007	0.63
C(112)	-0.009	0.89	C(212)	0.013	1.00
C(113)	0.011	0.87	C(213)	0.022	1.14
C(114)	-0.018	0.25	C(214)	0.002	1.14
C(115)	-0.008	0.58	C(215)	-0.028	1.69
C(116)	0.002	0.16	C(216)	0.000	0.01

Dihedral angles between least-squares planes for $[UO_2(HL^1)_2(EtOH)]$

Plane	Plane	Dihedral Angle (°)
2	3	12.11
2	4	4.74
3	6	15.71
4	7	20.05
6	7	1.09

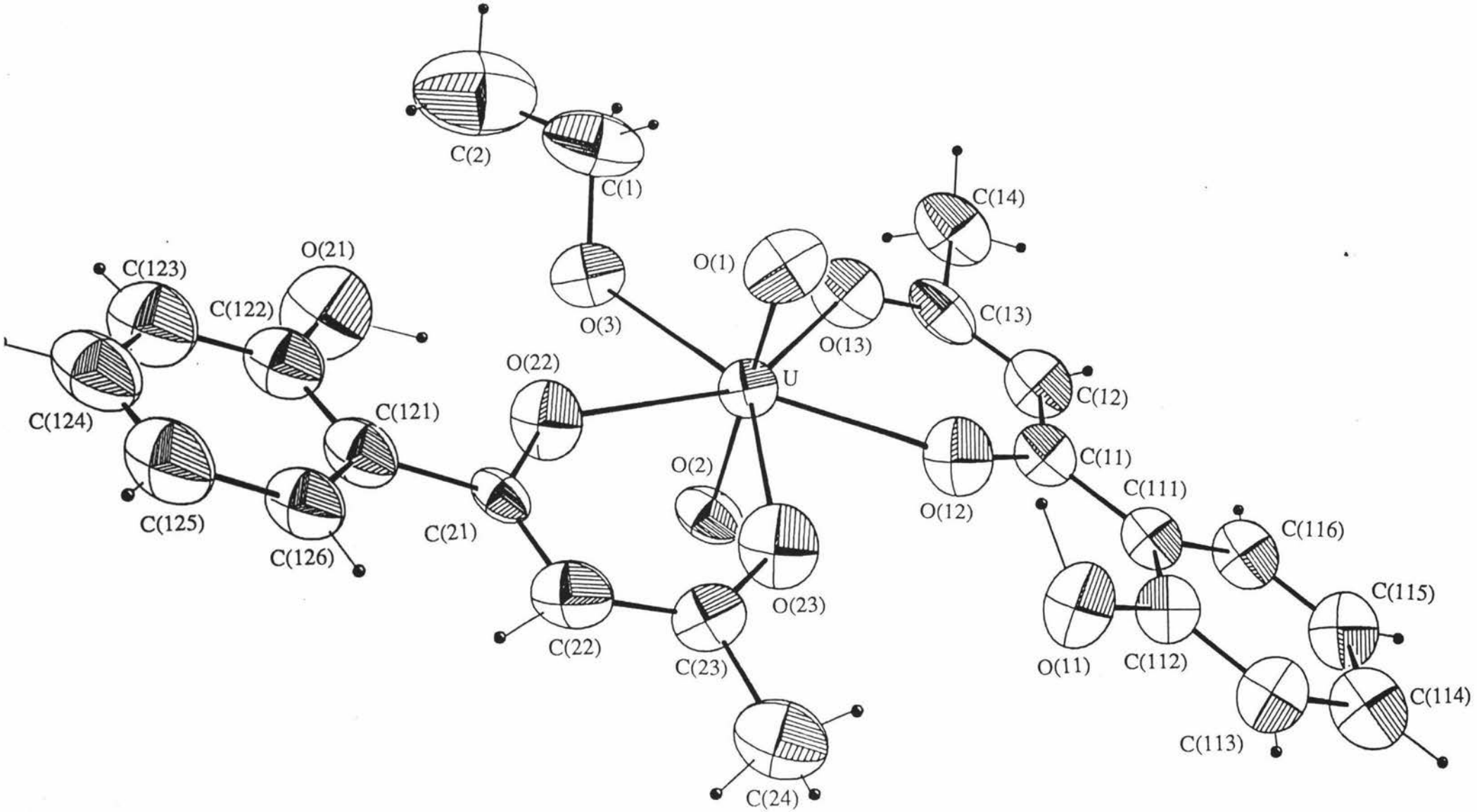

Figure 5.1 ORTEP Diagram of $[UO_2(HL^1)_2(EtOH)]$ showing the numbering scheme used. Ellipsoids are drawn at the 50% probability level. Hydrogen atoms have been included with arbitrary values for their ellipsoids

Figure 5.2 Unit Cell Packing Diagram for $[UO_2(HL^1)_2(EtOH)]$.

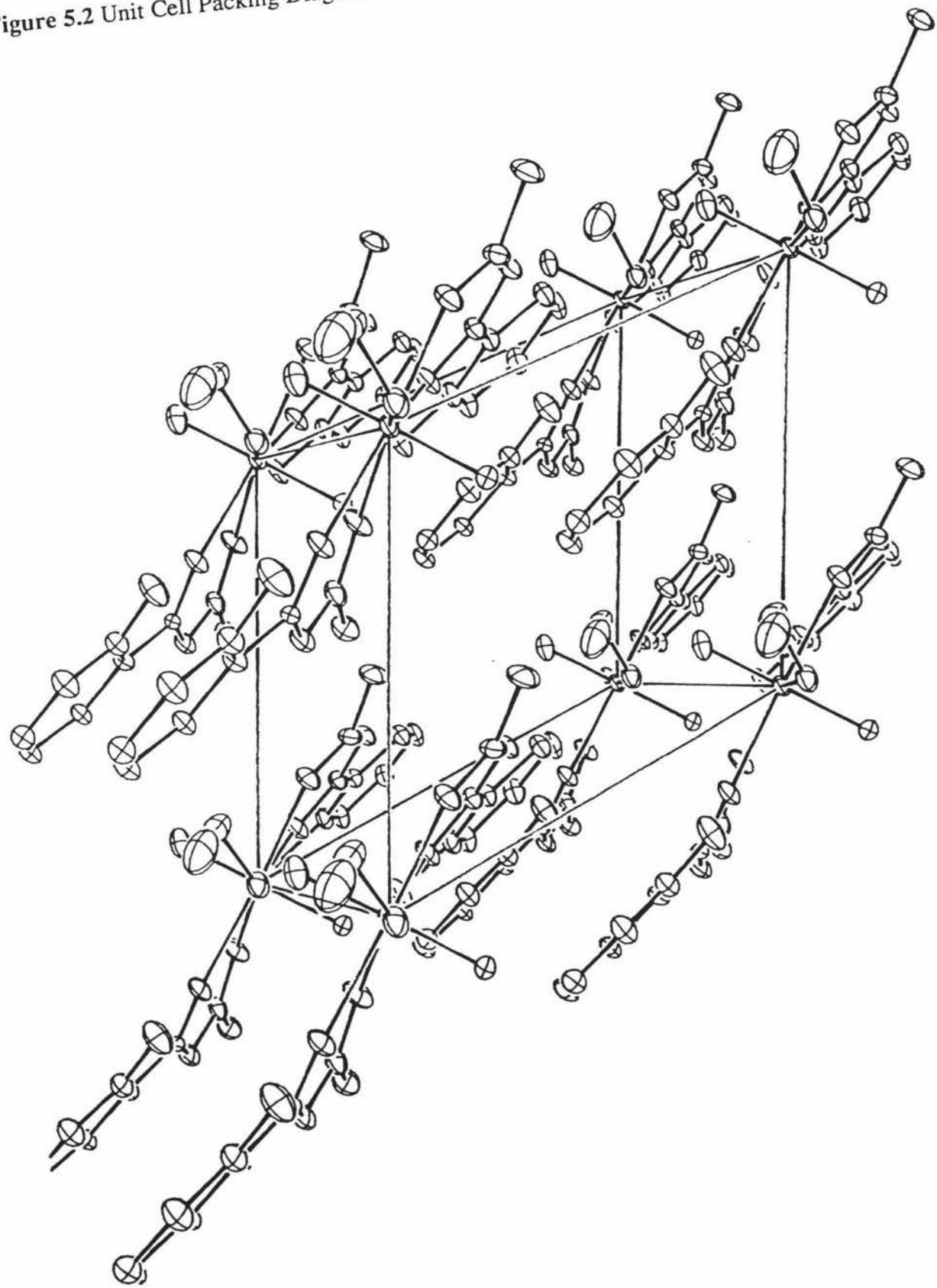

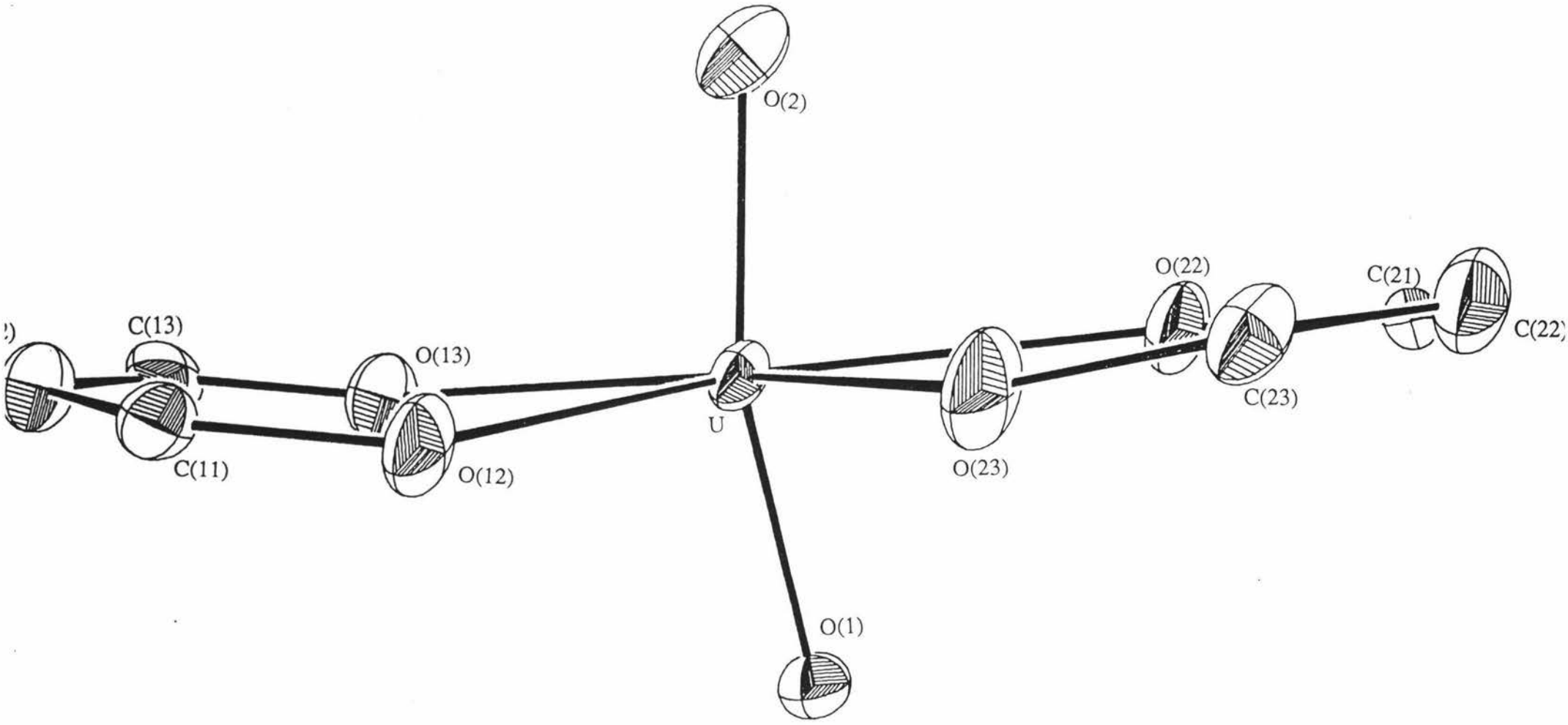

Figure 5.3 ORTEP Diagram in which only the uranyl ion and the ligand propanedione moieties are shown. The boat-like configuration is seen , as well as the distortion of the propanedione moiety O(22), O(23), C(21), C(22) and C(23)

TABLE 5.4. Selected bond distances for $[UO_2(HL^1)_2(EtOH)]$ and $[UO_2(HL^2)_2(EtOH)]\cdot EtOH$

(a) Bond lengths (Å)	$[UO_2(HL^1)_2(EtOH)]$		$[UO_2(HL^2)_2(EtOH)]\cdot EtOH$
Uranyl			
U-O(1)	1.784(15)		1.754(7)
U-O(2)	1.746(17)		1.760(8)
Pentagonal ring			
U-O(3)	2.460(7)		2.487(5)
U-O(12)	2.382(7)		2.376(6)
U-O(13)	2.376(8)		2.299(6)
U-O(22)	2.334(8)		2.409(6)
U-O(23)	2.303(8)		2.309(5)
HL(ligand1)			
O(11)-C(112)	1.366(12)		1.321(9)
O(12)-C(11)	1.286(12)		1.270(10)
O(13)-C(13)	1.217(26)		1.280(11)
C(11)-C(12)	1.385(13)		1.407(12)
C(11)-C(111)	1.461(13)		1.501(9)
C(12)-C(13)	1.383(30)		1.384(12)
C(13)-C(14)	1.586(27)	C(13)-C(131)*	1.497(9)
C(12)-H(12)	0.96		0.999(9)
O(11)-H(11)	1.094(8)		1.197(8)
C(111)-C(112)	1.408(13)		1.395
C(111)-C(116)	1.428(13)		1.395
C(112)-C(113)	1.393(13)		1.395
C(113)-C(114)	1.493(69)		1.395
C(114)-C(115)	1.372(73)		1.395
C(115)-C(116)	1.370(17)		1.395
		Ph (C-C)‡	1.395
HL(ligand2)			
O(21)-C(212)	1.338(19)		1.333(8)
O(22)-C(21)	1.360(19)		1.306(9)

(Table continued over page)

O(23)-C(23)	1.253(13)		1.283(10)
C(21)-C(22)	1.346(20)		1.391(11)
C(21)-C(211)	1.477(19)		1.474(9)
C(22)-C(23)	1.405(15)		1.397(12)
C(23)-C(24)	1.513(15)	C(23)-C(231)*	1.475(8)
O(21)-H(21)	1.024(13)		0.785(7)
C(22)-H(22)	0.96		1.076(8)
C(211)-C(212)	1.406(16)		1.395
C(211)-C(216)	1.404(15)		1.395
C(212)-C(213)	1.409(17)		1.395
C(213)-C(214)	1.399(27)		1.395
C(214)-C(215)	1.377(28)		1.395
C(215)-C(216)	1.390(16)		1.395
		Ph(C-C)‡	1.395

*Bond Distances associated with $[UO_2(HL^2)_2(EtOH)]\cdot EtOH$

‡ Phenyl rings have been refined as rigid groups with an expected C-C bond distance of 1.395Å

Table 5.5. Selected bond angles for $[UO_2(HL^1)_2(EtOH)]$ and $[UO_2(HL^2)_2(EtOH)]\cdot EtOH$

(b) Bond angles (°)	$[UO_2(HL^1)_2(EtOH)]$	$[UO_2(HL^2)_2(EtOH)]\cdot EtOH$	
Uranyl			
O(1)-U-O(2)	175.3(1.2)		178.0(3)
Pentagonal ring			
O(3)-U-O(13)	73.0(3)	O(3)-U-O(12)*	73.3(2)
O(3)-U-O(22)	74.5(3)	O(3)-U-O(22)	70.8(2)
O(12)-U-O(13)	69.2(3)	O(12)-U-O(13)	70.0(2)
O(12)-U-O(23)	71.2(3)	O(13)-U-O(23)	76.6(2)
O(22)-U-O(23)	72.4(3)	O(22)-U-O(23)	70.0(2)
HL(ligand1)			
U-O(12)-C(11)	138.8(6)		137.2(5)
U-O(13)-C(13)	134.2(1.4)		139.9(6)
O(11)-C(112)-C(111)	121.9(8)		123.9(4)
O(11)-C(112)-C(113)	116.3(9)		116.1(4)
O(12)-C(11)-C(12)	122.5(9)		122.3(8)
O(12)-C(11)-C(111)	114.7(8)		117.9(7)
O(13)-C(13)-C(12)	131.3(2.1)		121.9(8)
O(13)-C(13)-C(14)	112.4(2.1)	O(13)-C(13)-C(131)	115.5(7)
C(11)-C(12)-C(13)	120.2(1.3)		124.9(9)
C(11)-C(111)-C(112)	122.6(8)		119.3(4)
C(11)-C(111)-C(116)	121.9(9)		120.7(4)
C(111)-C(112)-C(113)	121.7(9)		120.0
C(111)-C(116)-C(115)	122.9(1.0)		120.0
C(112)-C(113)-C(114)	121.7(2.9)		120.0
C(112)-C(111)-C(116)	115.5(9)		120.0
C(113)-C(114)-C(115)	113.8(4.6)		120.0
C(114)-C(115)-C(116)	124.3(3.0)		120.0
		Ph(C-C-C)‡	120.0
HL(ligand1)			
U-O(22)-C(21)	136.6(9)		137.0(5)
U-O(23)-C(23)	137.1(7)		140.6(5)
O(21)-C(212)-C(211)	123.6(1.1)		124.1(3)

(Table continued over page)

O(21)-C(212)-C(213)	116.5(1.3)		115.9(3)
O(22)-C(21)-C(22)	121.2(1.3)		120.5(8)
O(22)-C(21)-C(211)	112.9(1.4)		117.5(6)
O(23)-C(23)-C(22)	125.0(9)		122.5(7)
O(23)-C(23)-C(24)	116.4(1.0)	O(23)-C(23)-C(231)*	115.8(7)
C(21)-C(22)-C(23)	125.9(1.1)		126.5(8)
C(21)-C(211)-C(212)	123.3(1.2)		120.2(4)
C(21)-C(211)-C(216)	117.8(1.1)		119.8(4)
C(211)-C(212)-C(213)	119.9(1.3)		120.0
C(211)-C(216)-C(215)	122.0(1.3)		120.0
C(212)-C(213)-C(214)	118.6(1.4)		120.0
C(212)-C(211)-C(216)	118.8(1.0)		120.0
C(213)-C(214)-C(215)	122.6(1.2)		120.0
C(214)-C(215)-C(216)	118.0(1.5)		120.0

* Bond angles associated with $[UO_2(HL^2)_2(EtOH)]\cdot EtOH$

‡ Phenyl rings have been refined as rigid groups, with a C-C-C bond angle of 120°

5.1.2(d) The Single Crystal X-Ray Structure of [(ethanol-κO)bis (1-(2-hydroxyphenyl)-3-phenyl-1,3-propanedionato-κO,O')dioxo uranium(VI)] Ethanol, $[UO_2(HL^2)_2(EtOH)]\cdot EtOH$.

A thermal ellipsoid diagram, showing the numbering scheme employed, is depicted in Figure 5.4; Figure 5.5 displays the crystal packing diagram. Bond distance and angle data are presented in Tables 5.4 and 5.5 respectively.

As in the former complex the uranium atom has adopted the pentagonal bipyramidal coordination geometry. However, whereas for both complexes the uranium is coordinated in the "O_4" site, the ligands are now arranged in a *cis* configuration in contrast with the previously described complex, in which the ligands are *trans* relative to each other. Thus , although the ligands are *trans* in the former complex so that the bulky phenolic rings are far from each other, the size and coordination geometry of the uranyl ion allows the accommodation of two relatively bulkier ligands, so that the phenolic hydrogen repulsions are minimised for the *cis* configuration.

The U-O(uranyl) and U-O(ligand) bond distances are similar to the values reported for the former complex, mean U-O(uranyl) = 1.757(7) Å and mean U-O(ligand) = 2.376(6) Å, and thus comparable with those of other uranyl(VI) β-diketonate complexes.The O(uranyl)-U-O(uranyl) bond angle is approximately linear (178.0(3)°) and the mean U-O(ligand) approaches the ideal pentagonal angle at 72.1(2)°.

As in the former complex the propanedione moiety dimensions of each ligand are indicative of a delocalised system; mean C-O and C-C bond distances are 1.285(10) and 1.395(12) Å respectively, whereas the mean C-C-O and C-C-C bond angles are 121.8(8) and 125.7(9)° respectively. The β-ketophenol ligands are inclined with respect to the coordination plane. However, whereas in the previously described complex the propanedione planes were tilted in the same direction to give a umbrella-like conformation, in this complex the propanedione planes are inclined such that one is "above" and one "below" the coordination plane to give a step-like conformation (Fig. 5.5) in which the propanedione planes are approximately parallel (the dihedral angle between them is 2.00°).

This step-like conformation, and the size and coordination requirements of the uranyl ion, allows the accommodation of two relatively bulky ligands such that intermolecular Ph---Ph and PhOH---PhOH repulsions are minimised. Those intra- and intermolecular H---H contacts which are <3.0 Å are listed below.

H(136) --- H(236)	2.38
H(1b) --- H(112)	2.92
H(2b) --- H(212)	2.98
H(113) --- H(135)'	2.87
H(114) --- H(215)'	2.53
H(114) --- H(134)'	2.95

As observed in the former complex, whereas one propanedione moiety is planar so that the chelate ring formed by including the uranium atom has a half-chair conformation, the other propanedione moiety, namely O(22), O(23), C(21), C(22), C(23), is sligthly distorted to give a skewed half-chair conformation to the chelate ring. O(23) is displaced in the opposite sense with respect to the other atoms of the propanedione moiety, and follows the umbrella-like pattern rather than the step-like conformation to give significant twist to the chelate ring. Least-squares planes and dihedral angles are given in Tables 5.6, 5.7 and 5.8 respectively.

The β-ketophenol ligands are not planar and within each ligand the phenol and phenyl rings are inclined, such that overall all rings are tilted in the same direction.

The phenol oxygen of each β-ketophenol ligand is hydrogen bonded to the adjacent carbonyl oxygen of that ligand (O(11) • • • O(12) = 2.54 Å and O(21) • • • O(22) = 2.53 Å), and the ethanol ligand and ethanol solvate are also involved in hydrogen bonding, O(3) • • • O(12) and O(4) • • • O(21) have values of 2.92 and 3.04 Å respectively.

The average Ph-C bond distance of 1.483(9) Å is comparable with partial double bond character (1.49(1) Å)[63] and therefore the benzenoid resonance structures may have a finite contribution to the bonding description of this complex.

Both the ethanol ligand and the ethanol of solvation have regular bond distances and angles.

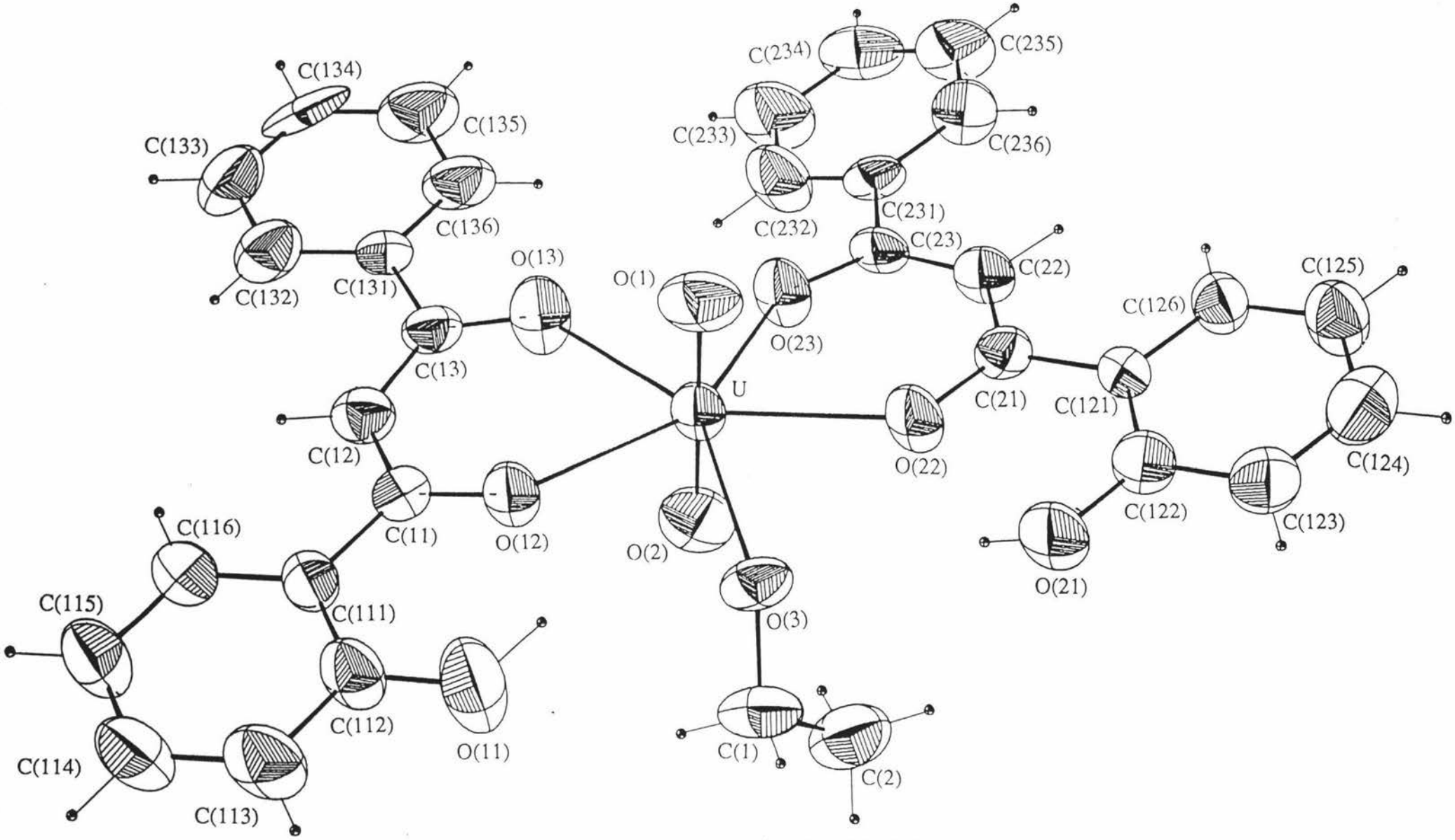

Figure 5.4 ORTEP Diagram of $[UO_2(HL^2)_2(EtOH)]\cdot EtOH$, showing the numbering scheme used. Ellipsoids are drawn at the 50% probability level. Hydrogen atoms are shown with

Figure 5.5 Unit Cell Packing Diagram for $[UO_2(HL^2)_2(EtOH)]\cdot EtOH$.

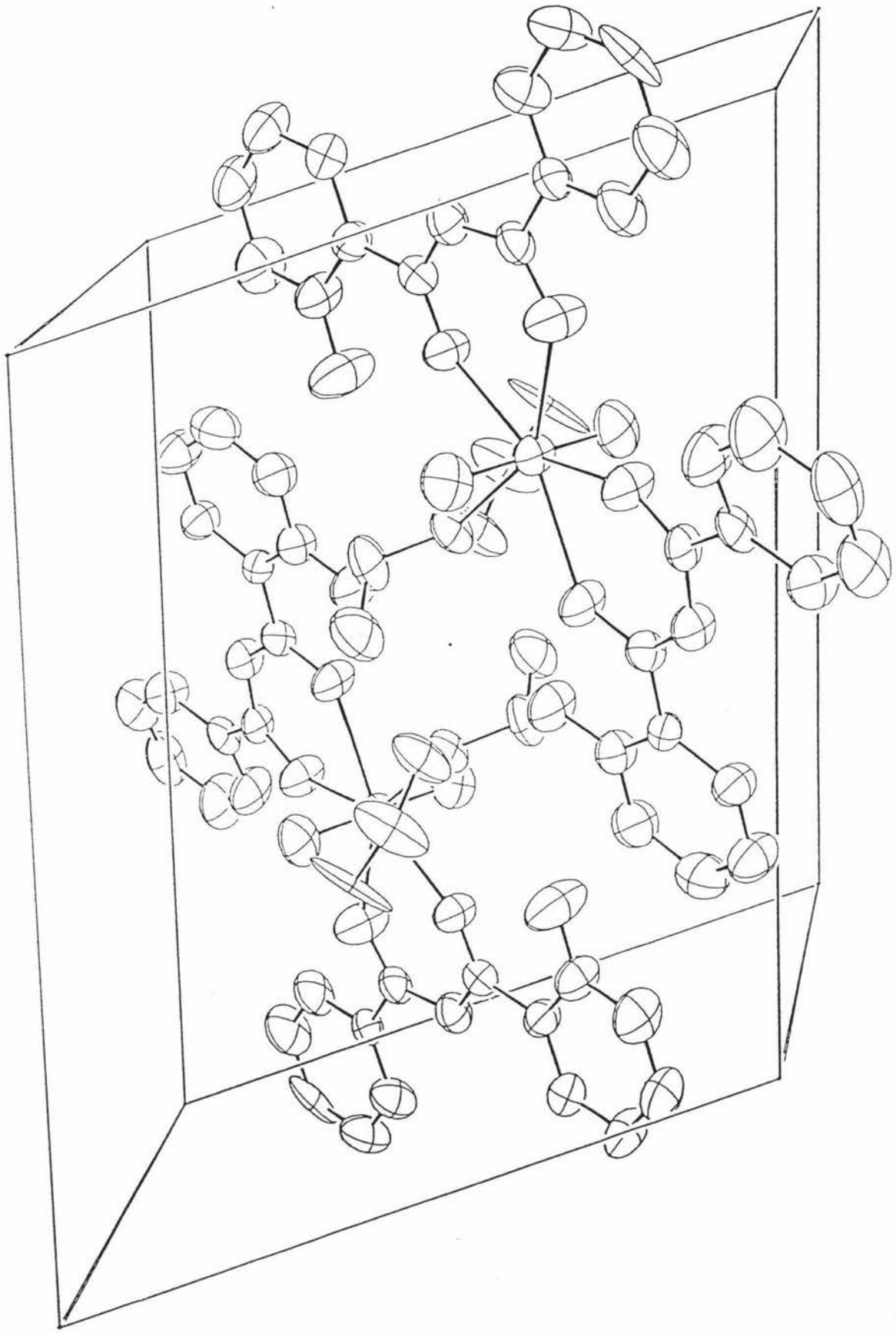

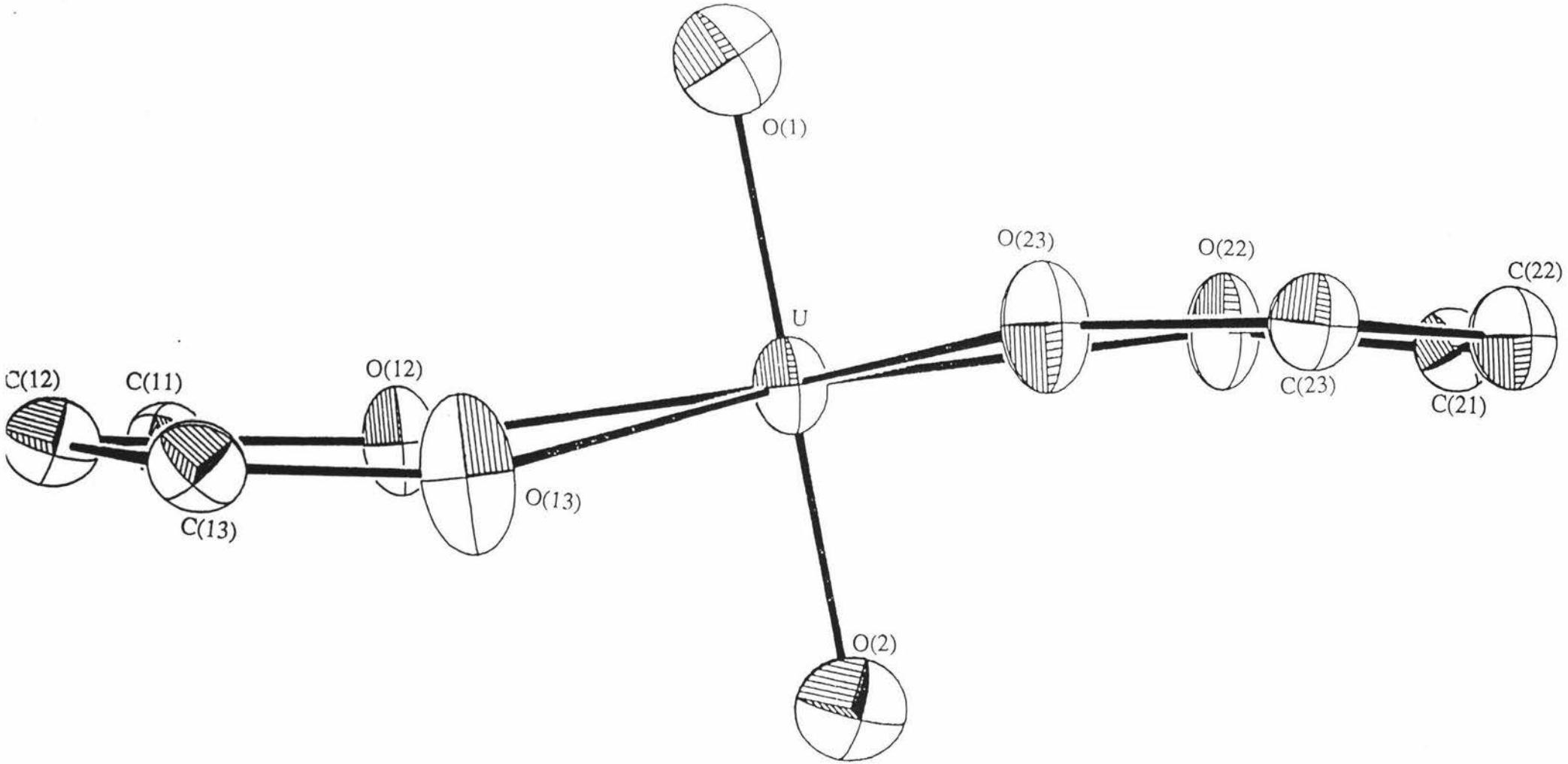

Figure 5.6 ORTEP Diagram showing only the uranyl and propanedione moieties. The step-like configuration is seen, as well as the slight distortion of the propanedione moiety O(22), O(23), C(21), C(22) and C(23).

Table 5.6 Planes of "best-fit" involving the uranyl coordination sphere of $[UO_2(HL^2)_2(EtOH)]\cdot EtOH$

Equation of Plane (1): 0.784x-0.164y -0.599z =2.636			Equation of Plane (2): 0.816x-0.139y-0.561z = 2.927		
Atom	Deviation(Å)	Dev / esd	Atom	Deviation(Å)	Dev / esd
U	-0.005	4.16	O(12)	0.067	10.49
O(3)	0.120	19.80	O(13)	-0.133	17.84
O(12)	0.001	0.12	O(22)	-0.066	10.38
O(13)	-0.057	7.64	O(23)	0.121	16.86
O(22)	-0.138	21.60			
O(23)	0.195	27.42			

Table 5.6(a) Planes of "best-fit" for the propanedione moieties of $[UO_2(HL^2)_2(EtOH)]\cdot EtOH$

Equation of Plane (3): -0.608x-0.401y-0.685z = -0.4572			Equation of Plane (4): -0.385x-0.421y-0.821z = -0.174		
Atom	Deviation(Å)	Dev / esd	Atom	Deviation(Å)	Dev / esd
O(12)	0.006	0.94	O(22)	0.020	3.14
O(13)	-0.002	0.25	O(23)	-0.021	3.00
C(11)	-0.024	2.50	C(21)	-0.046	5.26
C(12)	0.020	2.07	C(22)	0.007	0.78
C(13)	-0.006	0.62	C(23)	0.037	4.20

Table 5.7 Plane of "best-fit" showing the distortion of the propanedione moiety of ligand 2 of $[UO_2(HL^2)_2(EtOH)]\cdot EtOH$

Equation for Plane (5): 0.781x + 0.089y - 0.618z = 4.168

Atom	Deviation (Å)	Deviation / esd
O(22)*	0.005	0.71
C(21)*	-0.018	2.12
C(22)*	0.020	2.15
C(23)*	-0.009	1.02
O(23)	-0.115	16.17
U	-0.471	402.86

(* atoms defining the plane)

Table 5.7(a) Planes of "best-fit" of the phenol and phenyl rings in $[UO_2(HL^2)_2(EtOH)]\cdot EtOH$

Equation for plane (6): 0.765x-0.094y-0.637z = 2.766			Equation for plane (7): 0.770x-0.133y-0.625z = 4.473		
Atom	Deviation	Dev / esd	Atom	Deviation	Dev / esd
O(11)	-0.032	3.36	O(21)	-0.006	0.82
C(111)	0.005	0.91	C(211)	0.002	0.37
C(112)	0.008	1.57	C(212)	0.003	0.51
C(113)	0.006	1.09	C(213)	0.002	0.26
C(114)	-0.002	0.39	C(214)	-0.000	0.02

(Table continued over page)

C(115)	-0.005	0.87	C(215)	-0.002	0.31
C(116)	-0.002	0.35	C(216)	-0.001	0.18

Equation of Plane (8):

0.771x-0.063y-0.634z = 2.890

Equation of Plane (9):

0.791x-0.270y-0.549z = 5.122

Atom	Deviation	Dev / esd	Atom	Deviation	Dev / esd
C(131)	0.0004	0.06	C(231)	0.0002	0.04
C(132)	-0.0001	0.01	C(232)	0.0000	0.00
C(133)	-0.0001	0.02	C(233)	-0.0001	0.02
C(134)	0.0000	0.01	C(234)	0.0000	0.01
C(135)	0.0002	0.038	C(235)	0.0003	0.05
C(136)	-0.0004	0.07	C(236)	-0.0004	0.06

Table 5.8 Dihedral angles between Planes of "best-fit" for $[UO_2(HL^2)_2(EtOH)]\cdot EtOH$

Plane	Plane	Dihedral Angle (°)
2	3	12.23
2	4	11.09
3	4	2.00
3	6	8.29
3	8	6.57
4	7	5.24
4	9	13.59
6	7	1.09
8	9	19.87

5.1.2(e) NMR Spectroscopy

The crystal structures presented above illustrate two of the three isomers that are expected to exist for uranyl(VI) complexes of unsymmetrically substituted β-diketone ligands (Fig 5.7). There are two possible *cis* isomers corresponding to the ethanol ligand being either near the phenolic groups (as in the crystal structure of $[UO_2(HL^2)_2(EtOH)]\cdot EtOH$) or alternatively far from the phenolic groups. The *trans* isomer has the ethanol ligand near the phenolic group of one ligand and far from the phenolic group of the opposing ligand seen in the crystal structure of $[UO_2(HL^1)_2(EtOH)]$)

If the three possible geometrical isomers were to be observed on the nmr time scale, four sets of ligand resonances would be expected, one for each of the *cis* structures and two for the *trans* isomer due to one phenol group being near the ethanol ligand and the other distant from it. Variable temperature ^{19}F NMR studies on unsymmetrical fluorine-substituted β-diketonate uranyl(VI) complexes have shown fluxional behaviour , with three resonances for the *cis* and *trans* isomers of the complex $[UO_2(CF_3COCHCOCH_3)_2(DMSO)]$, DMSO = dimethylsulphoxide, being observed at low temperatures ($\Delta G = \pm 8.4$ kJ/mol for the equilibrium of the cis structures and so only one signal is seen), but the nature of this fluxionality is still a matter of debate[66-72].

The ^1H NMR spectrum of $[UO_2(HL^1)_2(EtOH)]$ was measured in $CDCl_3$ and showed peaks corresponding to both free and coordinated ligands indicating the occurrence of ligand dissociation, and this was confirmed by TLC. The methyl proton signals of the keto and enol isomers of the free H_2L^1 appear at lower frequency (2.15 and 2.30 ppm) than the broad singlet at 2.51ppm observed for the coordinated HL^1 (Fig. 5.8). Upon cooling to -30° another singlet appears at higher frequency at 2.75 ppm and at -60° there are three peaks at 2.44, 2.68 and 2.83 ppm associated with coordinated HL^1 due to the existence of *cis-trans* isomerism. Similarly the phenol proton signals at room temperature (20 °C) show one broad singlet at higher frequency (12.33ppm) from the two signals associated with the keto-enol tautomerism of the free H_2L^1 (11.89 and 11.98 ppm). On cooling to -60° C a spectrum containing three proton signals (12.45, 12.65 and 12.68 ppm) , at higher frequency relative to the two phenol

peaks of the free ligand, are observed as a result of geometric isomers of the complex (Fig. 5.9).

The ^{1}H nmr spectrum of $[UO_2(HL^2)_2(EtOH)]$ also displayed phenolic proton signals due to free and coordinated ligand at room temperature (20°C), with two signals arising from keto-enol tautomers of free H_2L^2 (11.94 and 12.13 ppm) and two broad signals at higher frequency (12.47 and 12.81 ppm) associated with the complex. Cooling this sample down in a stepwise manner shows the sharpening of one of the broad resonances, with two broad peaks at higher frequency flattening out (Fig 5.10).

There are several mechanisms (Fig. 5.11) that have been proposed to describe the fluxional processes observed for uranyl(VI) complexes of unsymmetrical β-diketonates[66-72]:

(i) rotation of the β-diketonate anions by momentarily opening one of the two coordinated rings and rotating the anion 180° about the remaining U-O bond and then closure to complete the ring again.

(ii) an anion rotation via a concerted intramolecular path.

(iii) an intramolecular migration of the solvent base via a face capped octahedral intermediate.

(iv) dissociation of the solvent molecule, giving an octahedral intermediate, followed by fast displacement of a bound solvent molecule by a free one.

Since ligand dissociation is already being observed and most likely contributing to the *cis-trans* isomerism, mechanism (i) involving the dissociation of one U-O(β-dike) bond is highly likely. If this is the case, then at some high enough temperature the *cis* and *trans* signals should coalesce, as is observed at 20°C in the NMR spectrum of $[UO_2(HL^1)_2(EtOH)]$. Heating a $CDCl_3$ solution of $[UO_2(HL^2)_2(EtOH)]$ to a temperature of 50°C yields a spectrum in which all the signals associated with coordinated HL^2 are coalescing to a broad singlet at 12.26 ppm with a shoulder at 12.40 ppm, again supporting the anion rotation mechanism (i). Since a conformational change to the axial O=U=O bond is most likely occur in mechanism (ii) it will be highly unlikely [69].

The crystal structure of $[UO_2(HL^1)_2(EtOH)]$ shows the ligands bent away from the coordination plane in the same direction and, thus, if this remains the case in solution it will provide a least hindered approach for the solvent circumnavigation of mechanism (iii). The

loss of hyperfine structure in the methyl and methylene proton signals of ethanol upon cooling and the probable lability of the coordinated ethanol give credence to mechanism (iv) occuring in this system.

Thus the ^{1}H NMR spectra of these complexes are difficult to interpret because not only does ligand dissociation occur in solution but there are clearly several other processes occurring.

Figure 5.7 Possible geometric isomers of $[UO_2(HL^1)_2(EtOH)]$ and $[UO_2(HL^2)_2(EtOH)]$

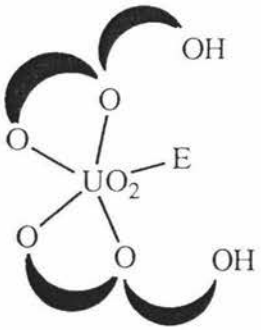

cis

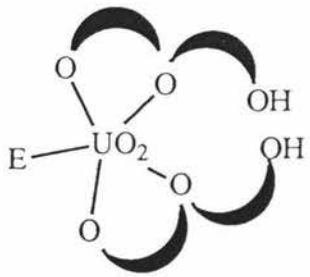

cis

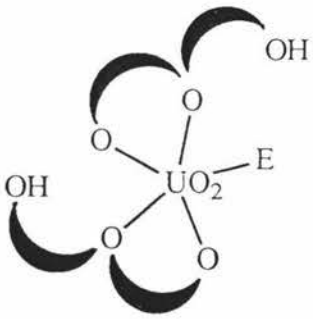

trans

=

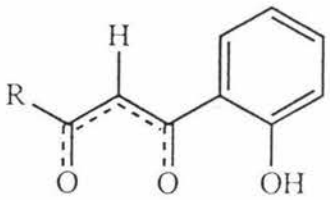

E = EtOH

R = Me, Ph

Figure 5.8 Variable temperature ^1H NMR spectra of $[UO_2(HL^1)_2(EtOH)]$ showing the methyl proton region at 20, -30 and -60 °C.

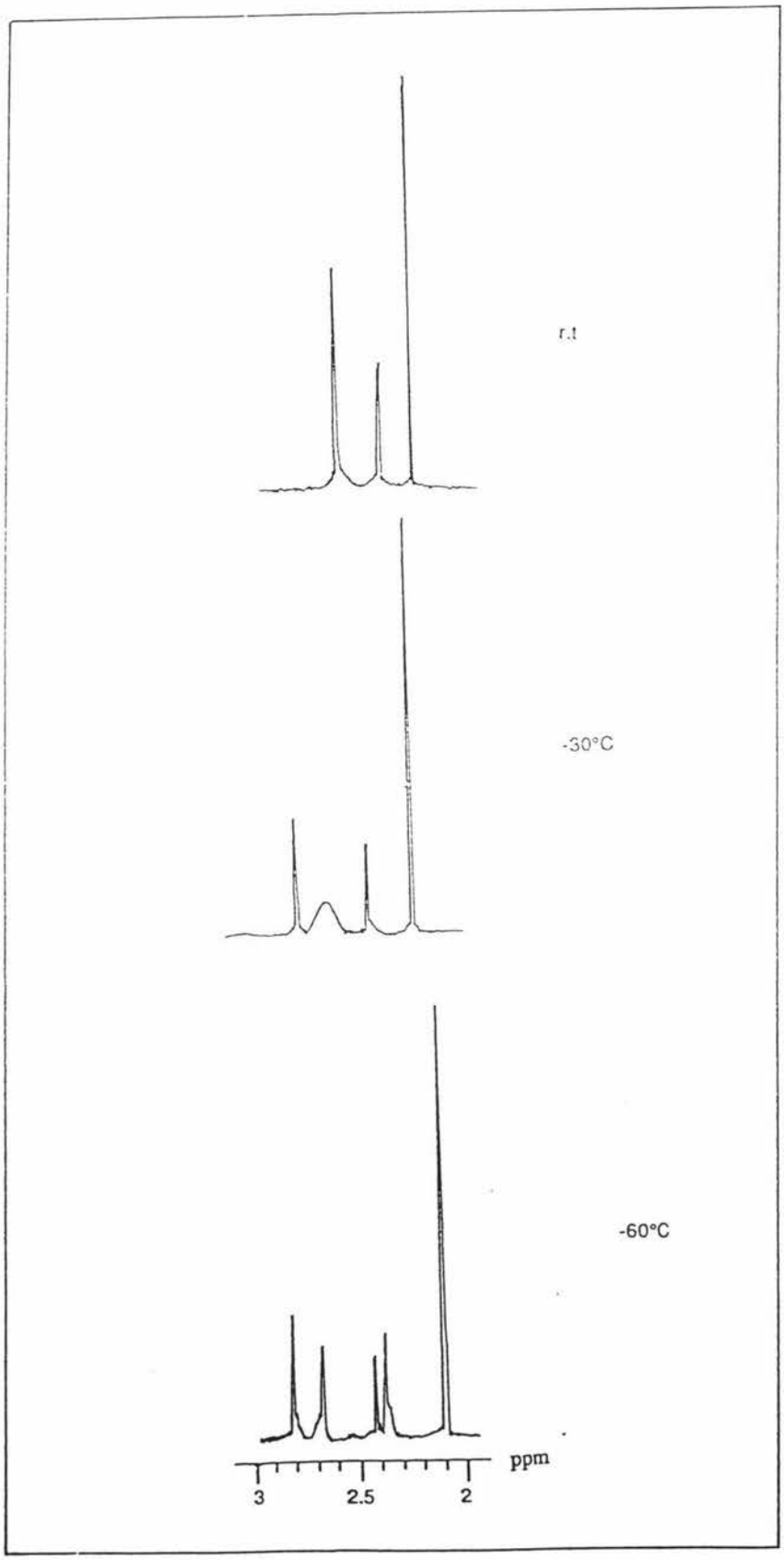

Figure 5.9 Variable temperature ^1H NMR spectra of $[UO_2(HL^1)_2(EtOH)]$ showing the phenol proton region at 20, -30 and -60 °C..

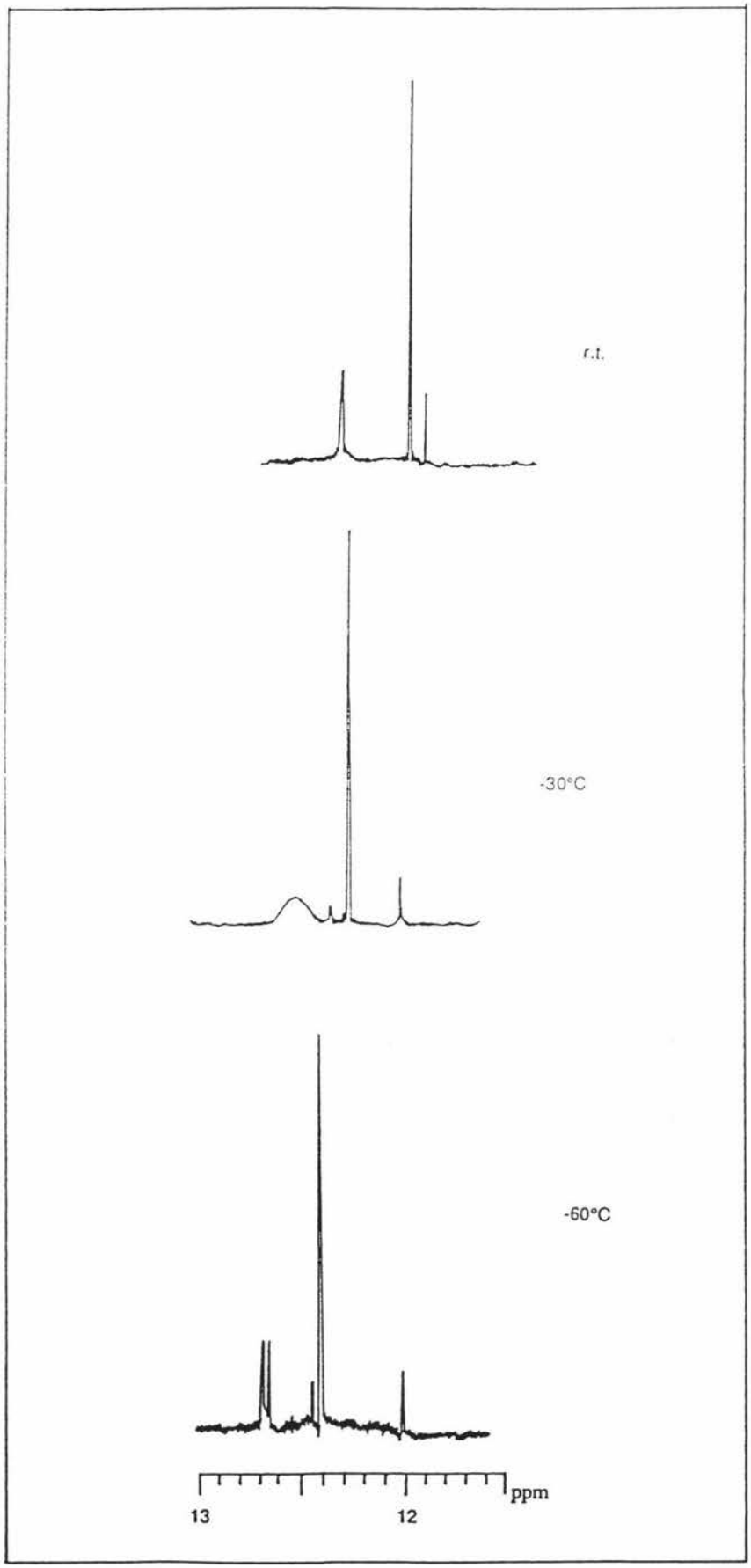

Figure 5.10 Variable temperature ^1H NMR spectra of $[UO_2(HL^2)_2(EtOH)]$ showing the phenol proton region at 50, 20, -10, -30 and -60 °C.

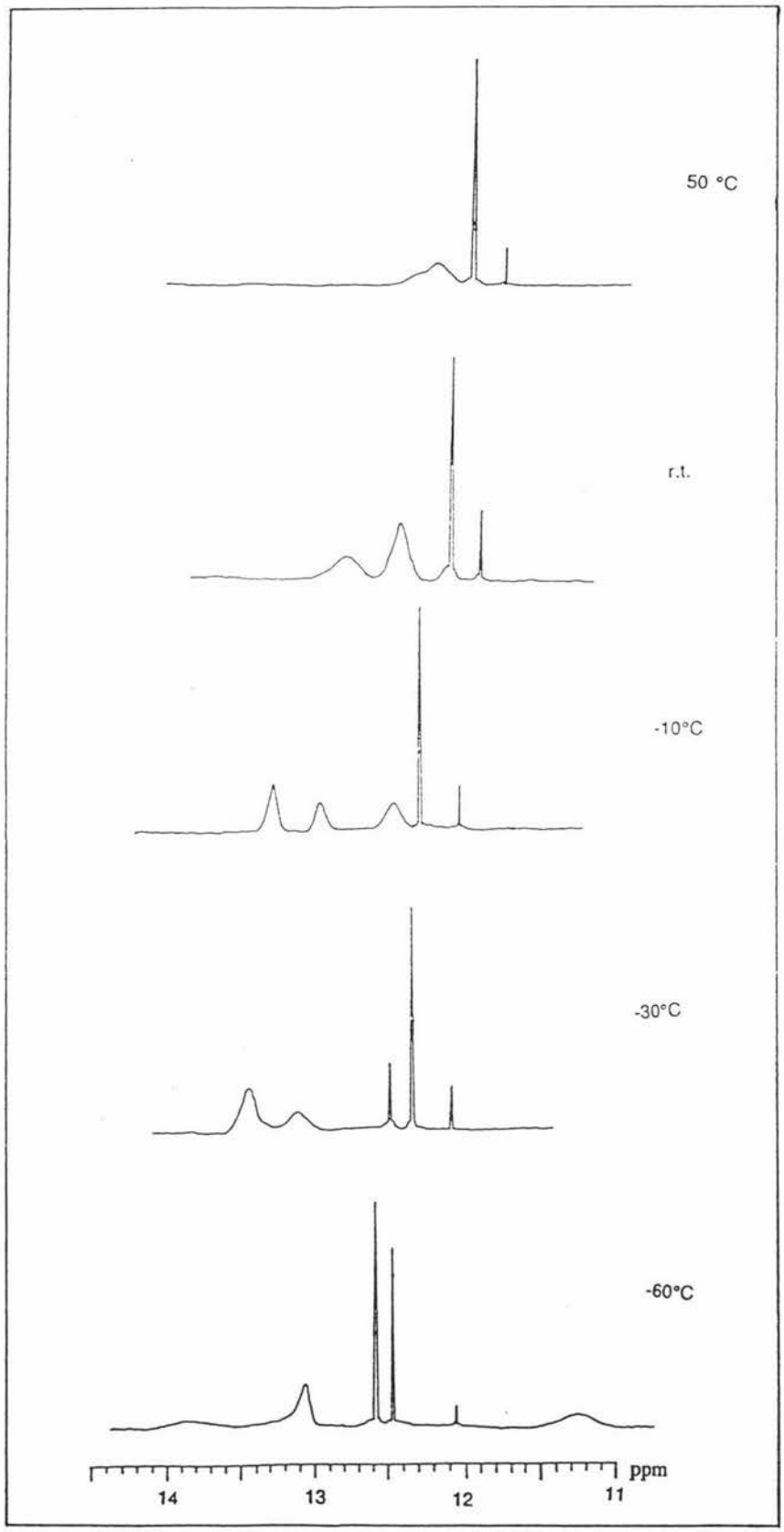

Figure. 5.11. Possible mechanisms for the geometric isomer interchange observed in the ^{1}H NMR Spectra of $[UO_2(HL^1)_2(EtOH)]$ and $[UO_2(HL^2)_2(EtOH)]$

Mechanism (i): anion rotation

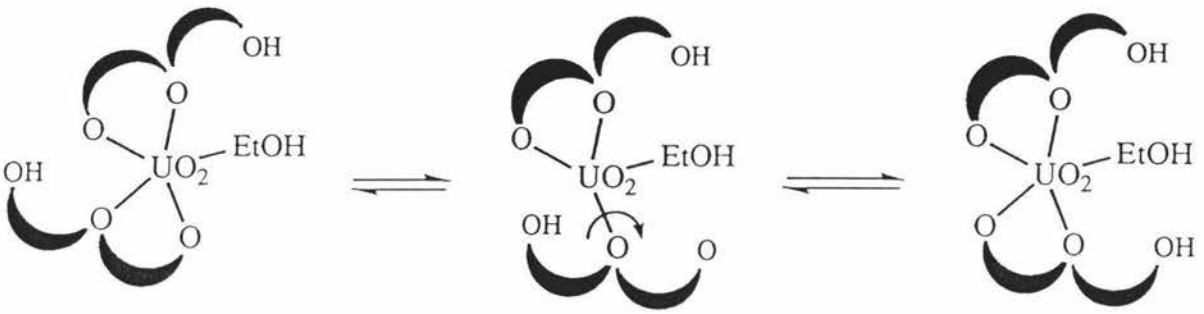

Mechanism (ii): concerted anion rotation

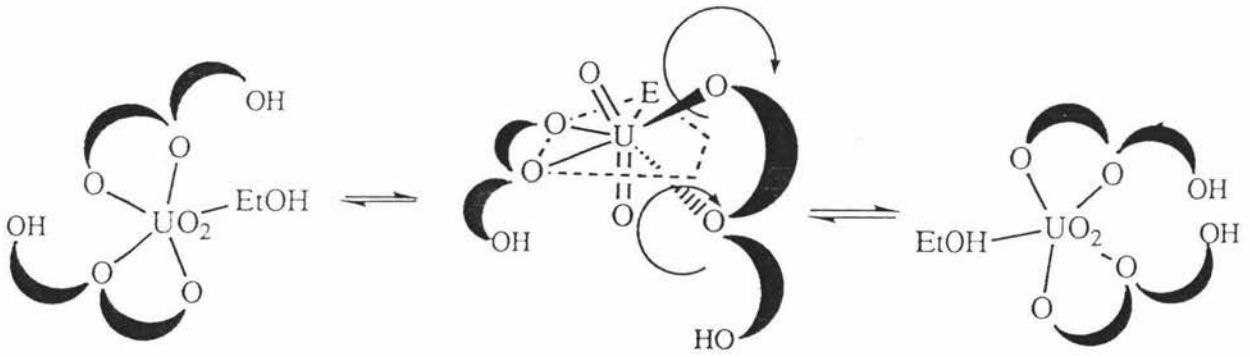

Mechanism (iii): intramolecular solvent migration

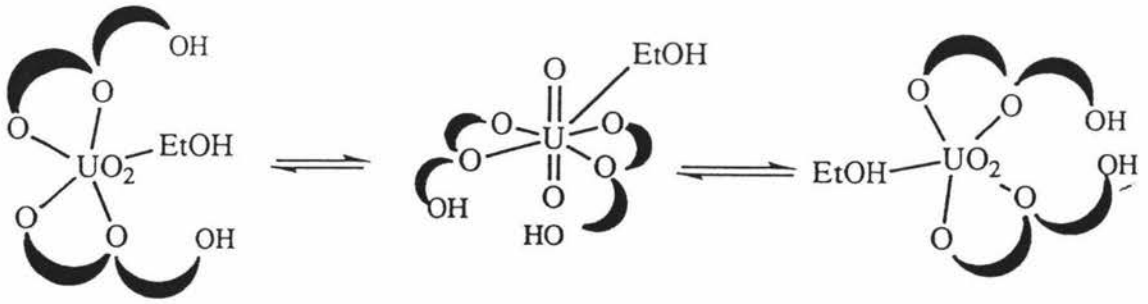

Fig. 5.11 (continued)

Mechanism (iv): intermolecular displacement of solvent

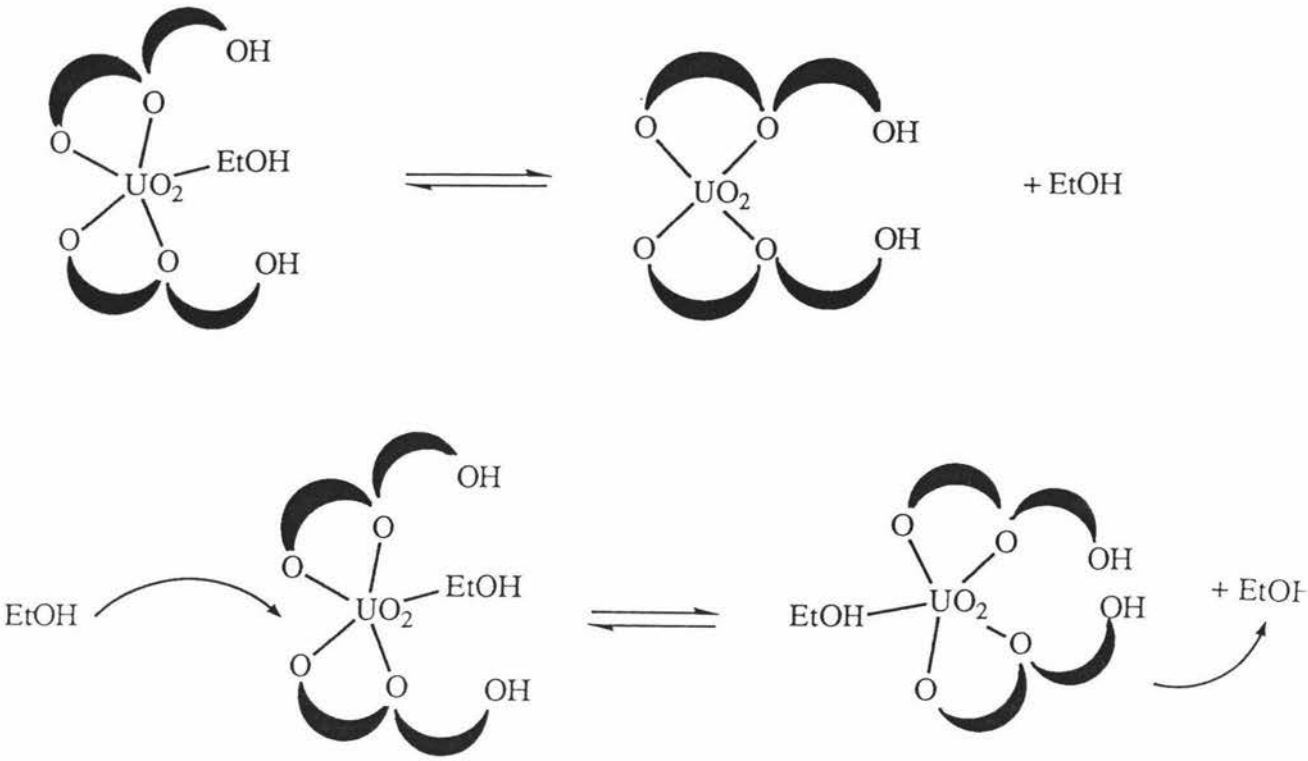

5.1.2(f) Summary

Uranyl(VI) complexes of the β-ketophenol ligands 1-(2-hydroxyphenyl)-1,3-butanedione, H_2L^1, and 1-(2-hydroxyphenyl)-3-phenyl-1,3-propanedione, H_2L^2, have been prepared by addition of uranyl(VI) diacetate to the non-deprotonated ligand.

X-ray crystallographic structures on $[UO_2(HL^1)_2(EtOH)]$ and $[UO_2(HL^2)_2(EtOH)]\cdot EtOH$ show the uranyl coordination geometry is pentagonal bipyramidal, the uranyl ion is coordinated in the "O_4" diketonato site as opposed to the "O_2O_2" phenoxy / ketonato site, and that there exists *cis* and *trans* geometrical isomers of these complexes. This evidence is in accord with the infrared, LSIMS and ^1H NMR spectroscopic results.

5.2 Heterodinuclear Complexes

5.2.1 Synthesis of the Complexes

Previous attempts at preparing heterodinuclear complexes containing uranyl(VI) and β-diketonate ligands such as 1,5-diphenyl-1,3,5-pentanetrione, 2,4,6-heptanetrione, H_2L^1 and H_2L^2 have been unsuccessful [41]. In this study metal exchange is the predominant reaction observed. For example the addition of copper(II) acetate to $[UO_2(HL^2)_2(EtOH)]$ in ethanol produces the copper(II) mononuclear complex $[Cu(HL^2)_2(H_2O)]$, whereas the use of nickel(II) acetate produces an equilibrium mixture of the mononuclear uranyl(VI) and nickel(II) complexes.

In contrast, when manganese(II) acetate was added to an ethanolic solution of the appropriate uranyl mononuclear complex, red microcrystals were isolated that could be formulated by elemental analysis as $[UO_2Mn(L^1)_2(EtOH)]\cdot 1.5H_2O$ and $[UO_2Mn(L^2)_2(EtOH)]\cdot 2H_2O$ respectively. The molar conductivity of ethanolic solutions of these two complexes give values very close to that of their parent mononuclear compounds, which are much less than values expected for 1:1 electrolytes.

5.2.2 Results and Discussion

5.2.2(a) Infrared Spectroscopy

The infrared spectra of $[UO_2Mn(L^1)_2(EtOH)]\cdot 1.5H_2O$ and $[UO_2Mn(L^2)_2(EtOH)]\cdot 2H_2O$ are very similar to those of the mononuclear chelates with small shifts in ν(C=O) and ν(C=C). The $\nu_{as}(O=U=O)$ stretching frequency is shifted to lower values relative to that of the corresponding mononuclear complex (Table 5.1).

5.2.2(b) Electronic Spectroscopy

The electronic spectra of the uranyl(VI) mononuclear complexes consist of two very strong bands at 340 nm (ε = 19,800) and 388 nm (ε = 16,200) for $[UO_2(HL^1)_2(MeOH)]$ and 352 nm (ε = 23,300) and 402 nm (ε = 24,500) for $[UO_2(HL^2)_2(EtOH)]$ respectively and are assigned to intense charge transfer bands arising from the ligand orbital to the 5f and/or 6d orbitals of uranium [26,73]. In each case the low wavelength absorption is perturbed on complexation of the manganese(II), with broad bands at 340 nm (ε = 13,300) and 372 nm (ε = 14,600) for $[UO_2Mn(L^1)_2(EtOH)]\cdot 1.5H_2O$ and $[UO_2Mn(L^2)_2(EtOH)]\cdot 2H_2O$ respectively, as has previously been observed for heterobinuclear uranyl(VI) complexes of Schiff-base ligands derived from 1,3,5-triketones [35]. In all cases ε_{max} values are approximate because of ligand dissociation.

5.2.2(c) Magnetic Susceptibility

The magnetic moment at room temperature for $[UO_2Mn(L^2)_2(EtOH)]\cdot 2H_2O$ is 5.92 BM which is close to the high-spin value for manganese(II)[74], however that for $[UO_2Mn(L^1)_2(EtOH)]\cdot 1.5H_2O$ is slightly lower at 5.41 BM suggesting some weak magnetic interaction between the manganese centres, and hence supporting the structure in Fig. 5.13b.

5.2.2(d) ESR Spectroscopy

Manganese(II) has five unpaired 3d electrons and a relatively long spin relaxation time, and ESR spectroscopy has been readily used to determine it's presence and coordination geometry in Mn(II) containing metalloproteins[75].

The ESR spectrum of Mn(II) in an octahedral environment shows signals with g-values at approximately 4.0 and 2.0 with a hyperfine structure of six lines, arising from hyperfine coupling of the unpaired electron with the Mn(II) nucleus ($I = \frac{5}{2}$)[76].

The ESR spectra of the two heterodinuclear complexes are typical 6-line spectra for d^5 Mn(II), centred near the free electron value. For $[UO_2Mn(L^1)_2(EtOH)]\cdot 1.5H_2O$ g = 2.054 , whereas for $[UO_2Mn(L^2)_2(EtOH)]\cdot 2H_2O$ g = 2.048 (Fig. 5.12). Both spectra have A values of approximately 90 Gauss. The A-value in Mn(II) depends strongly on the covalent bonding between Mn(II) and the ligand[77]. Thus the spectral pattern and the A-values observed for these two complexes is consistent with Mn(II) residing in a highly symmetrical coordination sphere of oxygen donors.

5.2.2(e) Mass Spectroscopy

The LSIMS spectrum of $[UO_2Mn(L^1)_2(EtOH)]\cdot 1.5H_2O$, using *m* -nitrobenzyl alcohol as the matrix, yielded the highest peak at m/z = 1357 (relative intensity = 25%) and this is designated as a dimeric species, $[(UO_2)_2(Mn)_2(L^1)_4H]^+$ (e.g. as in Fig. 5.13(b)) This observation is in line with the magnetic susceptibility results for the complex as discussed in Section 5.2.2(c).Further peaks at lower masses were assigned as follows; $[(UO_2)_2Mn(L^1)_4H]^+$ (1303, 35%); $[(UO_2)_2Mn(L^1)_3H]^+$ (1124, 46%); $[[UO_2Mn(L^1)_2H]^+$ (678, 100%); $[UO_2(L^1)_2H]^+$ (625, 90%); $[[UO_2Mn(L^1)]^+$ (501, 48%); $[UO_2(HL^1)]^+$ (447, 64%) and $[UO_2]^+$ (270, 57%).

The LSIMS spectrum of $[UO_2Mn(L^2)_2(EtOH)]\cdot 2H_2O$, in the "magic bullet" matrix, was measured and a peak assigned to [M - EtOH,1.5H_2O]+ (relative intensity = 51%) was observed. Higher masses were observed and are assigned to mixed ligand complexes involving the rearranged flavone ligand (L^4, page 96) derived from the ligand H_2L^2, e.g. $[UO_2(L2)(L4)_2H]+$ (m/z = 954, 100%); $[UO_2Mn(L2)(L4)_2)]+$ (1008, 27%).Other major

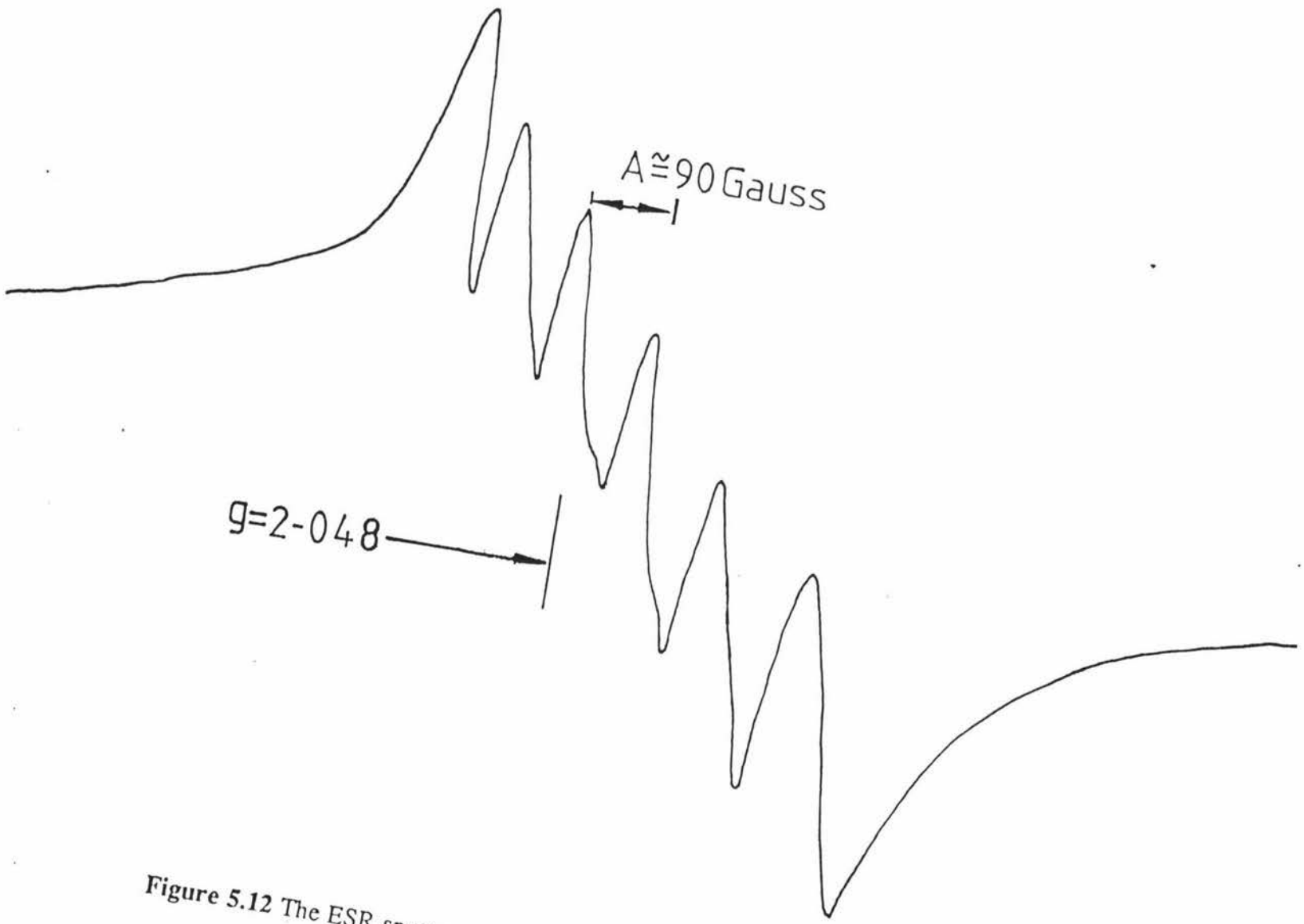

Figure 5.12 The ESR spectrum of $[UO_2Mn(L^2)_2(EtOH)]\cdot 2H_2O$

peaks observed are $[UO_2(L^4)_2H]^+$ (716, 90%), $[UO_2Mn(L^2)H]^+$ (563, 30%), $[UO_2(L^4)H]^+$ (492, 67%) and $[UO_2]^+$ (270, 100%).

5.2.2(f) Summary

Heterodinuclear complexes of the β-ketophenol ligands 1-(2-hydroxyphenyl)-1,3-butanedione, H_2L^1, and 1-(2-hydroxyphenyl)-3-phenyl-1,3-propanedione, H_2L^2, have been prepared by the addition of manganese(II) acetate to the appropriate uranyl(VI) mononuclear complex.

Without X-ray structural information for these heterobinuclear complexes, the question of where the manganese(II) atom is bound cannot be categorically answered, but to date it has not been possible to obtain suitable crystals. These complexes are soluble non-electrolytes and their ESR spectra are very similar to those of $Mn(II)O_6$ complexes, implying the manganese ion is most likely octahedral in coordination geometry.Mass spectral and magnetic susceptibility data would indicate a structure as depicted in Fig. 5.13(b) is a possibility for $[UO_2Mn(L^1)_2(EtOH)]\cdot 1.5H_2O$, whereas the structure of Fig. 5.13(a) is a possibility for the L^2 complex.

5.3 Experimental

The ligands, 1-(2-hydroxyphenyl)-1,3-butanedione(H2L1) and 1-(2-hydroxyphenyl)-3-phenyl-1,3-propanedione (H2L2), were purchased from Frinton Laboratories and uranyl(VI) diacetate from May and Baker Ltd.

Figure 5.13 Some possible structures for the heterodinuclear complexes presented: (a) Mn(II) is coordinated in the "O_2O_2" site
(b) dimeric structure involving bridging ligand oxygens.

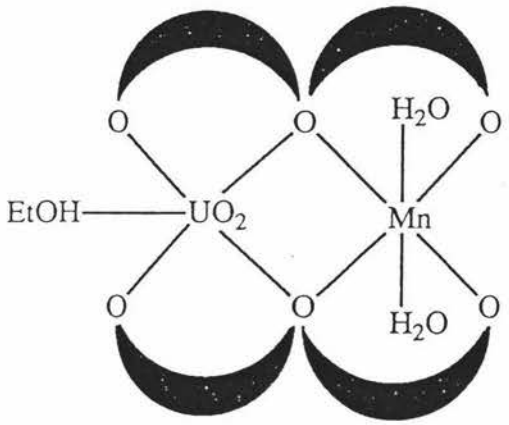

(a)

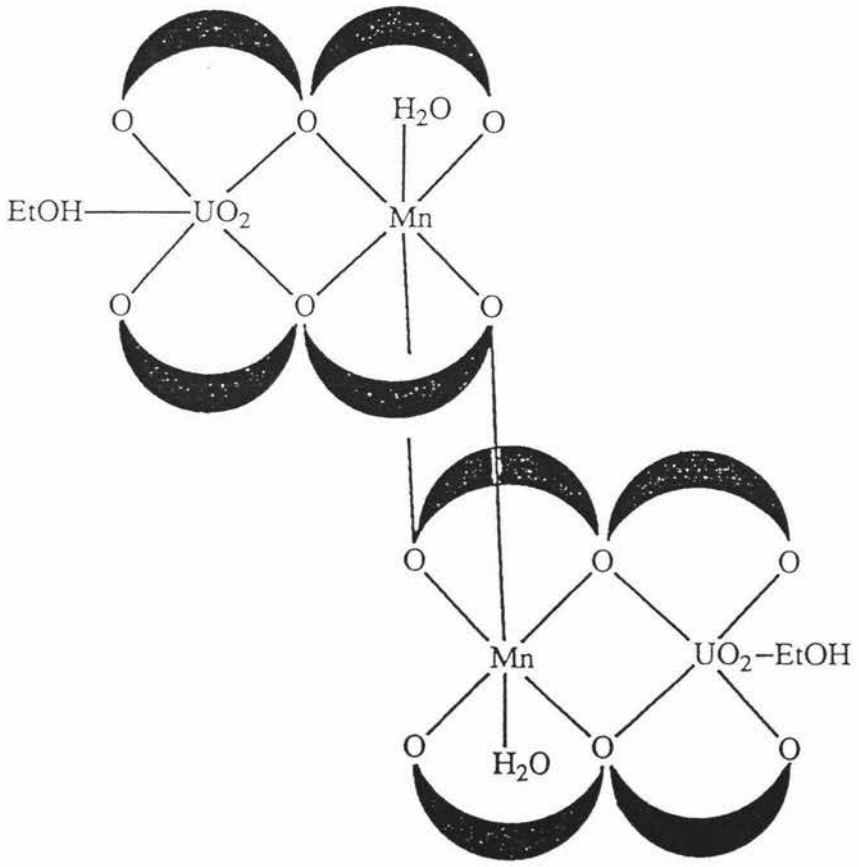

(b)

5.3.1 Preparation of the Mononuclear Complexes - $[UO_2(HL^1)_2(MeOH)]$ and $[UO_2(HL^2)_2(EtOH)]$

The method of synthesis was an adaption of the method employed by Vigato *et al* .[41]. To an ethanolic solution (40 cm^3) of the appropriate ligand (1 mmol) was added dropwise a solution of uranyl acetate dihydrate (0.5 mmol) in ethanol (15 cm^3). The resulting bright orange solution was left to stand for 48 hours yielding crystals which were filtered off, washed with a small amount of ethanol followed by diethyl ether, and dried *in-vacuo*. For the HL^1 complex, the product was washed with methanol, which resulted in a molecule of this solvent being incorporated into the complex. Yields of 93% and 87% were obtained for $[UO_2(HL^1)_2(MeOH)]$ and $[UO_2(HL^2)_2(EtOH)]$ respectively. Crystals of both complexes suitable for X-ray crystallography were obtained by slow evaporation of an ethanol solution of the appropriate complex.

5.3.2 Preparation of Heterobinuclear Complexes -$[UO_2Mn(L^1)_2(EtOH)]\cdot 1.5\,H_2O$ and $[UO_2Mn(L^2)_2(EtOH)]\cdot 2H_2O$

Manganese diacetate tetrahydrate (0.5 mmol) in ethanol (20 cm^3) was added dropwise to an ethanolic solution (50 cm^3) of the uranyl mononuclear complex (0.5 mmol), with gentle heating. The volume of the resulting red solution was reduced using a rotary evaporator until precipitation occured. The solid was collected by filtration, washed with small amounts of water, ethanol and diethyl ether, and dried *in-vacuo*. Yields *ca* . 50%.

5.3.3 Preparation of Adducts with Triphenylphosphine Oxide and Triphenylarsine Oxide- $[UO_2(HL^1)_2(Ph_3AsO)]\cdot 2H_2O$, $[UO_2(HL^2)_2(Ph_3PO)]$ and $[UO_2(HL^2)_2(Ph_3AsO)]$

Triphenylphosphine oxide or triphenylarsine oxide (0.5 mmol) in ethanol (5 cm^3) was added to an ethanolic solution (30 cm^3) of the appropriate mononuclear complex (0.5 mmol). The

solution was refluxed for an hour and the resulting yellow/orange precipitate was filtered, washed with ethanol, and dried *in-vacuo*. Yields *ca* . 70 - 90%.

5.4 The Crystal Structure Determination of [(ethanol-κO)bis(1-(2-hydroxy-phenyl -1,3-butanedionato-κ^2O,O')dioxouranium(VI)], $[UO_2(HL^1)_2(EtOH)]$

5.4.1 Crystal Preparation and Data Collection

The crystal was grown by slow evaporation of an ethanol solution.Data were collected using the general method described in section 2.10.3. All crystal data and parameters associated with data collection are summarised in Table 5.9.

5.4.2 Data Processing and Structure Solution

Data were processed as described in section 2.10.4. The diffraction symmetry was characteristic of the triclinic class and the unit cell volume indicated only one molecule per unit cell, suggesting that the space group was P1. The uranium was placed at the origin and a structure factor calculation based on this position gave a residual, R, of 0.15. Calculation of an electron density map, based on the phasing contribution of the uranium atom, revealed the positions of the oxygen donor atoms. A series of electron density maps and least-squares calculations revealed all non-hydrogen atom positions and gave a residual of 0.038. Hydrogen atoms were placed in calculated positions (C-H = 0.96 Å) and, except for the phenolic hydrogens (H(11) and H(21)), were constrained to ride on their associated carbon atoms.The isotropic thermal parameters of the hydrogen atoms were constrained to 0.06 and not refined. Anisotropic motion was assumed for all non-hydrogen atoms in the final stages of refinement. At convergence the "hand" of the molecule was reversed but the effect of this on on R and R_w was negligible. However inspection of the two uranyl U-O bond distances showed a significant difference between them: (U-O(1), 1.820(18); U-O(2), 1.718(17)Å) for the original "hand", whereas when the hand was reversed these distances were

clearlycomparable (U-O(1), 1.784(15); U-O(2), 1.746(17)Å). This latter form of the molecule was deemed to be correct. Final R-factors of R = 0.032 and R_w = 0.036 were obtained. Parameters associated with data processing and with structure solution and refinement are summarised in Tables 5.10 and 5.11 respectively. Atomic coordinates for all non-hydrogen atoms are given in Table 5.12. Anisotropic thermal parameters are listed in Table 5.13. Table 5.14 lists hydrogen atom coordinates and isotropic thermal parameters. Observed and calculated structure factors are listed on microfiche at the end of this thesis.

Table 5.9 Data Collection Parameter Summary For $[UO_2(HL^1)_2(EtOH)]$

Compound	$[UO_2(HL^1)_2(EtOH)]$
Formula	$C_{22}H_{24}O_9U$
Formula weight (a.m.u)	670.46
Crystal size (mm)	0.28 x 0.21 x 0.17
Space group	P1
a (Å)	8.077(1)
b (Å)	8.130(1)
c (Å)	10.162(1)
α (°)	108.50(1)
β (°)	112.26(1)
γ (°)	89.89(1)
V ($Å^3$)	580.3
Z	1
λ (Mo-Kα) (Å)	0.71073
μ (Mo-Kα) (cm^{-1})	66.7
F(000)	320
Number and θ range (°) of reflections used for determining lattice parameters	25,16.99 - 18.65
Temperature of measurement (K)	290
Scan mode	$\omega/2\theta$
ω scan angle (°)	0.80 + 0.34*tanθ
Detector horizontal aperture width (mm)	1.40 + 0.70*tanθ
Detector vertical aperture width (mm)	4
Incident beam collimator diameter (mm)	0.8
Prescan scan speed (° min^{-1})	8.24
Prescan acceptance $\sigma(I)/(I)$	0.5
Requested counting $\sigma(I)/(I)$	0.018
Maximum scan time (sec)	90
Maximum value of θ reached in intensity measurement (°)	30
Range of *h*, *k* and *l*	0 ->11, -11 -> 11, -13 -> 13
Standard reflections used to monitor intensity variation	-5 1 -3, 2 -4 -5, 7 1 -6
Requested $\sigma(I)/(I)$ for standard intensity measurements	0.012
Interval between standard intensity measurements (sec)	7200
Maximum permissable deviation between observed and calculated positions of standard orientation reflections (°)	0.10

Table 5.10 Data Processing Parameter Summary For $[UO_2(HL^1)_2(EtOH)]$

Total number of reflections measured	4895
Number of reflections considered unobserved from prescan data	128
Total x-ray exposure time (hrs)	182.1
Average standard intensity variation (%)	-2.3
Correction applied for intensity decay of standard reflections	Anisotropic
Method used for absorption correction	Empirical
Minimum transmission value (%)	51.1
Maximum transmission value (%)	99.9
Minimum absorption correction	0.751
Maximum absorption correction	1.000
Number of unique reflections measured	4895

Table 5.11 Structure Solution and Refinement Parameter Summary For $[UO_2(HL^1)_2(EtOH)]$

Method used to solve structure	Patterson
Criterion for recognising unobserved reflections during refinement	$F_{obs}^2>3\sigma(Fobs^2)$
Number of reflections used in refinement	4671
Method of locating Hydrogen atoms	Calculated positions
Weighting scheme§;k,g	1.0000, 0.010096
Parameters refined	299
Value of R	0.032
Value of R_w	0.036
Maximum and minimum height in final difference electron density map ($eÅ^{-3}$)	1.53, -2.82
Computer programs used	SHELX-76,SDP-PLUS package

§ weight = $k/\sigma^2(Fobs) + g^*(Fobs^2)$

Table 5.12 Fractional Atomic Coordinates for the Non-Hydrogen Atoms of[$UO_2(HL^1)_2(EtOH)$] (estimated standard deviations in parentheses)

Atom	x/a	y/b	z/c
U	0.0000	0.0000	0.0000
O(1)	-0.172(2)	-0.143(2)	-0.170(2)
O(2)	0.181(3)	0.136(2)	0.159(2)
O(3)	0.067(1)	-0.261(1)	0.074(1)
O(11)	-0.060(2)	0.432(1)	-0.173(1)
O(12)	0.061(1)	0.154(1)	-0.144(1)
O(13)	0.220(1)	-0.124(1)	-0.090(1)
O(21)	-0.161(2)	-0.210(2)	0.299(2)
O(22)	-0.161(1)	-0.002(1)	0.148(1)
O(23)	-0.174(2)	0.225(1)	-0.004(1)
C(1)	0.247(2)	-0.272(2)	0.179(3)
C(2)	0.247(4)	-0.411(4)	0.242(4)
C(11)	0.128(1)	0.129(1)	-0.244(1)
C(12)	0.230(2)	-0.004(2)	-0.272(1)
C(13)	0.264(3)	-0.117(3)	-0.190(3)
C(14)	0.406(2)	-0.246(2)	-0.214(2)
C(21)	-0.284(2)	0.092(2)	0.189(2)
C(22)	-0.358(15)	0.212(2)	0.126(1)
C(23)	-0.302(1)	0.273(1)	0.033(1)
C(24)	-0.404(2)	0.406(2)	-0.030(2)
C(111)	0.087(1)	0.252(1)	-0.3269(9)
C(112)	-0.003(1)	0.397(1)	-0.289(1)
C(113)	-0.045(2)	0.511(1)	-0.372(1)
C(114)	0.01(1)	0.49(7)	-0.50(6)
C(115)	0.098(2)	0.347(2)	-0.531(1)
C(116)	0.136(2)	0.233(1)	-0.452(1)
C(211)	-0.314(1)	0.056(2)	0.312(1)
C(212)	-0.253(2)	-0.086(2)	0.360(1)
C(213)	-0.284(2)	-0.109(3)	0.481(2)
C(214)	-0.372(2)	0.013(3)	0.553(2)
C(215)	-0.430(2)	0.155(3)	0.511(2)
C(216)	-0.403(1)	0.173(2)	0.388(1)

Table 5.13 Anisotropic Thermal Parameters for the Non-Hydrogen Atoms of $[UO_2(HL^1)_2(EtOH)]$ (estimated standard deviations in parentheses)

Atom	U11	U22	U33	U23	U13	U12
U	0.0406(1)	0.0323(1)	0.0313(1)	0.0147(1)	0.0193(1)	0.0123(1)
O(1)	0.039(5)	0.067(7)	0.032(4)	0.005(4)	0.016(4)	0.002(4)
O(2)	0.074(7)	0.040(4)	0.050(5)	0.024(3)	0.017(4)	0.015(4)
O(3)	0.058(4)	0.042(3)	0.047(3)	0.024(3)	0.021(3)	0.018(3)
O(11)	0.086(6)	0.041(3)	0.054(4)	0.024(3)	0.051(4)	0.026(3)
O(12)	0.067(4)	0.050(3)	0.058(4)	0.031(3)	0.046(4)	0.023(3)
O(13)	0.061(4)	0.053(4)	0.064(5)	0.032(4)	0.040(4)	0.027(3)
O(21)	0.107(10)	0.067(6)	0.083(8)	0.050(6)	0.061(8)	0.043(7)
O(22)	0.063(4)	0.047(3)	0.054(4)	0.027(3)	0.040(3)	0.025(3)
O(23)	0.077(5)	0.052(4)	0.079(6)	0.041(4)	0.057(5)	0.038(4)
C(1)	0.058(6)	0.064(8)	0.09(1)	0.045(9)	0.005(7)	0.008(6)
C(2)	0.12(2)	0.1(2)	0.12(2)	0.08(2)	0.00(2)	0.01(1)
C(11)	0.041(3)	0.033(3)	0.041(3)	0.013(2)	0.022(3)	0.008(2)
C(12)	0.051(4)	0.054(5)	0.053(5)	0.020(4)	0.033(4)	0.018(4)
C(13)	0.035(7)	0.048(7)	0.058(6)	0.017(5)	0.029(5)	-0.003(5)
C(14)	0.053(5)	0.057(6)	0.08(1)	0.028(6)	0.043(6)	0.026(4)
C(21)	0.023(4)	0.043(5)	0.032(3)	0.011(3)	0.017(3)	0.000(4)
C(22)	0.049(4)	0.065(5)	0.046(4)	0.034(4)	0.027(4)	0.026(4)
C(23)	0.056(4)	0.036(3)	0.041(4)	0.014(3)	0.023(3)	0.019(3)
C(24)	0.058(6)	0.063(6)	0.067(7)	0.038(5)	0.031(5)	0.027(5)
C(111)	0.040(3)	0.040(3)	0.034(3)	0.010(2)	0.019(2)	0.003(3)
C(112)	0.056(4)	0.033(3)	0.040(3)	0.014(2)	0.028(3)	0.008(3)
C(113)	0.068(6)	0.038(3)	0.041(4)	0.017(3)	0.026(4)	0.012(3)
C(114)	0.072(9)	0.052(6)	0.056(6)	0.007(5)	0.024(6)	-0.002(6)
C(115)	0.77(7)	0.051(4)	0.042(4)	0.014(3)	0.037(4)	0.005(4)
C(116)	0.054(5)	0.045(4)	0.046(4)	0.015(3)	0.030(4)	0.007(3)
C(211)	0.040(3)	0.060(5)	0.041(4)	0.029(3)	0.021(3)	0.018(3)
C(212)	0.050(4)	0.062(6)	0.048(5)	0.030(4)	0.024(4)	0.014(4)
C(213)	0.069(8)	0.09(1)	0.064(8)	0.053(8)	0.039(6)	0.023(7)
C(214)	0.047(5)	0.10(1)	0.048(5)	0.035(6)	0.022(4)	0.002(5)
C(215)	0.054(5)	0.11(1)	0.049(5)	0.038(7)	0.034(4)	0.018(6)
C(216)	0.045(4)	0.074(6)	0.039(4)	0.022(4)	0.025(3)	0.015(4)

Table 5.14 Hydrogen Atom Coordinates and Isotropic Thermal Parameters for $[UO_2(HL^1)_2(EtOH)]$

Atom	x/a	y/b	z/c	U
H(11)	-0.0100	-0.6615	-0.1140	0.06
H(21)	-0.1448	-0.1884	0.2077	0.06
H(1a)	0.3219	-0.3050	0.1231	0.06
H(1b)	0.2982	-0.1606	0.2574	0.06
H(2a)	0.3676	-0.4166	0.3081	0.06
H(2b)	0.1964	-0.5233	0.1652	0.06
H(2c)	0.1743	-0.3776	0.2995	0.06
H(12)	0.2897	-0.0449	-0.3395	0.11
H(14a)	0.4369	-0.2410	-0.2950	0.06
H(14b)	0.3552	-0.3636	-0.2365	0.06
H(14c)	0.5126	-0.2127	-0.1216	0.06
H(22)	-0.4495	0.2319	0.1656	0.12
H(24a)	-0.5000	0.4329	0.0030	0.06
H(24b)	-0.4523	0.3569	-0.1388	0.06
H(24c)	-0.3224	0.5107	0.0031	0.06
H(113)	-0.1121	0.6035	-0.3437	0.06
H(114)	-0.0159	0.5713	-0.5536	0.06
H(115)	0.1341	0.3269	-0.6138	0.06
H(116)	0.1355	0.2332	-0.4516	0.06
H(213)	-0.2458	-0.2066	0.5134	0.06
H(214)	-0.3921	-0.0028	0.6356	0.06
H(215)	-0.4861	0.2387	0.5642	0.06
H(216)	-0.4464	0.2691	0.3548	0.06

5.5 The Crystal Structure Determination of [(ethanol-κO)bis(1-(2-hydroxyphenyl)-3-phenyl-1,3-propanedionato-κ²O,O')dioxouranium(VI)]Ethanol, $[UO_2(HL^2)_2(EtOH)]\cdot EtOH$

5.5.1 Crystal Preparation and Data collection

The crystal was grown by slow evaporation of an ethanol solution.

Data were collected using the general method described in section 2.10.3. All crystal data and parameters associated with data collection are summarised in Table 5.15.

5.5.2 Data Processing and Structure Solution

Data were processed as described in section 2.10.4. A possible uranium site at (x,y,z) = (0.3330,0.2832,0.1250) corresponding to the Patterson vector 2x,2y,2z at (0.6660,0.5664,0.2500) was identified from the Patterson map and a structure factor calculation based on this position gave a residual, R, of 0.24.

Calculation of an electron density map, based on the phasing contribution of the uranium atom, revealed the positions of the oxygen atoms and several carbon atoms. A series of electron density maps and least-squares calculations revealed all non-hydrogen atom positions and gave a residual of 0.076.

In subsequent refinement, all phenyl rings were refined as rigid groups (C-C = 1.395 Å). Hydrogen atoms were placed in calculated positions (C-H = 0.96) and, except for the phenolic and vinylic hydrogens (H(11), H(21), H(12) and H(22)), were constrained to ride on their associated carbon atoms. The isotropic thermal parameters of the hydrogen atoms were constrained at U = 0.10. Anisotropic thermal motion was assumed for all non-hydrogen atoms in the final stages of refinement. Final R-factors of R = 0.033 and R_w = 0.033 were obtained. Parameters associated with data processing and with structure solution and refinement are summarised in Tables 5.16 and 5.17 respectively. Atomic coordinates for all non-hydrogen atoms are given in Table 5.18. Anisotropic thermal parameters are listed in Table 5.19. Table

5.20 lists hydrogen atom coordinates and isotropic thermal parameters. Observed and calculated structure factors are listed on microfiche at the end of this thesis.

Table 5.15 Data Collection Parameter Summary For $[UO_2(HL^2)_2(EtOH)]\cdot EtOH$

Compound	$[UO_2(HL^2)_2(EtOH)]\cdot EtOH$
Formula	$C_{34}H_{34}O_{10}U$
Formula weight (a.m.u)	840.67
Crystal size (mm)	0.28 x 0.28 x 0.21
Space group	$P\bar{1}$
a (Å)	12.184(3)
b (Å)	15.578(5)
c (Å)	9.035(2)
α (°)	91.05(2)
β (°)	103.20(2)
γ (°)	73.21(2)
V (Å^3)	1596.9
Z	2
λ (Mo-Kα) (Å)	0.71073
μ (Mo-Kα) (cm^{-1})	48.7
F(000)	784
Number and θ range (°) of reflections used for determining lattice parameters	25,14.93 - 15.69
Temperature of measurement (K)	290
Scan mode	$\omega/2\theta$
ω scan angle (°)	0.80 + 0.34*tanθ
Detector horizontal aperture width (mm)	2.50 + 0.80*tanθ
Detector vertical aperture width (mm)	4
Incident beam collimator diameter (mm)	0.8
Prescan scan speed (° min^{-1})	8.24
Prescan acceptance σ(I)/(I)	0.5
Requested counting σ(I)/(I)	0.020
Maximum scan time (sec)	90
Maximum value of θ reached in intensity measurement (°)	24
Range of *h*, *k* and *l*	-14 ->14, -18 -> 18, 0 -> 10
Standard reflections used to monitor intensity variation	-4 9 2, 3 9 4, 6 -6 -2
Requested σ(I)/(I) for standard intensity measurements	0.013
Interval between standard intensity measurements (sec)	7200
Maximum permissable deviation between observed and calculated positions of standard orientation reflections (°)	0.10

Table 5.16 Data Processing Parameter Summary For $[UO_2(HL^2)_2(EtOH)]\cdot EtOH$

Total number of reflections measured	6625
Number of reflections considered unobserved from prescan data	306
Total x-ray exposure time (hrs)	90.4
Average standard intensity variation (%)	-4.3
Correction applied for intensity decay of standard reflections	Anisotropic
Method used for absorption correction	Empirical
Minimum transmission value (%)	83.8
Maximum transmission value (%)	99.9
Minimum absorption correction	1.000
Maximum absorption correction	1.022
Number of unique reflections measured	6223
Number of equivalent reflections averaged	498
Value of merging R, based on intensity of observed reflections	0.022

Table 5.17 Structure Solution and Refinement Parameter Summary For $[UO_2(HL^2)_2(EtOH)]\cdot EtOH$

Method used to solve structure	Patterson
Criterion for recognising unobserved reflections during refinement	$F_{obs}^2>3\sigma(Fobs^2)$
Number of reflections used in refinement	3268
Method of locating Hydrogen atoms	Calculated positions
Weighting scheme§;k,g	1.3274, 0.000919
Parameters refined	368
Value of R	0.033
Value of R_w	0.033
Maximum and minimum height in final difference electron density map ($eÅ^{-3}$)	1.14, -1.21
Computer programs used	SHELX-76,SDP-PLUS package

§ weight = $k/\sigma^2(Fobs) + g*(Fobs^2)$

Table 5.18 Fractional Atomic Coordinates for the Non-Hydrogen Atoms of$[UO_2(HL^2)_2(EtOH)]\cdot EtOH$ (estimated standard deviations in parentheses)

Atom	x/a	y/b	z/c
U	0.3327	0.2871	0.1228
O(1)	0.2334(6)	0.3038(5)	0.2413(8)
O(2)	0.4358(6)	0.2714(5)	0.0090(7)
O(3)	0.4681(5)	0.3552(4)	0.3012(6)
O(4)	0.5339(7)	0.5997(6)	0.4180(8)
O(11)	0.6437(8)	0.1748(5)	0.5014(1)
O(12)	0.4690(5)	0.1686(4)	0.2907(7)
O(13)	0.2952(6)	0.1533(4)	0.0581(8)
O(21)	0.3273(6)	0.5663(4)	0.2406(8)
O(22)	0.2661(5)	0.4476(4)	0.0753(7)
O(23)	0.1874(6)	0.3249(4)	-0.0995(7)
C(1)	0.5830(8)	0.3579(8)	0.2913(12)
C(2)	0.5812(11)	0.4101(8)	0.1568(13)
C(3)	0.5654(16)	0.6479(11)	0.3114(16)
C(4)	0.6327(18)	0.7024(12)	0.3697(16)
C(11)	0.5055(8)	0.0835(6)	0.2925(10)
C(12)	0.4501(8)	0.0334(6)	0.1855(10)
C(13)	0.3468(7)	0.0688(6)	0.0761(10)
C(21)	0.1738(7)	0.5069(6)	-0.0059(9)
C(22)	0.1004(8)	0.4812(6)	-0.1290(9)
C(23)	0.1091(7)	0.3936(6)	-0.1736(9)
C(111)	0.6110(4)	0.0360(3)	0.4148(6)
C(112)	0.6736(4)	0.0862(3)	0.5093(6)
C(113)	0.7716(4)	0.0431(3)	0.6239(6)
C(114)	0.8069(4)	-0.0503(3)	0.6441(6)
C(115)	0.7444(4)	-0.1005(3)	0.5496(6)
C(116)	0.6464(4)	-0.0573(3)	0.4350(6)
C(131)	0.2864(5)	0.0120(4)	-0.0237(6)
C(132)	0.3255(5)	-0.0815(4)	-0.0054(6)
C(133)	0.2658(5)	-0.1328(4)	-0.1014(6)
C(134)	0.1670(5)	-0.0907(4)	-0.2157(6)

(Table continued over page)

C(135)	0.1279(5)	0.0027(4)	-0.2340(6)
C(136)	0.1875(5)	0.0541(4)	-0.1380(6)
C(211)	0.1537(5)	0.6013(3)	0.0346(6)
C(212)	0.2313(5)	0.6246(3)	0.1563(6)
C(213)	0.2100(5)	0.7136(3)	0.1972(6)
C(214)	0.1111(5)	0.7793(3)	0.1163(6)
C(215)	0.0334(5)	0.7560(3)	-0.0054(6)
C(216)	0.0547(5)	0.6670(3)	-0.0462(6)
C(231)	0.0309(5)	0.3748(4)	-0.3126(5)
C(232)	-0.0705(5)	0.4402(4)	-0.3886(5)
C(233)	-0.1415(5)	0.4201(4)	-0.5209(5)
C(234)	-0.1111(5)	0.3346(4)	-0.5772(5)
C(235)	-0.0097(5)	0.2693(4)	-0.5011(5)
C(236)	0.0613(5)	0.2893(4)	-0.3688(5)

Table 5.19 Anisotropic Thermal Parameters for the Non-Hydrogen Atoms of $[UO_2(HL^2)_2(EtOH)]\cdot EtOH$ (estimated standard deviations in parentheses)

Atom	U11	U22	U33	U23	U13	U12
U	0.0416(2)	0.0410(2)	0.0375(2)	-0.0010(1)	-0.0107(1)	-0.0100(1)
O(1)	0.052(4)	0.094(6)	0.060(4)	0.009(4)	-0.005(3)	-0.024(4)
O(2)	0.064(5)	0.085(5)	0.054(4)	0.000(4)	-0.009(3)	-0.020(4)
O(3)	0.047(4)	0.068(4)	0.042(3)	-0.003(3)	-0.004(3)	-0.026(3)
O(4)	0.095(6)	0.100(6)	0.054(4)	-0.013(4)	0.008(4)	-0.057(5)
O(11)	0.100(6)	0.50(5)	0.109(7)	0.002(4)	-0.041(5)	-0.009(4)
O(12)	0.052(4)	0.040(4)	0.054(4)	-0.002(3)	-0.017(3)	-0.011(3)
O(13)	0.082(5)	0.050(4)	0.076(5)	-0.006(3)	-0.039(4)	-0.019(4)
O(21)	0.053(4)	0.061(4)	0.075(5)	-0.13(4)	-0.026(4)	-0.11(3)
O(22)	0.050(4)	0.046(4)	0.061(4)	-0.004(3)	-0.023(3)	-0.007(3)
O(23)	0.062(4)	0.049(4)	0.048(4)	-0.002(3)	-0.021(3)	-0.008(3)
C(1)	0.043(6)	0.094(8)	0.065(6)	0.006(6)	0.003(5)	-0.027(6)
C(2)	0.072(8)	0.090(9)	0.083(8)	0.011(7)	0.008(7)	-0.034(7)
C(3)	0.16(2)	0.14(1)	0.081(9)	-0.023(9)	0.03(1)	-0.08(1)
C(4)	0.20(2)	0.17(2)	0.08(1)	-0.03(1)	0.04(1)	-0.13(2)
C(11)	0.043(5)	0.044(5)	0.047(5)	-0.12(4)	0.011(4)	-0.012(4)
C(12)	0.045(5)	0.057(6)	0.047(5)	-0.008(4)	0.006(4)	-0.015(4)
C(13)	0.038(5)	0.053(6)	0.050(5)	-0.010(4)	0.004(4)	-0.17(4)
C(21)	0.40(5)	0.045(5)	0.037(5)	0.002(4)	-0.001(4)	-0.013(4)
C(22)	0.046(5)	0.054(6)	0.039(5)	-0.001(4)	-0.008(4)	-0.011(4)
C(23)	0.031(5)	0.052(5)	0.038(4)	0.007(4)	-0.007(4)	-0.010(4)
C(111)	0.043(5)	0.040(5)	0.051(5)	0.004(4)	0.005(4)	-0.007(4)
C(112)	0.055(6)	0.052(6)	0.048(5)	-0.004(4)	-0.011(4)	-0.006(5)
C(113)	0.064(7)	0.085(8)	0.058(6)	-0.011(5)	-0.016(5)	-0.013(6)
C(114)	0.053(6)	0.074(8)	0.073(7)	0.013(6)	-0.006(5)	-0.001(6)
C(115)	0.06(7)	0.058(7)	0.08(7)	0.015(5)	0.004(6)	0.004(5)
C(116)	0.047(6)	0.053(6)	0.070(6)	0.010(5)	0.014(5)	-0.006(5)
C(131)	0.035(5)	0.048(5)	0.051(5)	-0.014(4)	0.003(4)	-0.014(4)
C(132)	0.077(7)	0.068(7)	0.062(6)	-0.018(5)	0.007(6)	-0.030(6)
C(133)	0.10(1)	0.060(7)	0.11(1)	-0.030(6)	0.028(8)	-0.033(7)
C(134)	0.085(9)	0.13(1)	0.097(9)	-0.062(8)	0.027(7)	-0.070(9)

(Table continued over page)

C(135)	0.067(7)	0.11(1)	0.081(8)	-0.022(7)	-0.006(6)	-0.039(7)
C(136)	0.054(6)	0.083(8)	0.072(7)	-0.024(6)	-0.000(5)	-0.029(6)
C(211)	0.033(5)	0.037(5)	0.048(5)	0.003(4)	0.006(4)	-0.006(4)
C(212)	0.048(5)	0.050(5)	0.044(5)	0.004(5)	-0.002(4)	-0.0012(4)
C(213)	0.055(6)	0.061(7)	0.077(7)	-0.019(5)	-0.007(5)	-0.018(5)
C(214)	0.082(8)	0.063(7)	0.092(8)	-0.018(6)	0.014(7)	-0.025(6)
C(215)	0.065(7)	0.054(6)	0.068(7)	-0.003(5)	-0.008(5)	-0.006(5)
C(216)	0.050(6)	0.044(5)	0.054(5)	0.002(4)	0.004(4)	-0.007(4)
C(231)	0.037(5)	0.061(6)	0.037(5)	0.090(4)	-0.006(4)	-0.022(4)
C(232)	0.058(6)	0.067(7)	0.055(5)	0.002(5)	-0.020(5)	-0.019(5)
C(233)	0.058(6)	0.105(9)	0.054(6)	0.002(6)	-0.021(5)	-0.027(6)
C(234)	0.056(7)	0.13(1)	0.048(6)	-0.026(6)	-0.002(5)	-0.033(6)
C(235)	0.064(7)	0.111(9)	0.079(7)	-0.051(7)	-0.018(6)	-0.020(6)
C(236)	0.056(6)	0.072(7)	0.072(7)	-0.026(5)	-0.016(5)	-0.004(5)

Table 5.20 Hydrogen Atom Coordinates and Isotropic Thermal Parameters for $[UO_2(HL^2)_2(EtOH)]\cdot EtOH$

Atom	x/a	y/b	z/c	U
H(3)	0.4438	0.3494	0.3770	0.10
H(4)	0.4686	0.5781	0.3696	0.10
H(11)	0.5708	0.2070	0.3881	0.10
H(21)	0.3552	0.5151	0.2300	0.10
H(1a)	0.6171(8)	0.3838(8)	0.3808(12)	0.10
H(1b)	0.6310(8)	0.2975(8)	0.2864(12)	0.10
H(2a)	0.6577(11)	0.4139(8)	0.1525(13)	0.10
H(2b)	0.5282(11)	0.4695(8)	0.1537(13)	0.10
H(2c)	0.5520(11)	0.3788(8)	0.0715(13)	0.10
H(3a)	0.4941(16)	0.6841(11)	0.2543(16)	0.10
H(3b)	0.6098(16)	0.6053(11)	0.2530(16)	0.10
H(4a)	0.6581(18)	0.7357(12)	0.3026(16)	0.10
H(4b)	0.7003(18)	0.6654(12)	0.4410(16)	0.10
H(4c)	0.5824(18)	0.7433(12)	0.4238(16)	0.10
H(12)	0.4824	-0.0331	0.1833	0.10
H(22)	0.0267	0.5334	-0.1924	0.10
H(113)	0.8146(4)	0.0776(3)	0.6889(6)	0.12
H(114)	0.8744(4)	-0.0800(3)	0.7230(6)	0.12
H(115)	0.7687(4)	-0.1647(3)	0.5635(6)	0.12
H(116)	0.6033(4)	-0.0919(3)	0.3700(6)	0.12
H(132)	0.3935(5)	-0.1104(4)	0.0732(6)	0.10
H(133)	0.2928(5)	-0.1971(4)	-0.0889(6)	0.10
H(134)	0.1259(5)	-0.1261(4)	-0.2818(6)	0.10
H(135)	0.0598(5)	0.0317(4)	-0.3126(6)	0.10
H(136)	0.1606(5)	0.1184(4)	-0.1505(6)	0.10
H(213)	0.2634(5)	0.7297(3)	0.2809(6)	0.11
H(214)	0.0964(5)	0.8406(3)	0.1445(6)	0.11
H(215)	-0.0347(5)	0.8012(3)	-0.0610(6)	0.11
H(216)	0.0013(5)	0.6509(3)	-0.1300(6)	0.11
H(232)	-0.0915(5)	0.4990(4)	-0.3499(5)	0.12
H(233)	-0.2113(5)	0.4651(4)	-0.5733(5)	0.12
H(234)	-0.1599(5)	0.3208(4)	-0.6683(5)	0.12
H(235)	0.0113(5)	0.2105(4)	-0.5399(5)	0.12
H(236)	0.1311(5)	0.2443(4)	-0.3165(5)	0.12

REFERENCES FOR SECTION TWO

1. H.A.O. Hill, **Chem. Brit., 12**, 119 (1976)
2. D.E. Fenton, **Pure & Applied Chem., 61**(5), 903 (1989)
3. T.N. Sorrell, **Tetrahedron, 45**(1) 3 (1989)
4. P.A. Vigato, s. Tamburini and D.E. Fenton, **Coord. Chem. Rev., 106**, 25 (1990)
5. U. Casellato, P.A. Vigato, D.E. Fenton and M. Vidali, **Chem. Soc. Rev., 8**, 199 (1979)
6. D.E. Fenton, U. Casellato, P.A. Vigato and M. Vidali, **Inorg. Chim. Acta., 62**, 57 (1982)
7. P. Zanello, S. Tamburini, P.A. Vigato and G.A. Mazzocchin, **Coord. Chem. Rev., 77,** 165 (1987)
8. R.L. Lintvedt, M.D. Glick, B.K. Tomlonovic and D.P. Gavel, **Inorg. Chem., 15**(7), 1646 (1976)
9. M.D. Glick, R.L. Lintvedt, D.P. Gavel and B.K. Tomlonovic, **Inorg. Chem., 15**(7) 1654 (1976)
10. D.E. Fenton and S.E. Gayda, **J. Chem. Soc. Dalton Trans.**, 2109 (1977)
11. A.R. Siedle, **Comprehensive Coordination Chemistry**, Vol **2**, p 365, Eds. G. Wilkinson, R.D. Gillard and J.A. McCleverty, Pergamon, Oxford (1987)
12. D.E. Fenton and R.L. Lintvedt, **J. Am. Chem. Soc., 100**(20), 6367 (1978)
13. L.L. Borer and W. Vanderbout, **Inorg. Chem., 18**(2), 526 (1979)
14. M. Atchayya, **Indian. J. Chem., 4**, 198 (1966)
15. Y. Taguchi, F. Sagara, H. Kobayashi and K. Ueno, **Bull. Chem. Soc. Jpn., 43**(8), 2470 (1970)
16. U. Casellato, S. Tamburini, P.A. Vigato, A. De Stefani, M. Vidali and D.E. Fenton, **Inorg. Chim. Acta., 69**, 45 (1983)
17. P. Lagrange, **Inorg. Chem., 24**, 80 (1985)
18. A.R. van Doorn, M. Bos, S. Harkema, J. van Eerden, W. Verboom and D.N. Reinhoudt, **J. Org. Chem., 56**, 2371 (1991)

19. W.F. Nijenhuis, A.R. van Doorn, A.M. Reichwein, F. de Jong and D.N. Reinhoudt, **J.Am. Chem. Soc., 113**, 3607 (1991)

20. H.I. Schlesinger, H.C. Brown, J.J Katz, S. Archer and R.A. Lad, **J. Am. Chem. Soc., 75**, 2446 (1953)

21. L. Sacconi and G. Giannoni, **J. Chem. Soc.**, 2368 (1954)

22. L. Sacconi and G. Giannoni, **J. Chem. Soc.**, 2751 (1954)

23. W.W. Wenalandt, J.L. Bear and G.R. Horton,**J. Phys. Chem., 64**,1289 (1960)

24. K. Nakamoto, Y. Morimoto and A.E. Martell, **J. Am. Chem. Soc., 83**, 4533 (1961)

25. E. Frasson, G. Bombieri and C. Panattoni, **Nature, 202**, 1325 (1964)

26. G.M.Kramer, M.B. Dines, R.B. Hall, A. Kaldor, A.J. Jacobsen and J.C. Scanlon, **Inorg. Chem., 19**, 1340 (1980)

27. J.C. Taylor and A.B. Waugh, **J. Chem. Soc. Dalton Trans.**, 1630 (1977)

28. J.C. Taylor and A.B. Waugh, **J. Chem. Soc. Dalton Trans.**, 1636 (1977)

29. J.C. Taylor and A.B. McClaren, **J. Chem. Soc. Dalton Trans.**, 460 (1979)

30. E.C. Okafor, A.B. Uzoukwu, P.B. Hitchcock and J.D.Smith, **Inorg. Chim. Acta., 172**, 97 (1990)

31. J.P. Fackler jr, **Prog. Inorg. Chem., 7**, 395 (1966)

32. J.C. Taylor, A. Ekstrom and C.H. Randall, **Inorg. Chem., 17**(11), 3285 (1978)

33. P.A. Vigato, U. Casellato, D.A. Clemente, G. Bandoli and M. Vidali, **J. Inorg. Nucl. Chem., 35**, 4131 (1973)

34. R.L. Lintvedt, M.J. Heeg, N. Ahmad and M.D. Glick, **Inorg. Chem., 21**, 2350 (1982)

35. R.L. Lintvedt and N. Ahmad, **Inorg. Chem., 21**, 2356 (1982)

36. R.L. Lintvedt, B.A. Schoenfelner, C.Ciccarelli and M.D. Glick, **Inorg. Chem., 23**, 2867 (1984)

37. R.L. Lintvedt, W.E. Lynch nd J.K. Zehetmair, **Inorg. Chem., 29**, 3009 (1990)

38. D.E. Fenton, J.R. Tate, U. Casellato, S. Tamburini, P.A. Vigato and M. Vidali, **Inorg. Chim. Acta., 83**, 23 (1984)

39. F. Texidor, J. Colomer, J. Casabo, J. Rius, E. Molins and C. Miravitlles, **Inorg. Chem., 28**, 678 (1989)

40. J. Casabo, J. Colomer, L. Escriche, F. Texidor, E. Molins and C. Miravitlles, **Inorg. Chim. Acta., 178**, 221 (1990)

42. D. Zheglova, N. Denkov and A.I. Kol'tsov, **J. Mol. Struct., 115**, 371 (1984)

43. B.D.M. Cunningham, P.R. Lowe and M.D. Threadgill, **J. Chem. Soc. Perkin Trans.II.**, 1275 (1989)

44. L.J. Bellamy, G.S. Spicer and J.D.H. Strickland, **J. Chem. Soc.**, 4487 (1954)

45. H.F. Holtzclaw and J.P. Collman, **J. Chem. Phys., 79**, 3318 (1957)

46. G.K.T Conn and C.K. Wu, **Trans. Faraday. Soc., 34**, 1483 (1938)

47. H.D. Bist, **J. Mol. Spectrosc., 16**, 542 (1968)

48. D.W. Barnum, **J. Inorg. Nucl. Chem., 22**, 183 (1961)

49. D.W. Barnum, **J. Inorg. Nucl. Chem., 22**, 221 (1961)

50. J.M. Haigh, D.A. Thornton, **J. Mol. Struct., 8**, 351 (1978)

51. R.D. Hancock and D.A. Thornton, **J. Mol. Struct., 4**, 377 (1969)

52. K. Nakamoto, Y. Morimoto and A.E. Martell, **J.Chem. Phys. , 32**, 588 (1960)

53. S.P. McGlynn, J.K. Smith and W.C. Neely, **J. Chem. Phys., 35**, 105 (1961)

54. L.K.L Dean, G.C. DiDonato, T.D. Wood and K.L Busch, **Inorg. Chem., 27**, 4622 (1988)

55. A.S. Plazaik, C. Zeng, C.E. Costello, S. Lis and M. Elbanowski, **Inorg. Chim. Acta., 184**, 229 (1991)

56. C. Reichert and J.B. Westmore, **Can. J. Chem., 48,** 3213 (1970)

57. M. Das, **Inorg. Chim. Acta., 77**, L65 (1983)

58. K.R. Jennings, T.J. Kemp and P.A. Read, **Inorg. Chim. Acta., 157**, 157 (1989)

59. D.A. Brown and S. Ismail, **Inorg. Chim. Acta., 171**, 41 (1990)

60. V.S. Sagoria, M.S. Gill, S.C. Jain, H.S. Ahuja and G.S. Rao, **Inorg. Chim. Acta., 121**, 233 (1986)

61. J.C. Morrow and E.B. Parker jr, **Acta Cryst., B29**, 1145 (1973)

62. G.J. Kruger and E.C. Reynhardt, **Acta Cryst., B30**, 822 (1974)

63. "International Tables for X-Ray Crystallograophy", Kynoch Press, Birmingham, 1962, Vol III, p 276

64. D.A. Clemente, G. Bandoli, M. Vidali, P.A. Vigato, R. Portanova and L. Magon, **J. Cryst. Mol. Struct., 3**, 221 (1973)

65. M.N. Akhtar and A.J. Smith, **Acta Cryst., B29**, 275 (1973)

66. G.M. Kramer, M.B. Dines, R. Kastrup, M.T. Melchior and E.T. Maas jr, **Inorg. Chem., 20**, 3 (1981)

67. G.M. Kramer and E.t.Maas jr, **Inorg. Chem., 20**, 3514 (1981)

68. B. Glavincevski and S. Brownstein, **Inorg. Chem., 22**, 221 (1983)

69. Y. Ikeda, H. Tomiyasu and H. Fukutomi, **Inorg. Chem., 23**, 1356 (1984)

70. D.T.Haworth and M. Das, **Inorg. Chim. Acta., 110**, L3 (1985)

71. D.T Haworth, G.Y. Kiel, L.M. Proniewicz and M. Das, **Inorg. Chim. Acta., 130**, 113 (1987)

72. W. Jung, H. Tomiyasu and H. Fukutomi, **Inorg. Chem., 25**, 2582 (1986)

73. I.L. KimBong, C. Miyakoe and S Imoto, **J. Inorg. Nucl. Chem., 37**, 963 (1975)

74. F.A. Cotton and G. Wilkinson, **"Advanced Inorganic Chemistry"**,5th Ed, John Wiley & Sons, New York (1988)

75. G.H. Reed and T.S.Leyh, **Biochem., 19**, 5472 (1980)

76. H. Sakurai, M. Nishida and T. Yoshimura, **Inorg. Chim. Acta., 66**, L17 (1982)

77. J.S. Wieringen, **Dis. Faraday Soc., 19**, 118 (1955)

Appendix 1

Purification of Solvents and Instrumentation

A1.1 Purification of Solvents

Dichloromethane was distilled from CaH_2. Methanol and ethanol were dehydrated by distillation from their respective magnesium alkoxides.These solvents were stored over type 4A molecular sieves.The deuterated NMR solvent $CDCl_3$ was used as supplied commercially (Aldrich Chemical Co).

A1.2 Instrumentation

Nuclear Magnetic Resonance spectroscopy was performed at 6.34 Tesla on a JEOL GX270W spectrometer operating in Fourier transform mode at 270.0 and 109.4 MHz for ^{1}H and ^{31}P nuclei respectively. Chemical shift data (δ) are expressed in parts per million (ppm) to high-frequency (downfield) shift from tetramethylsilane as an internal reference for the ^{1}H nucleus. ^{31}P chemical shift data are referenced with respect to 85% H_3PO_4 as an external standard.

Infra Red spectra were recorded on a BIO-RAD FTS-40 spectrophotomer as thin films of Nujol mulls between KBr discs.

Electron Spin Resonance spectroscopy was performed on a Varian E-104A spectrometer equipped with a Varian E-257 variable temperature accessory and operating at 110K.

Mass spectra were obtained using a Varian VG70-250S double focussing magnetic sector mass spectrometer by the method of Liquid Secondary Ion Mass Spectrometry (LSIMS) at the Department of Scientific and Industrial Research, Palmerston North. The samples were

dissolved in a suitable solvent and either *m* -nitrobenzylalcohol (NBA) or "magic bullet" employed as the matrix.

Electronic spectra were obtained on a HP8352A diode array spectrophotometer using a quartz cell of pathlength 1 cm.

Elemental analyses were carried out using standard techniques by the Microanalytical Laboratory, University of Otago, Dunedin.

Melting points were recorded using a Reichert hot-stage melting point apparatus and are uncorrected.